Document SC-CIEM01(08)4.1.Periodic Report

ANNUAL REPORT 2007

Asociación EURATOM-CIEMAT para Fusión

INDEX:

INTRODUCTION

The present document Is a report of the Association activities during 2007 following the thematic distribution of the approved 2007 Workprogramme.

This programme follows the standard pattern for all the associations and requires some specific adaptations for stellarator activities:

- Chapter I deals with the enhancement of the physics basis for the next step : ITER.

Here we report basic physics obtained in TJ-II which are applicable to the main tokamak line (momentum transport & turbulence), together with results obtained from experiments at JET and other devices: equilibrium reconstruction with EFIT, ITB formation, ELM propagation physics & plasma wall, or in technology devices: tritium retention prevention and Tritium removal

- Chapter II is devoted to the development of auxiliary systems: diagnostics, heating & CD, Control and DAC. Here we report developments both in TJ-II, JET and W7X, as well as developments for ITER

- Chapter III is the main section dealing with stellarator physics. It also includes general results from plasma theory.

Here we report TJ-II status and operation summary, operation highlights (Lithium coating) and a number of physics research results on: electric fields, magnetic topology, stellarator confinement scaling and momentum transport.

Theory activities include studies in TJ-II, JET and general plasma physics studies.

Finally we include in this chapter our activities on W7X engineering.

- Chapters IV & V Describe activities in technology, either under EFDA specific contracts or in preparation for expected activities

- Chapter VI covers other activities like: training & education, public information, socioeconomics, activities under the Broader Approach, preparation activities towards

the new fusion technology centre "Technofusion" and a report on Inertial Fusion keep in touch activities.

FINALLY, ANNEX I GIVES A LIST OF PUBLICATIONS & TALKS GENERATED BY THE ASSOCIATION.

I. PROVISION OF SUPPORT TO THE ADVANCEMENT OF THE ITER PHYSICS BASIS

I.1. Energy and particle confinement / transport

I.1.1. Momentum transport and role of turbulence

I.1.1.1. Parallel dynamics: Influence on electric electric field on Reynolds stress driven flux $<v_{||} v_{\theta}>$ component

The first experimental evidence of the dual role of electric fields as a stabilizing mechanism of plasma turbulence and as an agent affecting the parallel momentum balance via turbulence modification has been obtained. Then, turbulence driven momentum flux (via Reynolds stress) should be taken into account when considering the parallel momentum balance equation, particularly in high electric field shear regimes.

Applying a radial electric field generated by external biasing was seen to have a strong impact on the parallel Mach number profile in the edge of the TJII stellarator. The effect of the increased radial electric field shear on the radial profiles during an improved confinement regime due to external basing was investigated. A reduction of the radial-parallel Reynolds stress component as a result of the lower turbulence level was observed. However, the 'phase coherence' between the fluctuations was strongly enhanced inside the plasma, generating a gradient in radial-parallel Reynolds stress component of a magnitude comparable to the observed change in the friction term. This order of magnitude comparison of local measurements suggests that the turbulence driven momentum flux (via Reynolds stress) should be taken into account when considering the parallel momentum balance equation, particularly in high electric field shear regimes. The results presented in this paper show the dual role of sheared ExB flows as a fluctuation stabilizing term as well as an agent affecting the parallel momentum balance via turbulence modification [ref. I.1.1.1].

I.1.2. Equilibrium reconstruction studies and plasma peeling

I.1.2.1. Equilibrium reconstruction, modelling

Continued work on fortran 90 version of EFIT. During a visit to GA gathered information on optimal MSE representation to be introduced in code. JET version of efit-f90 installed

under svn version control. Ongoing work on pre-processor EFUN, to be re-written in fortran-90, including JET diagnostics.

I.1.2.2. Internal Transport Barrier physics

Study of plasma evolution towards critical equilibria and diamagnetism, carried out in 2D.

The evolution of the poloidal current density controls plasma diamagnetism locally, while the evolution of the toroidal current density controls criticality of the Grad-Shafranov equation. We investigated the possibility that transport barrier formation, likely to be associated with new solution branches of the non-linear Grad-Shafranov equation, may be an inescapable result of current profile evolution when localized current drive is applied. The work was presented at the 2007 International Sherwood Fusion Theory Conference, Baltimore, USA, April 23 - 25, 2007 [Ref I.1.2.2].

A study of conserved quantities in Grad-Shafranov equation, based on Derrick's theorem, initiated in collaboration with R. D. Hazeltine, IFS, Univ. of Texas at Austin.

I.2. MHD stability and plasma control

I.2.1. ELM propagation physics

I.2.1.1. Comparison of inboard-outboard temperature during type I ELM regimes

The good spatial and temporal resolution of the ECE heterodyne radiometer, make it an ideal diagnostic to study ELMs dynamics. New detailed measurements of the electron temperature perturbation caused by the ELM crash have been carried out. In general, good agreement has found between the Te pedestal profiles (before the ELM crash) determined by ECE (both LFS and HFS) and the edge LIDAR and High Resolution Thomson Scattering (HRTS) systems. At high densities, refraction effects need to be properly included in the data analysis. The most striking feature noted in comparing the temperature profile evolution before and after the ELM crash is that, for certain plasma conditions, the ELM affected region is similar for both the LFS and HFS profiles mapped onto the mid-plane. This leads to an asymmetric profile after the ELM crash when mapped onto normalized flux coordinates. At present, it is not entirely clear what the mechanisms are that allow the asymmetries to appear. The extension of the analysis to a larger database and a better understanding of mapping errors are in progress. [Ref I.2.1.1]

I.2.1.2. ELM studies at JET

Continued development of experimental proposal to study an ITER-relevant high T_e pedestal in JET. The plan is to develop a hot-ion-H-mode pedestal, with T_e~3-4 keV (the desired pedestal T_e for ITER). The interest of such plasma is that we could study in JET a pedestal with the same resistivity as the ITER pedestal. Low edge resistivity implies high edge current densities, which are to be expected in ITER. This can modify the balance of MHD instabilities that can trigger an ELM. Such plasmas would allow detailed pedestal evolution studies, study of MHD precursors and triggers to the ELM, and would be an ideal test-bed for ELM control or mitigation techniques in a plasma with an ITER-relevant pedestal. The proposal [Ref I.2.1.2a, Ref I.2.1.2b] has been accepted as an S1 experiment for the 2008 JET campaigns. It was presented at the 15th European Fusion Physics Workshop, 3-5/12/2007, Prague, Czech Republic [Ref I.2.1.2c].

I.2.1.3. ELM optimisation study for AT scenarios in JET

Diagnostic support for characterisation of plasma edge in AT plasmas, searching for optimum radiation levels to reduce ELMs while maintaining a pedestal compatible with Internal Transport Barrier formation and sustainment. [Ref I.2.1.3].

I.2.1.4. Test experimental set-up: influence of magnetic fields/radiation on fast camera performance, control system, up-grade optical coupling

After two months of operation (October – November 2006) no evidence of permanent damage on any pixel has been observed. However, further experiments at high neutron fluxes are needed to clarify the influence of radiation on the camera performance. These evaluations were carried out during C18 – C19 experimental campaign (January – March 2007). The integrated neutron fluence in the camera position after four months of operation is in the range of 4x1010 n/cm2. So far there is no evidence of permanently damaged pixels. Several disruptions were recorded, the camera withstanding field variations of up to 4 T/s.

I.2.1.5. First fast 2-D visualization of ELMs in JET

Maximum achieved recording speed has been 20 kHz during ELMs. Several fast phenomena like MARFE-Like rings, disruptions and plasma-wall interaction after ELM impact have been captured. The main future objectives of the fast visible camera in JET are the study of ELM structure, pellet ablation and impurity flows. The common IR/visible view will allow the joint interpretation of their data [Ref I-2.1.5].

Figure I.2.1.5: Image of the JET interior during an ELM

I.3. Power and particle exhaust, plasma-wall interaction

I.3.1. Studies of de-tritiation methods for ITER

I.3.1.1. Studies of nitrogen injection for co-deposited film inhibition

The drastic (up to 80%) decrease of QMB deposition upon injection of Nitrogen in the subdivertor region of Asdex Upgrade found in the 2004 experiments [Scav 1] was not reproduced in the nitrogen seeding experiments at JET in the 2006 campaign. Several locations of the gas inlet respect to the divertor inner leg were tried, although under reduced heating power. As a tentative explanation, the full ionization of N2 in the divertor plasmas foreseen in all scenarios could prevent the formation of radical species with enhanced chemical reactivity with the carbon film precursors, leading to a rather enhanced erosion of carbon surfaces in the divertor plates nearby [Scav 2]. A task in cooperation with FZJ has been initiated to include N driven chemical reactions in the ERO code.

I.3.1.2. Plasma-assisted removal of films with O and N

The effect, which metallic impurities, originated from the presence of mixed materials in ITER, will have on the efficient removal of carbon co-deposits by plasma oxidation, has been studied in laboratory experiments at CIEMAT. Mixtures of carbon films with Mg and Li, to simulate strong O gettering materials as Be, were prepared by effusion of these metals from an effusive oven during the PACVD of hard a-C: H films. The conclusion was that little effect of erosion yield by the reactive plasma (He/O_2) is to be expected if

metals are uniformly distributed into the film. However, a strong decrease in such yield was seen in layered structures with Li as contaminant [IVC07_1]

Alternatives to the use of oxygen, with possible deleterious effects on Be first wall, have been explored [IVC07_2]. The erosion of laboratory-produced a-C:H layers by H_2/N_2 and He/N_2 plasmas has been addressed. The layers showed erosion rates of 4 and 2.6 nm/min, respectively. However, thermal desorption of the films after exposure to the erosion plasmas indicates that some modifications of the binding states of H took place, leading to an increase of the temperature of desorption. Characterization of the plasma chemistry by differentially pumped mass spectrometry and Cryotraping-Assisted Mass Spectrometry was performed. HCN, C_2N_2 and acetylene are the main reaction products. The detection of acetonitrile in the reaction products provides a clear indication of chemical reactions being involved in the film removal mechanism under the reported conditions.

I.3.1.3. Testing of the role of atomic N in the scavenger mechanism in the PSI-2 linear device

Experiments at PSI-2 Berlin were initiated to elucidate the effect of free radicals on the deposition and inhibition of carbon films in a duct exposed to the species produced in the plasma region. It was found that radicals created by the plasma decomposition of injected nitrogen were able to prevent the formation of films in the ion-free region of the duct, where strong influx of carbon radicals leads to the deposition and erosion (by remnant H atoms produced in the plasma). Mass spectra showed that ammonia was largely produced by the plasma species and its concentration was ant correlated with the presence of methane in the plasma. Also, no net film erosion was seen by nitrogenic species produced in the plasma, the erosion being always dominated by the presence of H atoms. No scavenger effect was observed at all when Ne was injected instead of nitrogen into the plasma [Scav_3].

I.3.2. Edge instabilities and plasma-wall studies

I.3.2.1. Installation of fast camera diagnostic for plasma-wall studies in JET

The camera system provided useful information to study different fusion plasma relevant issues including plasma wall interaction, ELMs and disruption physics. However, the study of ultra-low intensity phenomena, like the continuous plasma wall interaction and the generation and dynamics of impurities requires a higher signal level. It was therefore

agreed to expand the original project to allow the addition of an image intensifier to the fast camera system. The upgraded diagnostic is expected to be installed in April 2008.

II. DEVELOPMENT OF PLASMA AUXILIARY SYSTEMS

II.1. Heating and current drive systems

II.1.1. NBI Heating studies (TJ-II)

II.1.1.1. Commissioning and start-up of NBI-2

Good Ion Source Plasmas were obtained in February. Arc discharges of 800 A, with smooth waveforms were stable for 100 ms. To obtain these Arcs in the Ion Source, several problems had to be solved:

- The piezoelectric valve throughput varies with temperature along operation
- The intermediate electrode connection was of poor quality
- The Ion Source Magnet supply is noisy
- The control electronics of the piezo valve is faulty

The grids were High Pot conditionned with a Glassmann Power Supply (50 kV). The Accel/Decel supplies connected to the grids in March. First Beams in March: severe problems related to the Accel switching circuit, the Decel Power Supply and the protection circuits (crowbar) appear. Extensive work on the grounding system is performed in April. Interlock PLC is replaced by a programmable logic based VME module (VPL0) during the summer break to accommodate new signals and provide room for future expansion. From October through December, commissioning of the High Voltage system continues:

- Decel supply: regulation circuit refurbished
- VPL0: filters installed, response delays adjusted and new Accel supply protection introduced
- Accel switching circuit: refurbished. The unwanted ("Spontaneous") switching of the Accel supply is suppressed

First time operation with the Motor Generator at 15 kV in continuous mode (previously, continuous operation was possible only up to 10.5 kV) on 27th November.

II.1.1.2. Beam conditioning up to 30 kV / 60 A (June-2007)

In spite of persisting problems in the protection, accel and decel systems, beam conditioning is carried out in June: beams of 27 kV, 45 A are obtained. First beams injected in TJ-II: 5th of July. Simultaneous injection with #1 and #2 beams: 5th of July: TJ-II shot number 17096.

II.1.1.3. Target Calorimeter for NBI-2: Port-Through Power (400 kW) measurement by Infrared Thermography: installation and commissioning (June-2007)

The Target calorimeter (identical to the one previously installed in NBI-1, [CCNB1_07] was installed in April 2007. The displacement mechanism is tested. The thermocouples installed and tested. There have been no beams in TJ-II with Injector #2 after the summer, therefore the target has not been put to use as yet.

II.1.1.4. First plasma operation with two co / counter NBI beams (December-2007)

Injection into TJ-II with NB#2 has not been possible after the summer due to a suite of problems with the High Voltage power supplies.

II.1.2. ECRH

II.1.2.1. ECRH system routine operation and improvements

The ECRH system of the TJ-II stellarator consists of two triode-53.2 GHz-gyrotrons, which can deliver a maximum power of 300 kW each, during 1s. Both gyrotrons are fed by a common high voltage power supply (HVPS) and driven by an anode modulator. During the last experimental campaigns the performance of the gyrotrons and the stabilization of the microwave power were limited by the HVPS, whose maximum output current was limited to 30 A and the ripple level of the output voltage was around 7%. In order to guarantee the reliability of the ECRH system and to improve the performance of the gyrotrons, a new HVPS has been installed during 2007 (the details are given in next section)

The TJ-II experimental campaign started in April 2007 after the commissioning of the new HVPS. The ECRH system was working with its two gyrotrons running together at

their maximum power - 600 kW - for the first time. High reliability has been achieved during the spring and autumn TJ-II experimental campaigns. The stabilization of the output power and the frequency has been proved.

The ECRH control system has to be improved and upgraded to implement the new signals of the power supply. Some new hardware components have been developed to include the HV safety signals and the fast and slow interlocks for the triggering and switching-off of the ECRH system.

The ionic pumps of the gyrotrons had to be electrically isolated and a remote control has been developed.

Improvements in the modules of the anode modulators were designed in order to implement new software to allow the remote control of the filament current power supply and the voltage of the anodes. The modules were installed during July 2007 and the software has also been finished. During 2008 the remote control will be available. (*This work has been carried out in collaboration with the Institut für Plasmaforschung of Stuttgart, Germany*).

The cooling system was working properly and the annual maintenance was carried out during the summer.

II.1.2.2. Commissioning of the new high voltage power supply

The new high voltage power supply was received at CIEMAT in February 2007 after the approval of the acceptance tests at the manufacturer in January 2007. The delay in relation to the scheduled plan was due to some problems in the development and manufacture of the prototype high voltage/ high frequency transformers.

The main specified characteristics were: maximum output voltage: -80 kV, maximum output current: 50 A, maximum pulse length: 1s, maximum switch-off time in case of a short-circuit: 5 ms, output voltage ripple: 1%, optimal regulation of the voltage in the connection and disconnection of the loads to avoid over-voltages and over-currents.

To achieve the specifications the solution includes a matching transformer, which isolates the AC input and provides the DC current for the 12 pulses SCR rectifier. The DC bus is connected to 32 IGBT invertors, which operate at 2,7 kHz. The pulse width modulated output of each converter is connected to a high frequency transformer, which provides the main isolation from the low voltage to the high voltage side. The square waveform obtained at the secondary of each transformer is rectified by means of a diode bridge. The connection in series of the diode bridges provides the required -80 kV d.c. at the output. In case of arcing in the gyrotrons the HVPS switches-off in less than 5μs, which limits the energy deposited in the gyrotrons and a crow-bar protection is not needed.

The final acceptance tests at CIEMAT in March 2007 proved most of the specifications, but the level of the output voltage ripple is now 2.5 % peak to peak and it has to be reduced with an additional filter, which is at present being developed.

Since April 2007 the HVPS and the gyrotrons are working properly and the performance of the ECRH system has been improved.

II.1.2.3. ECCD experiments in TJ-II and Heliotron-J

To continue with the characterization of the ECCD in the TJ-II stellarator new experiments have been carried out. The achievable maximum EC-driven current has been explored with a maximum power of 600 kW. A power scan was performed in order to obtain the experimental ECCD efficiency at different power levels and different signs of the induced currents. We have obtained values up to $\eta_{ECCD} \approx 0{,}0008 \times 10^{20}$ A W^{-1} m^{-2}. [Ref ECRH1]

More experiments need to be carried out in order to discriminate with more accuracy the bootstrap current and the EC-driven current. The reversal of the magnetic field direction will allow us to distinguish the EC current from the bootstrap current assuming that plasma parameters are comparable in discharges with different directions of B.

The TJ-II results are being compared with the experiments in another helical systems: Heliotron–J, CHS and LHD.

In Heliotron-J, several ECCD experiments were performed with the participation of persons of the TJ-II ECRH Group.The dependence of the current on the configuration was explored. The high ripple configuration with ripple top heating (5:4) shows a plasma current lower than the 5:3 configuration, were heating is also performed at the ripple top. The behaviour of the plasma current in relation with its sign reversal and its decay after the end of the discharge seems to be in agreement with the physical picture of the EC current drive where trapped particles play a fundamental role.[Ref ECRH2]

Then, ECCD experiments with reversed field were also performed. In the configuration 5:4, the bootstrap current and the ECCD were distinguished and the density scan showed that a low densities the toroidal current is mainly due to the ECCD. The toroidal current changes its direction in the 5:1 configuration, which has more trapped particles (it's a bottom ripple configuration) and the Ohkawa effect is dominant. The power scan from 135 kW up to 412 kW was carried out. A maximum current of -3kA was reached at 350 kW (the absorbed power was measured and more than 90%). The dimensionless current efficiency remained constant.

These comparisons give us a common understanding of the current drive physics in heliac machines [ref ECRH3]

This work has been carried out in the frame of the collaboration with the Kyoto University (Japan).

II.1.2.4. High frequency power modulation experiments

In order to determine the ECRH power deposition profile and the percentage of absorbed power, modulation experiments were performed at different modulation frequencies (6 and 9 kHz) and different launching configurations. Although the general findings as the dependence on modulation frequency, density and launching direction are consistent with the expected behaviour, the integration of the power deposition profile leads systematically to inconsistent values of the total absorbed power. This discrepancy is still not resolved, though it seems that the reason could be the non validity of the approximation that relates the experimental temperature modulation to the final absorbed power [Ref ECRH4].

II.1.2.5. Status of the Electron Bernstein Waves heating project

Electron Bernstein Wave heating (EBWH) is important for high-beta plasma experiments and will be used for heating over-dense plasmas on TJ-II. Previous work has shown that the most suitable scheme for launching EBWs in TJ-II is O-X-B mode conversion, which has acceptable heating efficiency for central densities above 1.2×10^{19} m^{-3}. A system based on a 28 GHz-100ms diode gyrotron will be used to deliver 300 kW through a corrugated waveguide. [Ref ECRH5].

The system has not been put into operation yet due to the problems with the high voltage power supply for the gyrotron. These problems could not be solved and a high voltage cable has been installed to connect the ECRH high voltage supply to this gyrotron. First high power testing of the gyrotron was carried out in September 2007 and 100 kW were achieved with -65 kV. The tube is very old and further conditioning is needed.

The waveguide could not be aligned due to a crack in the vacuum window. It has been already repaired and will be installed during 2008.

The microwave beam is directed and focused by a steering mirror located inside the vacuum vessel. The mirror was calibrated and it is already installed inside the vacuum vessel with its remote control system.

The polarizers have been also calibrated and installed. The remote control system is working properly.

The ellipsoidal mirrors that match the beam into the waveguide have also been installed.

II.1.2.6. Electron Bernstein waves emission diagnostic

Prior to the heating experiments, measurement of the thermal EBW emission from the plasma will be made to help determine the optimum launch angle for EBW mode conversion, and also to provide an indication of the electron temperature evolution in over-dense plasmas. A dual-polarized quad-ridged broadband horn will be used to measure the EBW emission at 28 GHz. Emission from the plasma is reflected from the internal steering mirror, propagates through a section of corrugated waveguide, and is then focused on the horn through a glass lens. A heterodyne radiometer system is used to process the emission signals. The antenna was installed in the TJ-II vacuum vessel in September 2007. The electronic components have been calibrated and are expected in February 2008. [Ref ECRH6].

This work has been carried out in the frame of the collaboration with the Oak Ridge National Laboratory, Oak Ridge (USA).

II.1.2.7. Verification of the gaussian beam parameters with an IR-camera

The shape of the microwave beam has been showed by means of a thermal camera. A target with some resistances used as references has been situated in the beam path to intercept it. A thermal camera was focusing the target, so its heating could be registered. The thermal images are transferred in real-time to a computer thanks to a GPIB-fiber optics communication. These images are treated by specific thermal imaging software in order to increase the contrast among the different temperatures. The tests have been performed in different places of the beam path [Ref ECRH7].

II.1.2.8. EC waves polarization control

For both EC heating systems (ECRH and EBWH), a complete control of the polarization of the launched waves is needed. In the case of the 53.2 GHz system which can perform perpendicular and oblique injection with each launcher, the good coupling of the quasi-extraordinary mode (QX) is desirable, particularly during ECCD on-axis experiments. The QTL1 has two corrugated polarizer mirrors. The QTL2 has only a $\lambda/4$-corrugation depth grooved mirror. Also, to reach an optimum Bernstein mode excitation, it is also mandatory to couple a pure quasiOmode under oblique injection. Its transmission line consists of a waveguide and matching optics mirrors. Two of them are also grooved mirrors and any polarization can be achieved at the intput of the waveguide.

The tools to control the polarization of the three EC beams launched in the TJ-II are developed. A code based on the 3-dimensional Jones matrix formalism allows the calculation of the resulting polarization of an output beam in the quasi-optical

transmission lines taking into account all smooth and corrugated mirrors. The code was calibrated at the existing TJ-II quasi-optical transmission line QTL1 using the signal from a directional coupler in one mirror at the end of the line. The $\lambda/4$ polarization twister of QTL2 will be replaced by a single deep grooved mirror which will also allow to vary the ellipticity of the output beam [Ref ECRH8].

This work has been carried out in collaboration with the EURATOM-IPP Association (Germany).

II.1.2.9. Influence of the controlled modulated power reflected back to the girotrón

New high power experiments have been performed with the gyrotrons of the TJ-II ECRH system to influence the microwave output radiation with a relatively weak wave returned from an external mechanically modulated reflector. The dependence of the gyrotron reaction on the frequency and the operation parameters was explored. A delay of some ms in the reaction of the gyrotron was found and it will be studied in detail during 2008.

[Ref ECRH9]

This work has been carried out in collaboration with the Institute of Applied Physics (Russian Academy of Science), Moscow and Nizhny Novgord (Russia)

II.1.2.10. Participation in the remote steering upper launcher of the ECRH system for ITER

Finally, the Front Steering design for the upper-port launcher of the ECRH system has been accepted as the reference solution and the Remote Steering remains as back-up design. No further development will be made in the RS and the participation of the ECRH is over for 2008.

This work has been carried out in collaboration with the EURATOM-FOM Association (The Netherlands)

II.2. Plasma diagnostics

II.2.1. Further development of TJ-II systems including

II.2.1.1. Reflectometry: installation of second channel (hopping reflectometer) for radial correlation studies

The second channel of the fast frequency hopping reflectometer was installed at TJ-II in February, becoming fully operative in March. Like the first channel, the second one was designed and constructed in collaboration with the IST reflectometry team. The frequencies of the two channels, which cover the whole gradient region in ECRH-discharges, can independently be switched on a very fast timescale, enabling the measurement of the radial correlation properties of the turbulence. First preliminary results on correlation measurements were presented in the 8th International Reflectometry Workshop in St. Petersburg [Ref II.2.1.1].

II.2.1.2. Fast particle detector: final installation and first measurements

This new diagnostic has been installed in the TJ-II stellarator for quantifying fast ion losses close to the plasma edge. The final goal of this study is to determine the energy and pitch angle distribution functions of the ions impinging onto a phosphor screen and to display these distributions in absolute scale. For this, we have developed, in parallel to TJ-II measurements, an experimental setup to perform basic studies on the response of this screen in the energy range of interest (E<35keV), with the aim of unfolding the distribution from the phosphor luminescence image. The first results obtained in TJII plasma discharges have been discussed within the physics of fast particles in stellarator devices (a more detailed report of this work can be found in [Ref II.2.1.2].

II.2.1.3. Diagnostic neutral beam injector in TJ-II: first radial ion temperature and velocity measurements

Charge-exchange recombination spectroscopy *(*CXRS), is an active spectroscopic technique, based on the localized measurement of the Doppler broadening and displacement of a spectral line emitted by hydrogen-like impurity ions that have captured an electron into an excited state after a collision with a neutral atom. For this a narrow beam of accelerated neutral atoms is injected into the plasma in order to stimulate such emissions. As a result of the localized interaction zone it is possible to determine the rotation velocity and direction, as well as temperature, of the original fully-ionized impurity ions that reside in the hot plasma centre.

During the TJ-I campaigns in 2007, the first impurity ion temperature profiles using charge-exchange recombination spectroscopy were obtained with the diagnostic neutral beam injector, and associated diagnostic systems, that had been installed on TJ-II in previous years [1,2]. For this the C VI spectral line at 529.2 nm was selected and its Doppler line broadening and line displacement were studied using a 24 channel spectroscopic system, that covered the plasma minor radius between $0.3 \leq r/a \leq 0.8$, for a broad range of plasma conditions. In the first instance, the resultant impurity ion

temperature profiles were found to be flat in the plasma centre and to fall off towards the edge, i.e. for r/a > ~0.7. In the second instance, in a systematic study of the C^{+6} ion for plasmas with line-averaged electron densities between 4 and 9 x 10^{19} m^{-3} (with fixed injected ECRH power), it was found that the impurity temperature has a minimum about 7 x 10^{19} m^{-3} [3]. This minimum was found to coincide with a change in the plasma poloidal rotation, also measured with this active diagnostic. Moreover, it was possible to relate this change in rotation direction with a transition in the radial electric field, from totally positive at low densities to negative at higher densities, with the transition starting at the plasma edge [4]. Such a transition is predicted by neoclasssical theory and is known as the electron-to-ion root transition. Finally, in a parallel study with fixed electron density, a similar tendency was observed when varying the injected ECRH potential (400 to 500 kW). The result suggested that the collision frequency for particles in TJ-II plasmas is an important control parameter for plasma dynamics. However further studies over a broader injected power range are needed to fully clarify this point.

1. K. J. McCarthy, R. Balbín, A. López-Fraguas, A. García, J. M. Carmona, J. Sánchez, and A. A. Ivanov, Rev. Sci. Instrum. 75 3499 (2004).

2. J.M. Carmona, K.J. McCarthy, R. Balbín, S. Petrov., Rev.Sci. Instrum. 77, 10F107 (2006).

3. J.M. Carmona, K. J. McCarthy, V. Tribaldos, R. Balbín, Fusion Sci.and Technol. (in press).

4. J.M. Carmona, K. J. McCarthy, V. Tribaldos, M. Ochando, Plasma and Fusion Research (in press).

II.2.1.4. Operation of second reciprocating probe system: test active gas injection for turbulence visualization using fast cameras

A second reciprocating probe system has been installed in TJ-II (sector B). In the last TJ-II campaign this system was holding a probe head containing a set of three groups of Langmuir probes (with 3 tips each) and a gas injector that will be used for turbulence visualization using fast cameras. Systematic experiments of edge turbulence visualization with active gas injections will start during 2008.

In the first step the whole system has been tested to ensure the correct work. Langmuir probes have been used routinely to measure the edge plasma parameters. The development of the new set of Langmuir probes (sector B) and the simultaneous operation of both systems located at two different toroidal positions (sectors D and B) makes TJ-II an ideal laboratory to study the presence of zonal flows in the plasma edge region. First experiments on toroidal cross-correlations between plasma edge magnitudes have been started in TJ-II [Ref II.2.1.4].

II.2.1.5. Test of optimised poloidal limiter and development and design of a new inner limiter and related diagnostics

A mobile diagnosed limiter to be inserted in the high field side of the TJ-II region close to the helical limiter has been designed and is under costruction. The limiter will include Langmuir probes and a set of thermoresistances for calorimetry measurements. The objective is to study the inner part of the plasma edge and how effective such a limiter defines the plasma separatrix as compared to the actual poloidal limiters situated at the outer plasma region. The complex mechanical design permits to install the limiter through a lower vacuum-port and once installed, during a plasma campaign, the limiter can be removed from the plasma or inserted with a diplacing-rotating movement. The vacuum flange includes a view-port to observe the limiter with a TV-camera.

II.2.1.6. Two color interferometer: transition from He–Ne to Nd-Yag second wavelength. Development of (three) multichannel system

To avoid a thermo-optical effect on the ZnSe windows the second wavelength of the two colour interferometer has been changed from HeNe laser 0.633μm to NdYAG 1.064 μm, also a window has been removed and an internal mirror included. The replacements involved changes in the optical and phase measurement systems. The results has been as foreseen, the thermal effect has been reduced more than ten times. The design of three channel interferometer has been completed and gathering of components is in process.

II.2.1.7. Upgrading of the Thomson scattering system: data acquisition support and calibration procedure

During the TJ-II summer shutdown, it was accomplished the complete migration of the Thomson Scattering diagnostic control system and data acquisition programs installed in the old Sun SPARC V to a new workstation Sun Blade 1500 (in collaboration with the FOM Institute for Plasma Physics, the Netherlands). As a result of this CIEMAT-FOM collaboration, a new, more stable, system for data acquisition has been implemented, keeping the old Sun workstation as backup. The upgrade was completed with a suitable backup system DAT 72 USB external tape drive (work leaded by Dr. J. Herranz).

The PC AT-386 computers in charge of data communication between Sunblade 1500 and the ICCD cameras have been equipped with uninterrupted electrical power systems in order to protect them against power line fluctuations.

A new calibration system for the Thomson Scattering diagnostic has been designed in 2007. This system will integrate the different light sources needed to calibrate the

diagnostic, i.e., spectral lamps (Argon and Helium), a continuous tungsten-halogen lamp, and a linear incandescent lamp equipped with small pinholes (200 micrometres) 20 mm from each other, in a common mechanical framework. This framework should provide the degrees-of-freedom needed for precise location of the different light sources used, and, in some cases, the adjustments to align them. The calibration system is to be finished at CIEMAT's workshop by early 2008, and is planned to be installed in the summer of 2008.

II.2.2. Development of plasma diagnostics in W7X

II.2.2.1. Participation in the definition of the two colour interferometer for W7-X: noise analysis, ADC phase meter studies and interferometer architecture

On the basis of experimental results in TJ-II, a study of several sources of noise has been done: cross talk, intermodulation and filter phase delay effect. Algorithm to reduce cross talk to be used with a phase meter based on an ADC has been presented [Ref II.2.2.1]. Some rules of design to limit the error to the desired level have been obtained with the aim to be applied to W7-X design.

II.2.3. Diagnostic exploitation and development in JET

II.2.3.1. JET radiometer upgrade

In the framework of the JET-EP2 project, a proposal sent by the Asociación EURATOM-CIEMAT to upgrade the existing heterodyne radiometer was approved by EFDA in 2006. The aim of the project is to extend the upper limit of the radiometer frequency bandwidth from 139 GHz to 205 GHz. This will allow *X*-mode second harmonic measurements at the wide range of the magnetic fields (1.7 T < B_T < 4 T) used in JET (currently central T_e data in X-mode is limited to B_T < 2.5 T). This upgrade will bring an increase in the associated cut-off densities, with the cut-off density for the second harmonic X-mode being twice that of the first harmonic O-mode.

The main activity during 2007 were: a) the following up of the three contracts with the industry (under article 7) launched in 2006 for procurement of 6 new microwave downconverter and the associated amplifiers and switching circuits; and b) to finalize the procurement of a set of waveguide components (under article 6). On the original plan all contracts should have been delivered to JET before September 2007. However, on the first contract, some minor technical problems occurred during the manufacturing and assembly of the downconverters induced a delay of about 3 months. Finally, the

donwconverters were delivered at JET in December of 2007. The other two contracts were delivered at JET before summer 2007 and the contracts have been closed. Performance tests of the components and the final assembly of the complete system will be carried out in JET during the first semester of 2008.

II.2.3.2. Integration of multiple diagnostics in EFIT

II.2.3.3. Diagnostic engineering activities in JET

The activities carried out in JET were concentrated in the diagnostics field. The objective is to ensure that the integration in JET of the EP2 diagnostic enhancements is successful. This involves ensuring that the design proposed by the associations is compatible with the JET requirements as well as designing the parts and mechanical systems with an interface function between the machine and the new diagnostics.

The CIEMAT seconded engineer has been mainly involved in the following EP2 projects :

- Work for FC7/KL8 fast visible camera diagnostic: Collaboration with CIEMAT in the design of the new KL8 system with intensifier compatible optics. Integration of components and verification of available space on the honeycomb panel. Calculation of stresses on the supporting structure and on the new supports for intensifier compatible optics. Writing of the mechanical design part of the design report for the new KL8 system. Writing of a stress analysis report for the new supports. Updating of final models and detailed 2D drawings of new KL8 system with intensifier compatible optics and image intensifier for JET approval in January 2008.
- Work for JET ITER like wall project: Stress analysis of vertical conduit in octant 4 for the embedded diagnostics of the ILW (ITER like wall). Writing of analyses report.
- Work for KM6T (tangential gamma ray spectrometer) pre-project: Checking and correction of existing KX1 models created from old blueprints. Conceptual design work for the KM6T/KX1-G diagnostic. Study of different lines of sight created by the different types and positions of collimators. Analysis of elements in the torus (inner guard and poloidal limiters, antennae, coils) intersected by the different fields of view. Integration in KM6T/KX1-G CATIA model of survey data defining the correct orientation of the KX1 pipe and position of BGO bore in bunker.

II.2.4. Diagnostic development in ITER

II.2.4.1. Reflectometry. Cluster IST / CIEMAT / ENEA / CEA

- **Coordination of the diagnostic integration into the port plugs and other port structures.**

ITER Diagnostic Procurement Package #1 includes the integration of two upper port plugs, Up01 and Up14. The port plugs provide the primary vacuum boundary as well as support for the diagnostics equipment, shielding and support for the blanket shield modules. Apart from the plasma position reflectometer, a number of EU- and non-EU-supplied diagnostics are to be integrated into these two port plugs. Together with the plasma position reflectometer gaps 4 and 5, the diagnostics to be integrated in Up01 are Bolometry (EU), Divertor Impurity Monitor (JA) and Soft X-Ray Array (UnC); whereas plasma position reflectometer gap 6 and Visible-IR TV DivertorViewing (US) are to be integrated in Up14. Besides, in both port plugs the installation of a Central Tube is also foreseen.

Gap 5 waveguides and antennas have been designed taking into account the plasma shape modification as different plasma scenarios are considered: the sightlines of the two channels have been selected to be normal to the LCMS in plasma scenarios 2 and 4. The location of gap 5 antennas has been chosen to minimize possible interfaces with other components inside the port plug and to facilitate the installation and removal of the blanket shield module. To properly study the integration and interfaces of all these diagnostics components inside Up01, CATIA models are required. Interfaces between the central tube and both, bolometer mini-cameras and gap 5 antennas can be envisaged unless the central tube does not reach the BSM front wall. At the port plug flange clashes are not expected though more information is required to be conclusive. No interfaces are foreseen inside Up14.

- **Coordination of in-vessel integration of waveguides and antennas.**

The reference designs for the in-vessel waveguides and antennas have been analysed and modifications have been introduced looking for more appropriate solutions. The main modifications can be summarized as follows:

An in-vessel waveguides flange shared by the two waveguides and with a central hexaedrical pin is proposed to ensure a good alignment of the waveguides and to avoid crosstalk between emitting and receiving waveguides. Preliminary ANSYS electromechanical analysis of the waveguides flange has been done and no structural problems are foreseen. However, a complete electromechanical analysis has to be carried out taking into account the complete model of waveguides, flanges and antennas.

The in-vessel waveguides routing has been slightly modified.

Although gap 4 and 6 antennas reference design appeared to be good from the viewpoint of the thermal studies, it has had to be modified due to the need of including an electric

insulator between the antennas and the waveguides that prevents the heat to be dissipated through the waveguides and supports to the vacuum vessel. A new design for the antennas is proposed that allows the heat to be dissipated through the upper blanket modules, keeping the thermal stresses to moderate levels.

Due to space restrictions, cut-outs in blanket modules 11 & 12 and 4 & 3 are proposed to accommodate the antennas and waveguides bends of gaps 4 and 6, respectively. Similarly, cut-outs along port-plugs #01 (bottom) and #14 (top) are proposed to make room enough for the waveguides of gaps 4 and 6, respectively.

- **Performance analysis in the area of antenna-plasma interaction**

The main activities on the performance analysis have been carried out by CEA and ENEA taking into account the designs of gap 5 as well as gap 4 and 6 antennas.

II.2.4.2. Visible-IR wide angle viewing system. Cluster CEA / CIEMAT / ENEA / HAS / IST

The work done by CIEMAT in the frame of the EFDA task "TW6-TPDS-DIADES Procurement Package 11". Ciemat contributions on this task include diagnostic optical design supervising and assessing proposed models for VIS-IR imaging, as well as to propose new solutions to assess. The initial optical design file has been rebuilt by taking into account the paraxial Zemax file and the cad file. The study of the optical positions in the available room gave rise to redefine the dimensions and integration of the Eq. Vis/IR WAVS in the port plug. Major changes in the number of relay lens systems and telescope design have taken place. In addition, the clarification of critical issues (like ELMs impact on divertor / first wall components) will require systems with a time resolution in the range of 10 - 20 microseconds. Fast cameras (CMOS technology) can run in the range of 100 kHz. The combined fast / slow visible monitors will greatly improve the performance of ITER visible/IR wide-angle viewing system.

II.2.4.3. Thomson Scattering. Cluster UKAEA / CIEMAT / FZJ / FOM / ENEA / HAS / IST

In 2007, a cluster of European Associations has been created to develop a Thomson Scattering system based on the LIDAR principle. This system should be able to measure plasma temperature and density profiles in the ITER Tokamak, with moderate spatial resolution (≈ 6 cm) and up to 100 Hz. The Cluster is leaded by the English Association (UKAEA), with contributions from other partners like FZJ (Germany), FOM (The

Netherlands), ENEA (Italy), CIEMAT (Spain), HAS (Hungary) or IST (Portugal) among others.

CIEMAT has contributed in 2007 with a conceptual engineering design to support and keep aligned mirrors # 3 and 4 in the so called "port plug interspace zone" of equatorial port # 10 where the LIDAR diagnostic is to be located. The design has taken into account issues related with suitable structural materials, clamping systems to the Port-Plug flange, remote access to the structure, mechanical and thermal computations (CATIA and ANSYS) to assess the stability of the proposed design and ray tracing and kinematical calculations to define the movements needed in case of re-alignment of the mirrors is required. A proposal and a conceptual design are made for the structural framework and mechanisms able to perform these tasks, based on proven commercial technologies like multi-axis piezoelectric motors or pneumatic gear-box mechanisms. This work has been carried out in close collaboration with the engineering group of TJ-II.

The police of buying spare parts for the system, as well as the maintenance visits for the ruby laser have been continued.

II.2.4.4. Magnetic sensors. Cluster CEA /CRPP /CIEMAT / IPP-CR / TEKES

Up to date, conventional coil sensors measuring dB/dt in combination with time integrators have been used in many TOKAMAK devices to obtain the magnetic field with sufficient stability and accuracy.

In ITER nuclear environment, this technique is expected to suffer from accumulated error due to radiation induced electromotive force in the coil and cabling being integrated in time. The result is that the low frequency spectrum of magnetic field will not be well determined in the pseudo steady state (dB/dt ≈ 0) phase of operation. To improve the low frequency spectrum of the measurements, sensors capable of measuring directly the magnetic field are being sought after. Currently, there is not a magnetometer that complies with all the specifications for ITER.

The purpose of this project (in progress since 2005 in the framework of the EFDA technology programme) is to advance towards the development of a magnetometer capable of measuring poloidal components of the magnetic field in the range of [0-2 Tesla] with a precision of 5mT, able to withstand high neutron doses (10^{22} n/m^2) in a high temperature environment (200 Celsius) with a thermal sensitivity less than 0.25mT/C. Within this context, the feasibility of three different magneto-resistive technologies have been studied: perovskite manganites of general formula La(1-x) AxMnO3 with A = Ca, Sr, (these are also known as LCMO when the alkaline element is calcium, and LSMO when the alkaline element is strontium), double perovskites Sr2-x

LaxFeMoO6 (SFMO) and magnetite Fe3O4. Result can be found in the TW5-TPDS-DIADEV-2c Task Report.

II.3. Plasma fuelling

II.3.1. Plasma fuelling in TJ-II

II.3.1.1. Distribution of the source and fuelling efficiency in normal and divertor configuration

Several locations of gas injection were tried in NBI heated TJ-II plasmas under Li wall conditioning. Since CX between the incoming beam and plasma protons is supposed to dominate the absorption of the neutral beam by the plasma, puffing of the gas in the path of the beam should have a net effect on the CX losses at the beam entrance, thus possibly modifying the coupling of the beam. Alternatively, NBI was injected in He target plasmas to check for a different beam-plasma coupling. Although no significant difference was seen between H_2 injection at the beam port and the farther location used, no conclusion about absorption by He target plasmas can yet be drawn [Li_2].

II.4. Real time measurement and control

II.4.1. Techniques for data storage and retrieval (ITER)

II.4.1.1. Evaluation of data compression techniques for ITER

Applications of the 'lossless cyclic delta' compression techniques [ref COMP_1] to images have been analysed. In particular, we studied the images of the JET high speed visible camera. These techniques were applied in two ways. On the one hand, the movies were compressed frame by frame with a bit allocation method valid for real-time applications. On the other hand, the technique was used as a delayed method and, therefore, the data pre-processing allows achieving much better compression factors.

To assess the compaction rates, the compression factor was defined as:

$$f = \left(1 - \frac{compressed\ storage}{uncompressed\ storage}\right) * 100$$

The factor f is the amount of storage that is saved. For example, a compression factor of 90% means that 10 bytes in compressed form have the same information content than 100 bytes before compression.

The average compression factor for real-time bit allocation methods is about 87% and the maximum compression rate of a movie was 94%. The use of the techniques as delayed methods is presently under development. In specific movies, the compression factor was above 99%. Currently, an article to describe these methods is in preparation.

II.4.2. Data mining techniques (pattern recognition)

II.4.2.1. Implementation of pattern recognition algorithms for TJ-II and JET

The activity in this field has been very intense and productive during 2007. It was focused on the development of optimised systems for data retrieval in massive databases. Instead of using a signal name and a shot number as input parameters to access data, a new model was proposed to look for data according to scientific and technical criteria. This model establishes the use of signal patterns as input to retrieve the shot numbers and the time instants where similar patterns appear within the database.

The main ideas about this were discussed in depth in both a JET seminar [ref PR_1] and an oral contribution to the 6th IAEA Technical meeting on Control, Data Acquisition and Remote Participation for Fusion Research [ref PR_2].

All research on intelligent data access and signal processing was carried out in collaboration with European Institutions, Spanish Universities and an Indian Laboratory. Different results were presented in several Conferences: 15th IEEE NPSS Real Time Conference 2007 (http://computing.fnal.gov/cd/rt07), 6th IAEA Technical meeting on Control, Data Acquisition and Remote Participation for Fusion Research (http://tm2007.nifs.ac.jp), International Workshop on Burning Plasma Diagnostics (http://www.ispp.it) and ICALEPCS 2007 (http://accelconf.web.cern.ch/AccelConf/ica07). It should be emphasised that it was held an invited session in the 2007 IEEE International Symposium on Intelligent Signal Processing (http://www.wisp2007.com). The session entitled "Information and knowledge extraction in massive databases" was co-organised between J. Vega (Asociación EURATOM/CIEMAT) and A. Murari (Associazione EURATOM/ENEA and JET Task Force D Leader). Most of the contributions have been published as refereed journal papers: ref PR_3, ref PR_4, ref PR_5, ref PR_6, ref PR_7, ref PR_8, ref PR_9 and ref PR_10. The rest of contributions appeared in the

respective proceedings of the Conferences: ref PR 11, ref PR 12, ref PR 13 and ref PR 14. An additional publication related to data mining was ref PR 15.

II.4.3. Development of TJ-II operation scenarios for dynamic control of magnetic configuration

II.4.3.1. Operation with dynamic variation in the magnetic fields

The TJ-II Control Group has developed new mode of operation, called mode C, which allows the magnetic configuration to be varied dynamically during the discharge. That means the currents do not reach a flat-top but ramp, up or down, during the pulses. They are allowed to vary in a small range, between a 5% and a 20% of the maximum values, practically between 0.2 and 1 kA. The basic principles of these experiments are.

- The change of the vertical field during an experiment intends to produce the dynamic control of the magnetic well.
- The change of the current in the helical coil during an experiment intends to produce the dynamic control of low order rational location.

Throughout the year 2007 some of the works for the development of this operation mode have been completed.

In this new set-up, coil current profiles are generated and controlled with millisecond timescales by the fast control system, located on the TJ-II control room, 200 meters far away from the power rectifiers.

In order to achieve this, new hardware and software features have been added to the TJ-II control system. The VMEbus slave, located on the electric building, is controlled by the master located on the TJ-II control room through a fibre optic link. The fast control system generates a digital signal reference that is converted to an analogical signal to be applied to the rectifiers. This sequence takes place during the interrupt response time at a rate of 1 millisecond and it extends throughout the whole pulse. The measurement of the response times and the delay of the signals between buildings will allow the complete development of the new operation mode during 2008. The development will include the design of the real-time protections during the pulse, and graphical user interfaces.

II.5. Mechanical engineering

II.5.1. Mechanical engineering

II.5.1.1. ITER Diagnostic Equatorial Port Plug Engineering and Integration

The tasks carried out in this area correspond to the EFDA Technology Work programme 2006 (EFDA Reference: TW6-TPDS-DIASUP)

Engineering activities related to the ITER port plug diagnostic integration are aimed to provide analyses not only for engineering design and thermal-mechanical calculations, but also for the development of standards and guidelines corresponding to the design engineering and integration. Within this framework, EFDA has launched several activities. Amongst these there is one performed by Ciemat under EFDA ref. TW6-TPDS-DIASUP/1430 task agreement, including the following supplies:

- Supply 1. Cooling circuit design for ITER reference equatorial diagnostic port plug.
- Supply 2. Study of a helping cantilever system for the assembly/disassembly of the ITER upper port plugs. Kinematical study of this process.
- Supply 3. Mechanical design of the Diagnostic Equatorial Port Plug BSM Attachment.

The objective of the supply 1 is to provide thermo-hydraulic calculations in order to optimise the reference equatorial port plug cooling circuit. It includes the cooling requirements of the Diagnostic Shielding Modules (DSM) defined by the studies carried out by other associations, mainly by UKAEA and CEA, as well as the BSM compatible with the water inlet at the lower part and the outlet at the upper part of the port plug. Supply 2 studies a helping cantilever system for the assembly/disassembly of the upper port plugs. This implies the integration of the wheel system into the plug structure, as well as the kinematical study of the plug insertion, the implementation of rails into the cask and into the port, the maintenance sequence and the functional description of the plug mover and of the handling tools.

Supply 3 is a contract extension of the main one, focused on the final design of the BSM attachment, taking into consideration all the previous designs. It comprises not only the conceptual design but also the structural and thermal analysis, the hydraulic evaluation of the coolant connection, as well as the assembly procedure definition considering remote handling requirements.

II.5.1.2. Ultrasonic Examination of the Divertor mock-ups manufactured with calibrated defects

The task in progress is focused on identifying a suitable non-destructive testing (NDT) procedure for the final acceptance of the Plasma Facing Components (PFC`s), in sight of the procurement of the ITER Divertor. The examination of the heat sink to armour joints by NDT is a crucial issue since it will be used to assess the quality of these PFC´s before

acceptance. Ultrasonic (US) tests along with Infrared thermography (IR) are those NDT foreseen to contribute to this task (EFDA Task TW5-TVD-FABCON).

Different sets of mock-ups containing calibrated defects have been fabricated with the aim of setting up experimental basis for the development of appropriate NDT procedure and subsequent definition of final acceptance criteria. The defects present in the mock-ups, are of different size and are placed in different locations. These samples have been fabricated by European industries using different technologies.

Ciemat was assigned to carry out the US inspections on the samples subcontracting for this job a specialized company, Tecnatom. During 2007, US inspections on several sets of samples have been performed.

The samples are high heat flux (HHF) tested in order to check the thermal behaviour of the joints and therefore the US examinations on each set have to be performed twice: before and after the HHF testing.

Regarding the US inspection before the HHF tests all the sets of samples have been examined and the results show the capability of the US method proposed by Tecnatom to detect, locate in position, and measure the extension of all the implanted defects in the different joints. The US examinations after the HHF tests carried out on one set of samples allowed the detection of defects and the size changes experienced as well as the detection of changes in the materials, in particular on copper and copper alloy microstructures.

The finalisation of the inspections of the mock-ups after HHF tests is expected to occur by mid 2008.

III. DEVELOPMENT OF CONCEPT IMPROVEMENTS AND ADVANCES IN FUNDAMENTAL UNDERSTANDING OF FUSION PLASMAS

III.1. Optimization of operational regimes for improved concepts

III.1.1. Influence of magnetic configuration in the development of core e-Internal Transport Barriers

III.1.1.1. The role of low order rational surfaces on confinement

Previous studies of integral confinement properties of the TJ-II - e.g. energy confinement time - have been revisited to develop local transport analysis based on power and particle balance methods [Ref III.1.1.1a]. Groups of steady state discharges belonging to scans of line density, edge rotational transform and ECH power have been analyzed to obtain effective transport coefficients. It is found that the electron heat diffusivity decreases with increasing plasma density especially in the outer half (in average radius) of the plasma. The rotational transform scan, on the other hand, suggests slightly better confinement but without a well defined radial region. The poorer accuracy of the iota exponent in the TJ-II scaling may be due to the fact that the detailed magnetic structure affects locally transport coefficients, namely through the presence of low order rational values of the rotational transform (magnetic resonances, in short), which are not ordered following, for example, the value of the edge iota. Finally, the heating power scan on these plasmas deteriorates transport through increasing thermal diffusivity in most of the plasma [Ref III.1.1.1b].

The effect of the magnetic configuration on transport, with particular emphasis on the role of magnetic resonances has been studied, in a first stage, on ECH plasmas of the TJ-II device. The plasmas have been analyzed and compared among them in conditions where the radial location of the magnetic resonances could be confidently inferred, e.g., in steady state low beta plasmas or in discharges with slowly varying poloidal magnetic fields due to ohmic induction. The studies reveal that such resonances are coincident with smaller effective electron thermal diffusivity in the typical low magnetic shear conditions of TJ-II plasmas. These works have promoted an international colaboration aimed at clarifying the robustness of stellarator plasmas versus magnetic resonances in terms of rotational transform and magnetic shear [Ref III.1.1.1c].

III.1.2. International stellarator confinement and profile data base and neoclassical transport

III.1.2.1. Participation in the on-going activities of the International Stellarator Confinement and Profile Data Bases during 2007

The Ciemat team has participated very actively in the above-mentioned activities through the participation in the Coordinated Working Group Meetings (CWGM) held along the year and the preparation of collaborative international papers presented in the 17th

International Stellarator/Heliotron Workshop (ISHW) that took place in October in Toki, Japan.

The second CWGM was organised by IPP-Greifswald in June. Three presentations were made by Ciemat members, dealing on:

- the rotational transform dependence of the confinement time in TJ-II [CWGM2_1]
- the effect of the low order rational on the effective diffusivity of the TJ-II ECH plasmas [CWGM2_2]
- the role of turbulence on momentum transport in stellarators and tokamaks [CWGM2_3]

The third CWGM was organised by NIFS at Toki, Japan, right after the ISHW in October. Two contributions from Ciemat were presented there:

- a proposal for further collaborative studies of the confinement dependence of the rotational transform and magnetic shear in stellarators, based on local studies and including the data from high shear devices (LHD, CHS) [CWGM3_1]
- a proposal for common collaborative momentum transport studies based on an experimentalist approach [CWGM3_2].

The results of the international collaboration on stellarators developed during the year were presented in several contributions to the 17th ISHW:

- an oral paper on the effect of the rotational transform and shear in the confienement of stellarators [ISHW_1]
- a poster contribution on the status of the stellarator /heliotron profile database [ISHW_2]
- an oral paper on the comparison of impurity transport in different stellarator magnetic configurations [ISHW_3]

III.1.3. Full lithium coating in TJ-II

III.1.3.1. Optimization of Lithium deposition set up by evaporation and Ne glow discharge in TJ-II

The production of homogeneous coatings of Li over the inner walls of TJ-II is challenging as a discrete set of ovens (4) was used for the deposition. Two alternative methods were tried for the task: Using a Ne glow discharge during the effusion of Li from the ovens, in order to provide some toroidal transport by the effect of plasma ionization and using a

background pressure of He during the deposition in order to spread the atomic beams created by the ovens by elastic collisions. Due to the large pressure required for running the GD in Ne, back-diffusion of the injected Li atoms led to localized deposition near the ovens, thus preventing the formation of a homogeneous coating across the full inner walls. The second method was more efficient if pressures in the order of 10^{-5} mbar of background gas were used. For these conditions the mean free path of Li is similar to the distance from the beam to the walls. Higher pressures again lead to back-diffusion of the Li atoms and localization of the coating near the ovens. In spite of these tests, it was found that a gradual improvement in coating dispersal was produced simply by the effect of plasma operation through sputtering of the initially covered areas and vacuum evaporation seems to be the best method for long-term operation [Li 1].

III.1.3.2. First operation of TJ-II with full lithiumization

The TJ-II stellarator has been operated under lithium coated first wall conditions for the first time. Particularly conspicuous has been the change in recycling associated to the new, low recycling walls, but also impurity content, with direct impact on radiative losses and total energy confinement is modified by the type of coating, as expected in a first-wall dominated plasma-wall interaction device. Lithium coating, tested for the first time in a stellarator, has proven a very effective method for particle control in TJ-II. Changes in the shot by shot fuelling characteristics as well as in the total particle inventory compatible with good density control have been recorded after the Li deposition. Thus, a factor of 4 increase in the fuelling rate at constant density compared with the B-coated walls was recorded, and even a higher value was estimated for the allowed H inventory in the puffing-controlled ECRH discharges. These changes have led to the production of much more reproducible plasmas. They were also mirrored in the radiation and edge radial profiles, with increased electron temperatures in some scenarios. This led to enhanced interaction with the poloidal graphite limiters, which had a deleterious effect on plasma performance. The lower instantaneous recycling also worked for the density control under NBI heating scenarios. Record values of plasma energy content were measured at densities up to $4.5.10^{13}$ cm^{-3} under Li-coated wall conditions. A replacement of edge main impurity, now sputtered Li, seems to be also involved in the different radial profiles of the parameters affecting the local power balance [Li 1].

III.2. Understanding of plasmas characteristics for improved concepts

III.2.1. Influence of electric fields on transport and MHD stability

III.2.1.1. Comparative studies (HIBP, probes, reflectometer, MHD activity) in ECRH and NBI plasmas (TJ-II): influence of magnetic configuration, heating power and plasma density

Magnetic fluctuations, both, ECRH heated pressure driven modes and NBI Alfvén Eigenmodes, have been studied during the 2007 TJ-II experimental campaign. These MHD events are detected by several diagnostics: Mirnov coils, microwave reflectometry and edge probes, enabling their temporal and spatial characterization [Ref III.2.1.1a].

In TJ-II ECH plasmas, a perpendicular velocity shear layer develops spontaneously at the plasma edge, above a certain line-averaged density. The transition for the shear layer formation has been characterized using Langmuir probes, Ultra Fast Speed cameras and microwave reflectometry. A parametric dependence of the critical density has been obtained studying plasmas confined in different magnetic configurations and heated with different ECH power levels. The studied data set shows positive exponential dependence on heating power and negative one on plasma radius, while the dependence on rotational transform has low statistical meaning. Besides, analysis of local plasma parameters points to plasma collisionality as the parameter that controls the inversion of the perpendicular rotation velocity of the turbulence [Ref III.2.1.1b].

III.2.1.2. Influence of electric fields on supra-thermal electrons (TJ-II): role of biasing

The spatial distribution of suprathermal electron losses have been monitored through their bremsstrahlung emission at the vessel walls [Ref III.2.1.2]. As expected, it has been found that some of the plasma parameters affect such losses and electron impacts are seen "to move" slightly as a function of heating conditions, electron density or plasma contamination. At the same time, a tight correlation between the electron cyclotron emission from the central part of the plasma and the flux of soft x-ray photons generated at the limiter surface is always seen, revealing that the monitored electrons were trapped in the plasma core.

In recent edge "negative biasing" experiments, it has been found that the signal of suprathermal losses detected at the poloidal limiter is reduced and, frequently, all of the ECE signals. Nevertheless, when a low order natural resonance is close to the edge, the outer ECE channels have an unexpected response (see the level increase of ECE(0.7) in Fig. III.2.1.2-a).

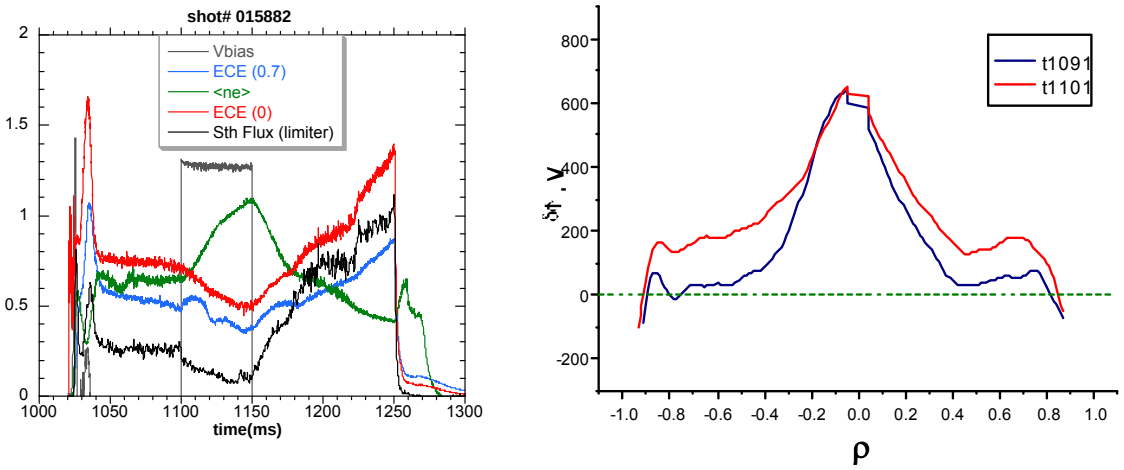

Figure III.2.1.2-a) Effect of biasing on the suprathermal electron losses to the limiter (Sth Flux signal), the averaged electron density and two ECE channels. b) radial profiles of plasma potential obtained with the HIBP diagnostic: blue- bias OFF; red- bias ON.

The effect of biasing on the plasma potential as deduced from HIBP data is more intense in the peripheral region (see Fig. III.2.1.2-b). The plasma core potential seems to remain unchanged in the studied configurations. For the apparent decoupling of the centre and the gradient region, we point two possibilities: the presence of the rational surface 3/2 or the decay length of the electric field induced shear. Nevertheless, a mix of both can be the answer. Up to now, no differences were found in the potential profile for the few explored configurations.

The purpose for next campaign is trying to obtain a more systematic correlation between losses, potential profiles and bulk confinement as a function of magnetic configuration.

III.2.2. Momentum transport

III.2.2.1. Parallel dynamics: Influence on electric electric field on Reynolds stress driven flux $<v_{||}\, v_\theta>$component

See section I.1.1.1

III.2.2.2. Relaxation of flows and radial electric fields in plasma regime

The importance of the ExB shear in flows as a stabilizing mechanism to control plasma fluctuations in magnetically confined plasmas has been widely established. Clarifying the driving/damping mechanisms of sheared flow remains a key issue for the development of fusion.

It has been previously shown that the development of the sheared flows at the plasma edge of the TJ-II requires a critical value of the plasma density or density gradient thet depends on the plasma conditions. Sheared flows have been also developed in TJ-II using an electrode that externally imposed a radial electric field at the plasma edge. The modifications in the plasma properties induced by electrode biasing depend on the plasma density, as the edge parameters and global plasma confinement depend in its turn strongly on it. The response of the plasma to bias is, therefore, different at densities below and above the threshold value to trigger the spontaneous development of ExB sheared flows. Two different time scales arise in the relaxation of externally induced electric fields in TJ-II: a slow time scale, in the range of the particle confinement time (tens of milliseconds) that evolves with plasma density, and a fast time scale in the range of few turbulence correlation times (10 – 100 μs).

- **Influence of plasma density and plasma position in the decay time of radial electric fields**

The fast time evolution of floating potential signals, when biasing is switched off, can be fitted to an exponential function. Results suggest an increase in decay times above the critical value of the control parameter (i.e. once edge perpendicular sheared flows are fully developed) (Fig. III.2.2a),[ref III.2.2.2a].

The emergence of the plasma edge sheared flow as a function of plasma density can be explained using a simple second order phase transition model. This simple model reproduces many of the features of the TJ-II experimental data and captures the qualitative features of the transition near the critical point (Fig. II.2.2b),[ref III.2.2.2b].

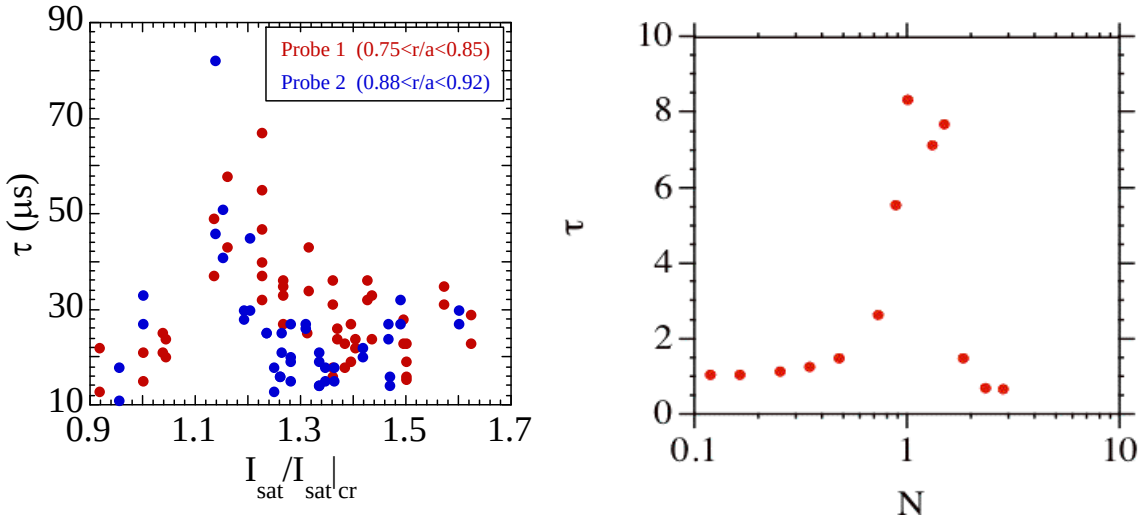

Fig. III.2.2.2 a) Relaxation time measured at the TJ-II plasma edge in two different toroidal sections, as a function of normalized ion saturation current measured after switch off the biasing. b) Decay time obtained by the model as a function of the local average ion saturation current normalized at the corresponding critical point (development of shear flow).

- **Comparative studies in the TJ-II stellarator and CASTOR tokamak and a critical test for anomalous and neoclassical damping mechanisms**

Similar electrode bias response has been reported in CASTOR tokamak: The characteristic relaxation time has been determined from the time evolution of floating potential signals with the same fitting function than in TJ-II being the obtained results in the range 10 - 20 μs. The similarity between decay time scales measured in TJ-II and CASTOR, being devices with different values of ripple (and consequently neoclassical viscosity), and the fact that measured fast decay times are in the range of few turbulence correlation times, suggests the important effect of anomalous (turbulent) mechanisms in the damping rate of sheared flows in the plasma boundary of fusion devices [ref III.2.2.2c].

III.2.3. Spectroscopy based studies

III.2.3.1. Comparative study of impurity and proton poloidal rotation in the TJ-II stellarator

We reported the poloidal rotation behavior in a previous work [ref III.2.3.1a]. We studied the rotation of an internal impurity (C^{4+}) in plasmas with different densities and we compared the deduced radial electric field with neoclassical theory. Since a strong discussion has taken place for the last decades on the comparison of intrinsic impurities and main ions rotation in tokamaks, this work wants to contribute to it looking at this interesting problem in an alternative configuration.

The poloidal rotation measurements have been carried out with an upgrade version of the system previously described [ref III.2.3.1b]. In order to cope with the lowering of spectral signal level produced by an efficient boronization, the fiber bundle length was shortened from 10 to 3 m. and 1 mm, instead of 200 mm core diameter fibers were used. In addition, a larger illuminated charge-coupled device (CCD) detector substituted to the previous front-illuminated one.

We choose a density scan as the operational frame to carry out this comparison, due to the robust behavior of impurity rotation for this scan. First results suggest that proton rotation deduced from the analysis of the H_a emission does not exhibit the change of poloidal rotation direction that was observed for C^{4+}, or at least it does not take place at the same density as impurities. We investigate the reasons and the role played by different effects: 1) diagnostic assumptions; 2) the distinct effects that neutrals could play on both type of ions and 3) if other mechanisms for driven rotation, apart from

radial electric field, could explain such a behavior (a more detailed report on this work can be found in [ref III.2.3.1c].

[1] B. Zurro, A. Baciero, V. Tribaldos et al., Fusion Sci. Technol. 50, 419 (2006).

[2] A. Baciero, B. Zurro et al., Rev. Sci. Instrum. 72, 971 (2001).

III.2.3.2. Suprathermal ion tails in ECR heated TJ-II plasmas

- **The role of a fast ion component on the heating of the plasma bulk**

Ion temperatures have been measured in the TJ-II stellarator using passive emission spectroscopy in parallel and perpendicular directions. A high energy component was observed from the tails of the Halpha line emission in both directions, suggesting a non-negligible population of suprathermal ions. The role of this fast ion energy component, which has been observed in both stellarator and tokamak plasmas when heated by electron cyclotron resonance heating in the additional heating of the plasma bulk is investigated by means of a simple model. The origin of such a fast component is discussed in terms of different mechanisms (a more detailed report of this work can be found in ref III.2.3.2a.

- **Study of suprathermal ion losses in the TJ-II Stellarator measured by means of a luminescence probe**

This work is focused on the study of the suprathermal population of ions associated to the electron cyclotron heating (ECRH) in the TJ-II device, whose detection is performed by means of a luminescent probe. Its behavior in TJ-II plasmas with the heating power and deposition position as well as with magnetic configuration is reported. The unfolding of its energy distribution for two selected cases has been presented (a more detailed report on this work can be found in ref III.2.3.2b.

- **Local emission profiles from impurity ions and visible bremsstrahlung in TJ-II Stellarator**

The goal of this work was to determine the local structure of impurity ion and visible bremsstrahlung emission. Local emission profiles can be employed to quantify spatial asymmetries, investigate plasma-NBI beam interaction, back up rotation measurements with poorer spatial resolution and derive Z_{eff} profiles.

A ½ spectrometer with a fast hexagonal rotating mirror collects the chord-integrated emission profile every 8 ms. Light intensity is measured, within the narrow range selected by the spectrometer, with a photomultiplier connected to a high-speed current amplifier.

The study was focused on visible bremsstrahlung, carbon and helium line emissions. Local profiles were calculated from chord-integrated data by using Fisher's tomographic inversion method. We also consider that local profiles were asymmetric. Comparisons between raw data and simulations of chord-integrated profiles were performed to check inversion method.

We investigated the rise of the central emission of non-intrinsic central ion lines during NBI heating phase and its relation with charge-exchange recombination between highly ionized ions and fast neutrals of the heating beam or its halo. We also studied emission profile asymmetries and its evolution along a TJ-II plasma pulse.

Finally, we estimated Z_{eff} profiles from visible bremsstrahlung local emission and we observed the variation of Z_{eff} with electron density for several TJ-II plasma pulses (a more detailed report on this work can be found in ref III.2.3.2c.

III.3. Other experimental activities

III.3.1. Remote participation

III.3.1.1. Development of a secure collaborative environment among CIEMAT/CEA/IST

Security is an essential element in remote participation to develop protected collaborative environments. Efforts during 2007 were centred on creating a common security infrastructure for EFDA sites by means of federated resources. To this end, two different distributed authentication and authorization systems (PAPI and Shibboleth) were analysed. A PAPI federation was put into operation among six partners: CIEMAT, CEA, CSU Garching, IST, JET and KFKI/HAS. It was presented as an oral contribution to the 6th IAEA Technical meeting on Control, Data Acquisition and Remote Participation for Fusion Research [ref FED_1] and a detailed description has been published [ref FED_2].

Two additional contributions regarding security and remote participation were sent to the above Conference. On the one hand, an adaptation of PAPI to Shibboleth was presented [ref FED_3] and, on the other hand, a summary of current tools for the EFDA remote participation collaboration was described [ref FED_4].

III.4. Theory and modelling

III.4.1. Transport analysis and modelling

III.4.1.1. Transport modelling in TJ-II

We have developed a model to study transport in LHD and TJ-II stellarators, based on previous transport analysis in such devices. This model includes a neoclassical franction as well as an anomalous and was able to predict the appearance of electron internal transport barriers in ECH plasmas [ref III.4.1.1a].

Our work has contributed also to establish the general properties of the regime called CERC (Core Electron Root Confinement) in stellartors. Particularly, beyond the high power density effect, we have introduced the effect of low order rationals in triggering the CERC [ref III.4.1.1b]. Morevover, the role of rational surfaces on heat transport has been explored extensively in TJ-II, showing that the presence of rationals is able to modulate the transport showing an improvement of the confinement in a wide range of plasma minor radius [ref III.1.1.1b].

III.4.1.2. Internal transport barrier studies at JET

Continued development of experimental proposal to study a diamagnetic ITB trigger at JET: typically ITB formation corresponds to both the formation of a local diamagnetic region in the plasma, and (often) local shear reversal. It is possible in JET to create a scenario, with off-axis LHCD, in which local diamagnetism is produced before local shear reversal. An experiment has been designed with Task Forces T and S2 to test plasma diamagnetism as an ITB precondition. It has been combined with experiment S2-2.3.2 for the JET 2008 campaign [ref III.4.1.2].

III.4.2. Modelling of kinetic effects on transport

III.4.2.1. Kinetic Simulation of Heating and Collisional Transport in a 3D Tokamak

The mutual influence of microwave heating and plasma transport has been observed experimentally in several fusion devices, but there is a lack of numerical results. We have adapted the ISDEP code (Integrator of Stochastic Differential Equations for Plasmas) to include quasi linear wave-particle interaction and the geometry and profiles of a virtual tokamak with ripple. In spite of ISDEP originally solves linear kinetic equations, we have introduced nonlinear terms in order to study the heating in a more accurate way. This is

done modifying the background temperature, increasing it according to the test particles profiles [ref III.4.2.1a].

We have simulated the device with and without heating and studied the differences in the behavior of the system. We have measured several transport quantities: confinement times, energy and particle fluxes, poloidal and toroidal velocities, temperature and velocity distribution function. The main results are the increment of the outward fluxes and modifications of the distribution function [ref III.4.2.1b].

III.4.3. Statistical description of transport processes in fusion plasmas based on the use of probability distributions for individual particle motion

III.4.3.1. One-dimensional model for the emergence of the plasma edge shear flow layer with momentum conserving Reynolds stress

We have formulated a one-dimensional version of the second-order transition model based on the sheared flow amplification by Reynolds stress and turbulence supression by shearing. We have included a form of the Reynolds stress which explicitly conserves momentum. After performing a linear stability analysis of the critical point, we have studied the dynamics of weakly unstable states, which is determined by a reduced equation for the shear flow. In the case in which the damping term is diffusive, the stationary solutions of the reduced equation are those of the Ginzburg-Landau equation [CalCar_PoP2007].

III.4.3.2. Fractional generalization of Fick's law

In the study of transport in inhomogeneous systems it is common to construct transport equations using Fick's law. This is justified if the following two conditions are met. First, finite characteristic length and time scales associated to the dominant transport process must exist. Secondly, the microscopic transport mechanism must satisfy a specific microscopic symmetry which we call global reversibility. However, many complex systems have been shown to lack finite characteristic scales. We have derived a generalization of the inhomogeneous Fick law which does not require the existence of characteristic scales while still satisfies global reversibility. We call it fractional Fick's law because it is formulated in terms of fractional differential operators [CalSanCarMil_PRL2007].

III.4.3.3. Models of fractional transport in periodic systems

We have formulated the Continuous Time Random Walk in one-dimensional periodic systems and rigorously performed the hydrodynamic limit when Lévy distributions are involved. The hydrodynamic equation is written in terms of a periodic version of the Riemann-Liouville fractional differential operators. In some special cases (which may be of interest for transport in fusion plasmas along the poloidal or toroidal directions) we are able to give analytical solutions [CalCarSanMil_JPhysA2007].

III.4.4. Theoretical EBW studies and heating studies

III.4.4.1. EBW studies

The investigation of the properties of electron Bernstein waves (EBW) in TJ-II together with the development of a suitable dispersion relation for the study of such waves in any magnetic configuration has been continued. We have introduced the relativistic effects on the EBW dispersion relation in order to explore the modification of wave properties due to such effects in TJ-II and in other magnetic configurations. Some relevant modifications of the wave trajectories and absorption coefficient that introduces non-negligible changes in the power deposition profile have been found [castejon_FST07].

III.4.4.2. The dispersion Relation

The activities on developing the fully relativistic dielectric tensor have continued. In the frame of these activities, a small mistake has been found in a former publication [castejon_pop07], and the study of the dispersion relation in complex frequencies is under development.

III.4.5. Eirene code studies

Calculations of the comprehensive Monte-Carlo code Eirene, as adapted to the geometry and requirements of the TJ-II device, have been coupled to a transport code in order to study electron transport coefficient profiles in steady state discharges with different average densities [ref III.1.1.1a]. Only ECH plasmas have been studied, which narrows considerably the line density range. However, two particle transport regimes are found depending on a threshold that is linked to the emission of X-rays above 20 keV. For densities below the threshold, energy and particle confinement times are comparable and thus the latter are considered to be too small. Above the threshold, particle confinement times are some four or five times larger than energy confinement times. Comparison

with studies about the dependence of the electrostatic potential on the line density indicate that the improved confinement above the threshold happens when the radial electric field is no longer positive all over the plasma. The X-ray signals, in turn, point to fast particles generated by the ECH as responsible for the positive electric field and poor confinement found below the threshold.

III.4.6. Gyro-kinetic codes

Collaboration with the Max Plank IPP at Greifswald has been established for the development of a global non-linear gyro-kinetic code suitable for being applied to tri-dimensional stellarator geometry, in particular to W7-X and TJ-II relevant configurations. The TORB code has been installed in the Linux cluster and the ALTIX servers at CIEMAT. The performance of the code using different libraries for sparse matrix (WSMP, SPOOLES and the TORB inner routines) has been studied. Tests for studying the dependence of the energy conservation (numerical noise) on different input parameters of the code (integration time step, number of markers, number of Fourier modes/spatial grid size, loading optimization and Fourier mode filtering) have been carried out.

An extension of the optimization loading, previously done in two dimensions of the phase space, for allowing optimized loading in tri-dimensional cases is under development.

Collaboration has also been initiated with the Barcelona Supercomputing Center for the development/exploitation of the global gyro-kinetic code. TORB has also been installed in the Marenostrum supercomputing cluster where performance tests have been initiated.

III.4.7. Grid and Volunteer computing

Grid computing offers a large amount of research resources, provided that the structure of the applications is suitable to be adapted to this architecture. There are several fusion applications suitable to run in this kind of infrastructure, i. e., those with low level of parallelism, especially Montecarlo-based codes and processes that are based on running the same job many times with different input parameters. Several fusion applications have been selected and ported to the grid, giving scientific relevant results [castejon_EGEE07].

Many of the applications that are suited to run in the grid can be ported to the volunteer computing infrastructures. The use of BOINC (Berkeley Open Infrastructure for Network Computing) allows one to deploy the application in a distributed computer integrated by

the personal computers given by citizens. The first experience of deployment of an application in a supercomputer based on the spare CPU time of the citizens have been done in the city of Zaragoza (Spain), in the frame of the collaboration of BIFI (http://bifi.unizar.es/) and CIEMAT. The result of this experiment is the availability of an average of 800 CPUs during 45 days. This infrastructure was used to obtain relevant results for fusion research [castejon_sn110].

III.5. Stellarator engineering

III.5.1. Engineering support for Wendelstein 7-X project

One engineer from CIEMAT has been seconded to the W7X team in Greifswald and has been active in the following areas:

III.5.1.1. Central Support Elements (CSE).

Connection Inconel bolts and fastening elements between the coils (planar and non-planar coils) and the Central Support Structure (CSS) or central ring. Procurement monitoring and project management of two main contractors: P&S (Switzerland) for the Superbolts (tensioners) and Tempelmann (Germany) for the rest of Inconel elements (stud bolts, bolts, nuts, washers, pressure plates). Supervision of the Stainless Steel 1.4429 elements manufactured by IPP Techniche Dienste workshop.

Non-Conformities and Change Notes management.

III.5.1.2. Non Planar Coils testing frame and other structures for the new testing facility at FZK Forschungszentrum Karlsruhe (TOSKA).

Conceptual design and structural assessment of the testing frame and base plate. Detail manufacturing drawings. Manufacturing and load test technical specification. (Up to now the coils are being tested in the CEA Saclay test facility. To have another parallel testing facility for safety reasons and to minimize the coil testing time (critical) was decided to upgrade the TOSKA cryostat to test non-planar coils from W7-X. Due to the smaller cryostat diameter of Toska cryostat than the Saclay one a new testing frame design has been needed)

III.5.1.3. GRP (Glass Reinforcement Plastic) tube of the cryolegs (cold mass supports).

Manufacturing and qualification test technical specification (first draft). Potential suppliers analysis.

III.5.1.4. Overpressure safety device for the plasma vessel.

Bursting discs and safety valves. Pre-analysis of technical solutions and potential suppliers analysis (safety valve: WEKA; rupture discs: REMBE, Elfab, Bormann, GEFA).

III.6. TJ-II Engineering and Operation

III.6.1. Basic Machine Engeneering

The engineering activities in TJ-II and its auxiliary systems have been focused in three aspects:

- The technical operation of the experimental device.
- The maintenance and repairing of the components and systems.
- The installation of new facilities.

III.6.1.1. Technical operation of TJ-II

The development of the pulses during the experimental campaign requires the proper operation of the auxiliary systems of the TJ-II (power supplies, cooling systems, etc.) and the good behaviour of the components (coils, structures, etc.). All this elements are supervised by the control and safety systems under the surveillance of the engineer in charge. Two shifts per day are performed for this task.

III.6.1.2. Maintenance tasks.

The maintenance activities in the TJ-II components and systems have been developed within the predetermined programs. The following aspects can be mentioned:

- Cooling System: the maintenance of the last year has reduced the non-programmed stops of the system to nearly zero. Revision of electrical circuits, pumps, etc, were carried out as usual. The most frequent activity needed is cleaning the cooling tower and the refrigeration circuits filters of the cooling plant.

- The maintenance of the crane bridges installed in the different buildings related to the TJ-II facility has been performed as usual. This task is considered an important safety aspect.
- Power supplies: during the routine maintenance tasks a low insulation against ground was detected on the secondary winding of the TF coil rectifier transformer. This transformer is an oil transformer, it has a voltage relation of 15000/956V, a power of 2x22000kVA each 3 seconds and its weight is almost 14 tons. TF transformer has two secondary windings, one with star connection and the other with delta connection. The last one had a very high isolation against ground (more than 4 GOhm) but on the contrary, the star winding isolation was rather low (0.24 MOhms), this value being unacceptable for its operation. An evaluation of the possibilities of the fault location was done and finally it was discovered in the electrical feed-through which allowed the repair on site. It was necessary to extract more than 500 litres of oil for the disassembly of the LV terminals. Due to fact that these low voltage terminals do not exist on the market, new ones were specially manufactured. Lastly, the old terminals were replaced by new ones and the isolation increased its value up to more than 4 GOhms, an acceptable value for a safe operation.

III.6.1.3. New facilities

Several modifications have been introduced on existing systems to allow new possibilities and better performance on the experiment and the plasma heating systems:

- Power supplies: Since 2003 the pulse generator had been able to work in two different modes of operation. The first one is the impulse way of operation in which the generator works with no-load and with a low output voltage (1.5 kV) in between TJ-II shots. Before each shot the generator increases the voltage to its nominal value (15 kV) during a few seconds and provides all the output power to TJ-II. In the second mode of operation the pulse generator only provides energy to NBI (it is not compatible with TJ-II shots) and it maintains an output voltage of 9 kV during more than one hour.

During 2006 a third mode of operation was developed. In this new mode the pulse generator should maintain continuously its nominal output voltage (15 kV) during the full eight hours period of the working day and it should be able to provide the required electrical energy for the TJ-II shots and for the NBI conditioning pulses. It is clear that this type of operation has a big impact in the whole installation: it affects the generator

from the electromagnetic and also the thermal points of view and it also affects the excitation, cooling and protection systems and the DC pony motor among others.

Due to the fact that the motor-generator cooling system will have to dissipate a higher thermal power and in order to know in detail the current dissipation power, the water flow levels through the different heat exchangers have been measured with an ultrasound system. This measurement has demonstrated that the heat exchangers are currently dissipating less power than they are able, so the cooling system has some margin, but still is uncertain whether this reserve is enough for the new type of operation. To know in detail the new expected thermal losses, a large number of calculations of the behavior of the machine under the new conditions have been done.

- Cooling system. Pellet Injector for TJ-II: It is foreseen the installation of a pellet injector system in the next future. The cooling system for the Helium compressor (part of the cryocooler) was completed during year, installing the connection pipes between the chiller (located in the cooling water plant) and the He compressor located in the TJ-II Torus Hall, and the instrumentation and valves.

Some problems appear during the commissioning and were solved doing some adjustment in a not well settled instrument. Hydraulic tests have been performed and the system is ready waiting for the assembly of pellet injector.

- Torus hall: three distribution boards have been renewed and enlarged to allow the connection of new vacuum pumps in the secondary vacuum for diagnostics.
- Control system (Upgrade of the access control system): A new access control system has been installed, based on barcode scanners, more reliable than the old one based on magnetic cards. The software for the monitoring and control of the access doors to the experimental room has been designed using the C# language and has been installed into a personal computer dedicated to this purpose. The remote monitoring TV system has been updated through a dedicated network that allows viewing all cameras, both from the control room of the TJ-II as from the control room of NBI. A set of three new cameras has been added, two cameras located in the high voltage room, and another one in the NBI transformers room. With these actions the access control system has been fully renovated and is operating successfully.

III.6.1.4. Update of the control system.

The control system of the TJ-II was developed by TJ-II team members in early 1992. Therefore, the definition of the system and the selection of the hardware were decided in

that date. In order to assure the continuity and the maintenance of the system it is necessary to update the hardware and software of the control system.

The most significant changes according to plan are the following ones:

- Replacement the real time operating system OS9, by VxWorks.
- Replacement of the old processors MVME147, 68040 a 33 MHz, by the new ones MVME5500, MPC7455 @ 1 GHz..
- Development of Java applications, for the entire graphical user interfaces, instead of old graphics cards.
- Removing the hard disks in all embedded systems.

The strategy to follow for the renovation of the entire system is to gradually replace each of the subsystems. The first system chosen to undergo the change has been the Ground Loop Supervision System hereafter described.

New Ground Loop Supervision system: The TJ-II stellarator has a complex AC power distribution system to power diagnostic equipment, vacuum, and cooling. During the pulse, the existence of ground loops between these systems can cause damage or compromise the performance of the associated equipment. The real-time detection of these ground loops in the grounding system is crucial to the productive operation of the machine.

The new ground fault supervision system is capable of detecting ground loops with impedances between 1 Ω and 20 KΩ. The number of monitoring channels has been increased since 8 up to 16. The new design reduces by two the area of location of the ground loop and adds the possibility of measuring the impedances with different frequencies, allowing the measure of both, real and imaginary components of the loop impedance. Continuous monitoring is accomplished without breaking ground wire connections. The system has been designed to function in an environment that includes harsh electrical noise.

The monitor runs continuously between pulses to detect faults as they occur The outputs are displayed in the control room by means of the graphical user interface, and simultaneously in one electronic panel located in the experimental room.

The structure of the new grounding system is based on the standard VME bus with embedded MPC7455 PowerPC processor, running the real time operating system VxWorks. . The system architecture is show in the figure X2.

For graphical user interfaces we have developed a Java application, figure X3, which shows the impedance of each channel and facilitates the adjustment of the main

parameters of the system. The system works successfully and has been integrated into the control system TJ-II.

III.6.2. Operation of TJ-II

The 2007 spring campaign was shorter than usual because the completion of the new ECH power supply suffered a four months delay caused by technical problems during the construction period. The campaign took place between April and June, with 27 days of operation and 939 shots. The autumn campaign occurred between October and December with 16 days of operation and 622 shots. The main remarks that must be mentioned as regards TJ-II operation in 2007 are:

- The new ECH power supply has worked very reliably. It allows routine and steady ECH plasma operation at the maximum available power of 600 kW (two gyrotrons, 300 kW each)
- The co-NBI injector has reached a rather steady operation at 31 kV, 60 A, voltage and current levels, respectively. These beam parameters correspond to a port-through injected power into the TJ-II vessel of about 450 kW.
- The counter-NBI injector produced the fist beams into the TJ-II vessel in July this year but it is still in the commissioning phase. Intense effort is devoted to bring it to a steady, reliable operation state.
- The old 28 GHz gyrotron of the EBW heating system, which is planned to be tested along 2008 (proof-of-pinciple) in TJ-II, was successfully tested in September. For these tests, it was fed, through an adapted HV cable, by the new ECRH power supply
- A permanent -although still not final- "lithiumization" system for the lithium coating of the first wall (four ovens with their corresponding manipulators and control systems) has been installed in ports distributed symmetrically along the torus.

A summary of the experimental sessions performed, along with the number of shots allocated to each experiment/activity, is listed below:

- Start-up, commissioning of control and data acquisition systems and diagnostics: three sessions, 71 shots
- ECRH studies: calibration, power deposition profile (modulation) and ECCD experiments: seven sessions, 240 shots

- Rotational transform and plasma volume scan: three sessions, 88 shots
- NBI plasmas (experiments devoted to optimize the coupling of the neutral beam to the ECH target plasma: working gas, magnetic configuration and plasma volume scans, ECH providing on/off axis heating, electrode biasing, etc): thirteen sessions, 379 shots
- Electron ITB´s and low order rationals: one session, 15 shots
- Comparison of profiles measured with different diagnostics: one session, 38 shots
- Electrode biasing and electric fields: tw0 sessions, shots
- Power/density scan: two sessions, 85 shots
- Characterization of ECH plasmas after lithium coating of the vacuum vessel: eight sessions, 258 shots.

IV. UNDERLYING TECHNOLOGY: OVERVIEW OF THE ACTIVITIES ENVISAGED TO COMPLEMENT THE EFDA TECHNOLOGY PROGRAMME

IV.1. Physics Integration: Ceramic insulators

IV.2. Physics Integration: TIEMF in coated cables for in-vessel coils

To try to avoid cold work of mineral-insulated (MI) cables, several ceramic-coated have been obtained. We measured their TIEMF values using a new and much more sensitive system. It includes a small oven with a rather narrow thermal gradient and highly reduced noise, able to examine the fine structure due to

The 3 measured cables (from CaliforniaWire, Ceramawire and Expocable) are based on wires consisting of Cu-Ni , SS 304 and Cu conductors respectively covered with a thin ceramic coating.

We found that in ceramic coated cables TIEMF effects are not entirely avoided. Although their absolute magnitude is relatively similar there are important differences in structure. The best one (lower TIEMF) was the Expocable. It is worth mentioning that the coating of

the first two cables is easily lost so they do not seem good candidates for a fusion environment. Comparing these coated cables with MI cables taking also into account insulation and mechanical reliability only the Expocable seems more suitable than MI cables (with values of TIEMF around 0.2 μV at 90ºC) but thermal treatments at 200 ºC induces an increase of TIEMF values.

Recent measurements with a new concept of cables (Sultzer cable) which consist of a twisted Cu pair with fibre glass insulator (furnished by UKAEA) shows the best results so far (70 nV compared to 200 of Expocable). Thermal and radiation effects must still be studied to assess it.

IV.3. Long Term: Heat treatment effects on ODS steels

IV.3.1. ODS and non ODS Fe-Cr alloys

Two Fe-12 wt% Cr alloys, one containing 0.4 wt% Y_2O_3 and the other Y_2O_3-free, were produced by mechanical alloying followed by hot isostatic pressing [Ref. Fecre1]. The alloys were characterized in the as-HIPEd state and after tempering by transmission electron microscopy (TEM) and atom probe tomography. The as-HIPed alloys exhibited a microstructure of martensite laths and small voids with sizes < 10 nm. An intra-granular dispersion of nanoparticles was observed in the ODS alloy, although nanoparticles were also found by carbides or on grain boundaries. Small voids with sizes < 2 nm were often seen next to the ODS nanoparticles or the carbides. Tempering at 1023 K for 4h led only to a partial recovery and recrystallization of the alloys.

IV.4. Tritium Breeding and Materials: Breeding blanket

IV.5. Development of ITER subsystems

IV.5.1. NBI Heating

IV.5.1.1. Alternative concept of a Residual Ion Dump: Magnetic RID. Design of the magnetic coil and integration with the passive and active magnetic shielding of ITER

CIEMAT has carried out work as contribution to the EFDA task TW6-THHN-NBD1, subtask 3.7.1 [TW6-THHN-NBD1spec]. This part of the task was aimed to the conceptual design of a magnetic Residual Ion Dump (MRID) for the ITER Neutral Beam Injectors. The design has been done in collaboration with UKAEA. CIEMAT work was to define an adequate magnetic system with coils external to the injector vacuum vessel, calculate the resulting magnetic field and provide UKAEA with the 3D field distribution to be used to compute ion trajectories and the power densities deposited on the collecting plates.

For this work CIEMAT has relied on the assistance of ELYTT Energy for the magnetostatic calculations and magnet design. The magnetic system has to include a magnetic screen to shield the neutralizer from the magnetic field and must be integrated in the magnetic field reduction system devised for the injector.

The main points of the MRID study are summarized as follows:

- Analysis of different options for the MRID.
- Initial solutions to the out-of-vessel design. Detailed modelling of the magnet with coils encircling the poles.
- Effect of modifications of the magnetic screen on the stray field at the neutralizer
- Study of the saturation influence on the field distribution
- Integration of the magnetic system in the NBI vessel and passive shield.

The results of the work are described at [Elytt_MRID]

IV.5.1.2. Electrostatic Residual Ion Dump of ITER: physics studies and viability

CIEMAT has carried out work as contribution to the EFDA task TW6-THHN-NBD1, subtask 3.1.3 [TW6-THHN-NBD1spec]. The work concerns the Electrostic Residual Ion Dump (ERID) of the ITER NBI. It is basically a study of space-charge and plasma formation effects inside the ERID channels, which could affect the deflection properties of the ERID giving rise to operational risks. The electric field inside the ERID may be affected by space-charge effects due to ion beam separation, and by the creation of a plasma through ionization of the deuterium gas present in the ERID. The thermal gas re-emission has been studied and included in the ionization gas target. The role of the stripped electrons and secondary electrons has been taken into account.

An MD code has been written that simulates the trajectories of the beam components emerging from the neutralizer and subjected to the electric field of the ERID. The particle deposition patterns on the ERID panels have been obtained.

The deuterium gas re-emission from the panels has been studied with the help of the code TMAP7. The outgassing process accounts for approximately one fifth of the base density in the ERID channels due to diffusion from the ion source and neutralizer.

The different ionization processes of this gas target due to the beam components, stripped electrons and secondary electrons are then studied. The total ionization density rate is found to be two orders of magnitude smaller than the critical ionization density rate for plasma creation.

The possible extension of the neutralizer plasma into the ERID channels needs to be studied, since it may have an effect on the plasma formation inside the ERID as well as on the behaviour of the stripped electrons coming from the neutralizer.

The results of the study are presented in [CIEMAT_ERID_080415]

IV.5.1.3. Maintenance by remote handling

Computer simulations have shown that during ITER operation, the NB cell (3 H&CD NB + 1 DNB) will become progressively precluded to man access because of radio-activation and T contamination (~several 100μSv/h) except for short interventions (say in the order of ~1h - tbc). As a consequence, most NB maintenance operations, routine as well as unforeseen interventions, will have to be performed without direct man intervention. It has been established that remote maintenance operations are to be performed from the top, and the vessels and BL components are being redesigned with the requirement of top maintenance compatibility.

CIEMAT has carried out work related to the Remote Handling Activities in the ITER Neutral Beam Cell, under EFDA Task TW6-TVR-NBRH, commended to CIEMAT under EFDA contract FU06-CT-2006-00142 (EFDA/06-1456).

As specified in the Contract Specifications, the areas of CIEMAT activities are as follows:

- Gather and rationalize the expected maintenance requirements for the ITER NB Beam Line Components (Neutralizer, RID and Calorimeter), NB gate valve, beam duct bellows and Fast Shutter.
- Examine (using an appropriate 3D CAD or virtual reality approach) the logistics and space availability within the NB cell in relation to the transport of various components from the NB units to the hot cell access point and temporary in-cell storage of components removed to allow for maintenance operations.

- Develop an engineering design for an overhead crane necessary to transfer NB components within the NB cell (including design calculations to demonstrate compliance with the necessary lifting gear and nuclear regulations relevant to operations in the ITER NB cell).
- Develop the design of a specific sub-set of RH equipment and/or tooling identified as being necessary for the cut/weld/inspection operations inside the BL vessel.

Task breakdown

The Project Management Plan (PMP_TW6-RH) delivered to EFDA in February 2007 established the following distribution of CIEMAT activities:

Gathering and rationalization of maintenance requirements is being performed entirely by CIEMAT technical staff with the support of EFDA, the European Associations and ITER.

Space availability and logistics activity was subcontracted to IBERTEF with the supervision of CIEMAT technical staff.

Crane design was also subcontracted to IBERTEF with the supervision of CIEMAT technical staff.

Cutting, welding and inspection activity was subcontracted to TECNATOM, counting also with the supervision and advice of CIEMAT technical staff.

The Task has been completed and the main results can be found in the following references:

The ITER NBI Maintenance requirements are presented in the Intermediate Report of the EFDA task [CIEMAT_TW6-NBRH_IntRep]

The Space availability and logistics are best summarized in [IBERTEF-EA 18-10-07]

The different solutions proposed for the crane can be seen at [IBERTEF-Sen 18-10-07]

A preliminary study of the cut/weld operations on the NBI components is contained in [Tecnatom-Ciemat_071018].

IV.5.2. Divertor

IV.5.3. EISS5 - CONTRIBUTIONS TO STUDIES IN SUPPORT OF RPRS

EFDA Technology Work programme 2005 (EFDA Reference: EISS5-SL-53)

The EISS-5 project aims to complete a number of activities that shall allow the establishment of the ITER team and the start of ITER construction in Cadarache. Following the French regulatory procedure, after "Dossier d'Options de Sûreté, DOS" a so-called "Rapport Préliminaire de Sûreté, RPrS" must be written in order to prepare the demand for construction of the installation, "Décret d'Autorisation de Création, DAC". CIEMAT is responsible of three subtasks that belong to Task SL53: Studies in support of RPrS.

The tasks have been coordinated by a group of people composed by members of the Laboratorio Nacional de Fusión at CIEMAT, the spanish national waste management company ENRESA, and of the CIEMAT Safety and Decommissioning Group. A specialized company with previous experience on ITER safety analysis has been subcontracted.

IV.5.3.1. Subtask SL53.2: Safety Operational limits and correlation of the experimental programme

Under this task, two different studies have been peformed:

- Safety important components classification
- Operational limits and conditions
- Safety important components classification

The results of this work have been compiled in the final report of the task (Safety Important Components. Final Report of EFDA task EISS5-SL53.2. CIEMAT. IN-IT-EISS-002. May, 2007), which includes the list of safety-important structures, systems and components (SIC) of the ITER design. A cross-checking with the reference sequences of the safety analysis has been performed with the aim of demonstrating that the list of the components classified as SIC is exhaustive. This information is prepared for subsequent inclusion in the RPrS (Rapport Préliminaire de Sureté).

Operational Limits and conditions

- The purposes of this subtask have been to revise the complete list of the Operational Limits and Conditions
- To derive a minimum set of conditions which define the main safety parameters that should be retained with regard to the DAC (Décret d´Autorisation de Création)
- The results of the study are compiled in the final report of the task: Operational Limits and Conditions. Final Report of EFDA task EISS5-SL53.2. CIEMAT. IN-IT-EISS-

003. May, 2007. A summary table of all of the OLCs, classified according to French practice has been also included.

IV.5.3.2. Subtask SL53.4a: Outline description of the maintenance programme

The objective of this task was to provide a breakdown of the scheduled hands-on maintenance operations that must be carried out on components/systems located in potentially radioactive/contaminated areas in the Tokamak Complex during normal plant operation.

The study refers not only to the maintenance of SIC components but also to the maintenance of any system or component located in an area with radiological monitors. The results are presented in the final report: Outline Description of the ITER maintenance Program. Final Report of EFDA task EISS5-SL53.4. CIEMAT. IN-IT-EISS-001. May, 2007. The document structure is such that it can be easily updated in the future as the design evolves.

IV.5.3.3. Subtask SL53.8b: Hotcell and Radwaste – Functions during ITER dismantling and phases of Hotcell and Radwaste dismantling

The objective of this subtask is to present the main functions of the Hot Cell and Radwaste Buildings during the ITER dismantling and to analyse how the dismantling of the Hot Cell and Radwaste buildings themselves can be integrated into the ITER dismantling phase. The work performed is compiled in the final report of the EFDA task: Hotcell Functions during ITER dismantling and Phases of Hotcell and Radwaste Buildings Dismantling. Final Report of EFDA task EISS5-SL53.8b. CIEMAT. IN-IT-EISS-004.December, 2007. This document has four appendices which summarize the work performed:

- Review of the document "Dismantling Reference Scenario of ITER" and identification of the hot cell functions during ITER dismantling phase
- Descriptive and comparative studies of two dismantling scenarios of the hot cell building
- Hot cell dismantling reference scenario
- Radwaste Building dismantling reference scenario

As a first step, a peer review of the EISS Cadarache document "Dismantling Reference Scenario for ITER", SL 5 DEL 2002 0002 Rev 1 and a complete description of the potential use of the hot cells during ITER dismantling have been carried out. Next two dismantling scenarios of the Hot Cell Building (higher to lower risk / top to bottom) have been described and compared, concluding that the first option could be more adequate. The chosen scenario has been described in detail (appendix C), including the processes description, the sequence of dismantling operations, the identification of tools and equipment, etc. Finally, a potential dismantling reference scenario for the radwaste building has been proposed and a description of the main phases, their sequence, dedicated tools and equipment has been made, underlying the main aspects to consider in the decommissioning of this building.

V. GENERIC DESCRIPTION OF AREAS INTENDED TO BE COVERED BY EFDA TASTKS

V.1. Physics Integration: Ceramic insulators

V.1.1. Assesment alternative radiation resistant glasses

Several works have shown that both KU1 (high OH content) and KS4V (low OH content) quartz glasses exhibit very good behaviour when exposed to a radiation field particularly in terms of radioluminescence and radiation induced optical absorption. Consequently these materials are being considered as the main candidates to be used in ITER as windows and optical components. KU1 and KS4V are high purity silica, basically pure SiO_2, in contrast to other glasses which are made of different oxides. An study of the radiation induced absorption and luminescence of two type of alternative multicomponent glasses has been carried out at CIEMAT [Ref V.1.1]. The samples were provided by SCK-CEN and the nominal composition of both types of glasses in weight percentage was 75%SiO_2 22%Na 3%CaO. One of the types was 0.05% Cerium doped meanwhile the other type was undoped.

The two types, Ce doped and undoped, materials have been studied in terms of radioluminescence, photoluminescence and radiation induced optical absorption. In order to perform such study the samples were 1.8 MeV electron irradiated at 15, 100 and 200 C up to a dose of 190, 60 and 60 kGy respectively and during irradiation different

radioluminescence and optical absorption measurements were performed at different doses. Also photoluminescence and optical absorption measurements were performed before and after irradiation making use of commercial spectrophotometers.

The two materials studied exhibit very high sensitivity to radiation in terms of optical absorption and radioluminescence. Particularly the radiation induced optical absorption reaches values of the order of 10 cm^{-1} in optical density after only 50 kGy at 15 C. In order to anneal the coloration during irradiation the temperature of the glass has to be increased up to 200 C. However when the optical absorption is measured during irradiation the absorption is clearly higher showing that the annealing is not completely effective. When the material is doped with Cerium the coloration occurs a little bit slower within the visible range but on the other hand introduces high absorption within the UV range. The radioluminescence for both types of glasses is higher than in the case of KU1 quartz glass and Ce-doped type of glass exhibit high photoluminescence.

V.1.2. Dielectric loss and thermal conductive

No new activities have been developed during 2007 into this topic.

V.1.3. SiO / SiO2 mirror coatings

Radiation enhanced degradation of reflectivity of different commercial mirrors as a function of irradiation temperature and time (dose) in different environments (vacuum, nitrogen, air), as well as enhanced corrosion in a humid environment are being studied.

Problems have been encountered with the as-received commercial mirrors concerning reflectivity and overcoating, since commercial specifications are not completely reliable [ref. MC 1].

For new commercially available mirrors (general broad band use and UV enhanced), provided by Thor, the reflectivity changes after gamma irradiation up to 60 MGy in dry nitrogen at 170 ºC were examined. No measurable degradation of reflectivity in the VIS-NIR range is observed. The problem is the manufacturer specifications, since the 4 broad band mirrors (with nominal SiO overcoating), provided as identical, show two different reflectivities and the XPS analysis of the surface shows in one group Thorium (Th) and Fluorine (F) (not referenced by the manufacturer) and the other group shows that is completely SiO_2 overcoated (not SiO). The UV enhanced (4 mirrrors), nominally MgF_2

show similar reflectivities, but Mg and F were not found, only SiO_2 is present, that it is not the specified coating.

Also two commercial mirrors from PGO (Präzisions Glas & Optik) have been gamma irradiated up to 50 MGy in dry nitrogen at 170 ºC. One cold mirror (SHD) with multilayer dielectric coating (unspecified by manufacturer). Other mirror (SEA-VIS) enhanced aluminium with dielectric overcoating (unspecified). Both mirrors show good radiation resistance.

V.1.4. Window assemblies and seals, radiation enhanced T diffusion

A system has been developed to measure the radiation induced diffusion of H, D, and He will for 6 simplified window assemblies. The different window assemblies are mounted in a special irradiation chamber mounted at the end of the beam line of a Van de Graaff accelerator. One face of the window assembly is in vacuum and exposed to a 1.8 MeV electron beam meanwhile the other face was subjected to pressurized hydrogen, deuterium or helium. Gas leakage through the window assembly during irradiation will be measured with a helium/hydrogen leak detector. The system has been tested successfully during the last year. Also optical absorption measurements will be carried out before and after irradiation. Once irradiated the gas chamber pressure will be increased up to 3 bars in order to check mechanical failure of the assemblies.

The window assemblies are produced at UKAEA and will be shipped to Ciemat during 2008. Such window assemblies consist of sapphire with edge brazed AuCu bond on titanium, fused silica, with Al-diffusion bond on tantalum, crystal quartz with Al-diffusion bond on 316 stainless steel,. silicon nitride with Al-diffusion bond on titanium, silicon nitride with Al-diffusion bond on titanium, and fused silica with a eutectic braze (lead-silver compound) welded on 316 stainless steel.

V.1.5. Radiation enhanced diffusion of H isotopes in Silica

Different oxides, mainly fused silica and aluminium oxide, are candidate materials to be used in different systems of ITER. Some applications require their use as confinement barriers for tritium and other radioactive products. The effect of radiation on diffusion mechanisms of fused silica was studied. To help clarify this phenomenon in a qualitative way, radiation effects on the behaviour of the implantation profile of deuterium are measured for fused silica. Deuterium has been introduced into the samples by 50 keV ion implantation and later on irradiated at different temperatures to induce diffusion. The

modification of the implantation profile has been determined by Elastic Recoil Detection Analysis (ERDA) using Si ions. It is observed that high dose rate ionizing irradiation (over 100 Gy/s) induces changes in the D profile even at room temperature. No significant effects are observed for lower dose rate ionizing radiation effects or displacement radiation effects from 1.2 MeV Si ion irradiation.

V.1.6. Radiation induced defects in fused silica

KU1 (high OH content) and KS-4V (low OH content) silica glasses, considered as the main candidate materials for optical diagnostic and remote handling components in ITER, have been gamma irradiated at doses from 10 kGy up to 12 MGy together with five commercial types of silica. After each irradiation the optical absorption of the different grades has been obtained, and the concentration evolution of each defect has been compared for the different silica types. This comparison allowed us to determine which defects are intrinsic and which depend on the impurity level or fabrication method.

The results obtained confirm that precursors (impurities and defects), produced during the manufacturing process of the silica samples, determine the type and concentration of defects after gamma irradiation, at least up to 12 MGy doses; hence radiation induced optical absorption depends on the material grade. E' centers are present in all the silica types after irradiation, although its concentration is different for each one. The type and concentration of the E' center precursors also depend on the silica grade. No correlation was found between the optical absorption and the OH content. Among the different silica grades those with fewer impurities, clearly show lower optical absorption. KS-4V shows the lowest optical absorption at room temperature at the studied gamma doses. [ref. RDFS_1]

By other hand, the photoluminescence emission around 4.4 eV, induced by UV and vacuum ultraviolet excitation, in neutron irradiated KU1 and KS-4V and for comparison commercial silica Infrasil I301 has been studied at temperature from 300 to 10K. The neutron fluences have been 10^{21} n/m^2 and 10^{22} n/m^2. At the same temperature and neutron fluence KU1, KS-4V and I301 show similar excitation spectra shape. Neutron irradiated samples show intense excitation bands, related to ODC(II) defect, around 4.95 and 6.8 eV. Relative intensity of 7.3 eV band, associated to ODC(I) defect, is greater at lower temperature. Band intensities are different depending on silica grade. At the present neutron fluences, photoluminescence excitation spectra are very affected by high optical absorption in this spectral region. KU1 grade shows the lowest photoluminescence. [ref. RDFS_2]

V.1.7. Radiation damage modelling in fused silica

Molecular dynamics calculations have been made to study the radiation effect in amorphous silica with different percentage of H atom. Feuston and Garofalini interatomic potential modified have been used in this study [Webb 94]. These studies have showed the evolution of number of defects in function of the hydrogen atoms percentage and in addition the behaviour of the H atoms under irradiation. In addition, we have studied the diffusion coefficient at different temperatures and the migration energy of the H atoms in the bulk of amorphous silica.

This study has been made in several steps:

- Characterization of the different positions of H atoms in the bulk of simulation box.
- Study of the defects evolution under irradiation in different simulation box with different Hydrogen atoms concentration (0, 1, 10%).
- Calculations of migration energies of H atoms inside of amorphous silica simulation box.

Result:

- The H atoms mainly occupy two specific position. H atoms bonded to an oxygen atom with 1-fold coordination, that is, the H atom is bonded to NBO (Si-OH, O-H binding distance 1.3 Å). The second position is the H atoms free. [Mota 08a, Mota 08b]
- It has been found that the evolution of defects point evolves in different ways in different simulation boxes with different percentages of Hydrogen atoms [Mota 07]. In addition, it has been observed that all defects evolve in similar form, they increases when increasing Hydrogen concentration and then decline again when they reach a certain concentration of H. We have also observed that the lattice is modified to assimilate the energy deposited by the PKA, that is, the rings distribution is modified: Increase the rings size smaller and bigger (size 3, 4 and 8) and decrease the 6-fold and 5-fold rings size, the center of rings size distribution [Mota 08a]
- Calculations of the migration energies of Hydrogen atoms. We have found two characteristics different migration energies. E1 = 0.5 eV corresponding to the energy needed by the H to migrate until to find a nearest neighbour vacancy where link and E2 = 2 eV it is the energy needed to break the O-H binding plus energy needed to migrate [Mota 08b]. We have found experimental comparisons for these two values [Brückner 71, Pacchioni 00].

[Brückner 71] R.Brückner, "Properties and structure of vitreous silica. II" Journal of Non-Crystalline solids 5 issue 3, (1971) 177-216

[Webb 94] E. B. Webb and S. H. Garofalini " Molecular dynamics simulations of the approach and withdrawal of a model crystalline metal to a silica glass surface" J. Chem. Phys. 101 [11] 10101-10106 (1994)

[Pacchioni 00] G.Pacchioni, " Ab initio theory of point defects in SiO2",

NATO Science Series, II. Mathematics, Physics and Chemistry –Vol 2 (2000), 161

V.1.8. Radiation damage modelling and H isotopes in diamond

After a revision of available codes for molecular dynamics two of them have been selected: *MDCASK and LAMMPS.* The former because it is well adapted to calculate damage cascades generated by PKA atoms and the later for its larger versatility (low energy atoms).

The Brenner potential was introduced in the *MDCASK* code, task that required quite a lot of work due to the potential complexity.

At this first stage of the work programme, we studied the equilibrium position of Hydrogen in the perfect diamond lattice and also located at carbon vacancies. We obtained good agreement with several configurations obtained by *ab-initio* codes which add confidence to our future calculations. As a first results C vacancies seems to act as H traps.

V.1.9. Surface degradation under ion irradiation of insulator materials

Different types of electrical degradation of insulators are known to occur when these materials are subjected to a radiation field. Electrical degradation may occur within the bulk and also at the surface of the material. Susceptibility and rate of degradation is believed to depend strongly on the ratio between displacement and ionization processes which occur during material irradiation. Two different types of oxides have been studied: silica and sapphire. The behaviour of these two materials when subjected to a radiation field is known to be very different. Radiolytic processes giving rise to oxygen vacancy production occur within the bulk of silica while in the case of sapphire such processes do not occur, knock-on collisions being necessary to produce oxygen displacements Sapphire and silica samples were irradiated with 1.8 MeV electrons (high electronic excitation but low displacement), and with 54 keV He^+ (high electronic excitation and

high displacement) at 450 ºC. For both types of irradiation the experimental set-up permitted one to measure the surface electrical conductivity at different doses and as a function of temperature [Ref V.1.9].

Severe surface electrical degradation occurs when either sapphire or silica are subjected to electron irradiation. Such degradation is a consequence of the loss of oxygen from the irradiated surface. A comparison with the 54 keV He^+ irradiations indicates that the electrical surface degradation is mainly due to the ionizing radiation component rather than to the knock-on displacements. This could have serious consequences for the use of alumina ceramics in fusion reactors where the gamma radiation alone may induce the loss of oxygen from the vacuum surface of the ceramic insulators eventually producing degradation of the electrical insulation. Other works clearly demonstrated that severe surface degradation of oxides after either proton or alpha particle characterized by oxygen loss, electrical conductivity degradation, and optical absorption increase. The experimental results indicate that both 1.8 MeV electron irradiation and 54 keV He^+ implantation produce basically the same surface effects: drastic reduction of oxygen content and as a consequence an enormous increase in electrical conductivity. However, the magnitude of the fundamental damage processes for each type of irradiation is very different in principle. In the case of 54 keV He^+ implantation there is a high number of atomic displacements within a very thin layer (of the order of 0.8 μm), high electronic excitation and also physical sputtering, while in the case of 1.8 MeV electron irradiation the number of atomic displacements is extremely low and physical sputtering is negligible. The observed preferential loss of oxygen suggests that the fundamental process taking place is extremely selective, and that a type of preferential radiolytic sputtering induced by the ionizing component is the main mechanism giving rise to drastic oxygen loss. Oxygen loss induces a band gap reduction. Although the processes seem basically the same, the magnitude of the surface degradation in terms of surface conductivity and induced optical absorption is much less for electron irradiation. This must be a consequence of the higher density of energy deposition in the case of He implantation. In addition the much higher rate of displacements due to He bombardment in comparison with 1.8 MeV electron irradiations must also play an important role in the surface degradation process.

Refractory oxides such as sapphire are known to be extremely resistant to gamma radiation damage in the bulk, however the experimental results demonstrate that severe vacuum surface degradation may occur in an ionizing radiation environment. In the case of a fusion reactor the situation will be worse because the insulators not only will be

subjected to gamma and neutron irradiation, but also to energetic particle bombardment due to the presence of electromagnetic fields and ionized residual gas.

V.1.10. Radiation bolometers development

In-reactor tests of JET type bolometers (Au meanders on mica), considered for use in ITER, highlighted several problems: rapid Au to Hg transmutation, mica swelling, meander detachment, and unreliable spring loaded electrical contacts. To address these important limitations alternative radiation resistant substrates have been examined during the last five years [ref report 07].

High temperature bolometers fabricated with thin ceramic substrates as the foil with a platinum meander sensor and an absorber have been analysed in terms of their temperature behaviour and radiation tolerance. Basic prototypes with sputtered Pt meander sensors on alumina and aluminium nitride ceramic substrates were tested during electron and neutron irradiation, with results up to 0.013 dpa showing acceptable behaviour of both substrates and better radiation resistance response of Pt compared with Au. But electrical connection to the thin Pt meander proved to be unreliable.

During last year, research was devoted to develop new bolometer configurations with special attention to attain more robust electrical contacts. Several technical materials have been taken into account in an attempt to improve particularly the isolating frame. First, the bolometer was supported on a Macor machinable glass ceramic but its resistance to neutron radiation was questioned. Alumina frames were then tested being the perfect choice for the application but expensive and too fragile during mechanization. Supports of anodized aluminium were finally considered, giving an optimum electrical isolation even at the bolometers operation temperature (450C). A comparison of the electrical resistance of the differently supported prototypes was here presented as a function of temperature and ionizing radiation. Conclusions were also evaluated comparing with older devices and actual mica bolometers. Temperature behaviour is independent of Pt-depositing substrate, the design of the meander-like sensor, and the deposition method. Ionizing radiation due to electron irradiation has little effect on the sensor resistance values [ref SOFT 08]. Resistance variations (≤ 0.5 %) over periods of time far greater than one ITER shot can be accommodated. Prototypes were send to the SCK-CEN (Mol, Belgium) experimental reactor BR2 to final characterization under neutron irradiation.

V.1.11. Assessment of Li ceramics fabrication routes

Previous results point out the difficulties on obtaining lithium ceramics from commercial powders. The low sintering temperatures that are needed to avoid lithium diffusion resulted on low densified ceramic bodies with limited mechanical stability. Therefore, better results could be obtained from lab-synthesized lithium titanate and zirconate powders following wet chemical methods. Most of the research was dedicated on the optimization of sintering parameters from different precursors. Modifying sintering temperature and time, 100% of the stequiometric phase was obtained before 1100C with porosity between 20 and 15%. The used synthesis methods allowed less temperature densifying processes due to the formation of smaller and softer particulate powders, compared to commercial ones. The synthesized powders were granulated with water or PVA on spherical particles, being recommended the mixture of different diameters to achieve better packing. The ceramic characterization of the sintered spherical particles is under development now. Anyhow, 80% densified ceramic rods have been characterized previously to ionizing radiation exposure. Scanning electron microscopy was used to study the microstructure and chemical analysis of the as-sintered and polished samples in order to define the phase ratio and its mean grain size, and the formation of glass phase, being possible to suggest the followed sintering mechanism.

Concerning lithium metasilicate, the powder lab-synthesis was successfully achieved from a mixture of the convenient oxides and carbonates, obtaining almost theoretical density on sintered samples. Difficulties were found when synthesis of lithium orthosilicate and lithium aluminate was approach. As a consequence of a lack of reaction between reactives, parasitic phase formation was identified resulting on low densified ceramics. Optical characterization was concentrated on the monophasic lithium metasilicate product. The registered radioluminiscence bands could be associated to oxygen vacancies, peroxide radicals, free SiO_2, and intrinsic metasilicate cell features. The dielectric behaviour of silicates and aluminate is very similar. At room temperature, the frequency spectra show peaks at GHz and below1MHz, while the permittivity data point out the existence of real relaxation processes better than a pure DC conductivity. Micro spheres from these powders are now under preparation with the aid of a spray-dryer.

V.2. Vessel In-Vessel: Radiation tolerance of alternative radiation hard “O” rings

V.2.1. Report on the Outcome of the irradiation and subsequent testing of the hydraulic seal carriers: Progressive gamma irradiation of Hydraulic Seals

The main CIEMAT contribution to the present task centred on irradiation of a number of seal carriers developed jointly by IHA (Finland) and Gradel (Luxembourg)

Three different polymers have been tested as possible seals and O-rings: PEEK, polyethylene (UHMW-PE), and polyurethane. Specimens of each material have been irradiated with ^{60}Co γ-rays up to 10 MGy in water and in dry nitrogen. Following irradiation mechanical testing (tensile and microhardness) and microstructural observations of the fracture mode were carried out.

Remarked results:

The results show that PEEK is outstanding, showing excellent mechanical behaviour for the doses and irradiation conditions studied. Up to 10 MGy, neither hardness nor tensile strength were modified. In the case of polyethylene and polyurethane, the tensile failure mechanism was modified with irradiation and gave rise to a lower ability for bending. However, up to 10 MGy the measured tensile strength and hardness data are still acceptable.

The irradiation in water has been observed to have no additional effect, the mechanical damage and the results are very similar for the irradiation carried out in dry nitrogen for the three materials. [Ref V.2.1]

V.3. Long Term: Structural materials

V.3.1. Mechanical and microstructural characterization of Eurofer ODS steels

The charpy and fracture toughness properties of the EU ODS-EUROFER steel, normalized in Ar at 1100°C/30'plus tempered in Ar at 750°C/2h/air cooled, have been studied in two products forms: plate of thickness 16 mm (Heat HXX1115) and rod of diameter 20 mm (Heat HXX1116). The impact and fracture toughness characteristics of this alloy have been investigated in the TL and LT orientation for the plate and L orientation for the rod. The DBTT has been calculated as the temperature corresponding to USE/2.

The EU ODS-EUROFER has shown the following DBTT values: -38°C for the TL orientation, -24°C for the LT orientation and -2.6°C for the rod. These values mean a

significant shift of the DBTT compared with the Eurofer'97 (DBTT = -107°C). The difference of the DBTT between the orientation and the product form could be attributed to the fitting procedure. The USE decreased, compared with the Eurofer'97, by 15% for the rod and around of 40% for the both orientations of the plate.

Turning next to the fracture toughness properties of EU ODS-EUROFER, this steel has been tested using small bend pre-cracked specimens (KLST geometry) in the transition region. Results shows that fracture toughness of this material obtained with this specimen geometry can not be described by the Master Curve. The main reason is that the data do not present clear transition behaviour with a sudden shift up to the upper shelf region and the fracture surfaces are not entirely cleavage. This alloy presents poor fracture toughness properties, independently the product form and the orientation.

V.3.2. Eurofer and Eurofer ODS new heats. Milling effects

Y_2O_3 dispersion strengthened (ODS) and non-ODS EUROFER, produced by hot isostatic pessing (HIP) [Ref. C1], have been subjected to isochronal annealing up to 1523 K. The evolution of the open-volume defects and their thermal stability in these materials have been investigated using positron lifetime and coincidence Doppler broadening (CDB) techniques along with transmission electron microscopy (TEM) [Ref. C2, C3]. Three-dimensional vacancy clusters were detected in both materials in as-HIPed condition and after annealing at T≤623 K. In the temperature range 823 – 1323 K, other new species of vacancy clusters appear to be nucleated and became into cavities. Above 1323 K, some cavities were unstable and annealed out. However, those associated to oxide particles and some small precipitates remained stable up to 1523 K.

V.3.3. W alloys development

Small laboratory scale batches of W and W-Ti(Y2O3) have been produced by mechanical alloying and consolidation by hot isostatic pressing (HIP) [Ref. W1]. The microstructural, compositional and wear characteristics of these materials have been investigated. Samples of these materials have been delivered to perform welding experiments and mechanical tests by the ESTRUMAT groups at the Rey Juan Carlos University and the Polytechnique University of Madrid. The HIP treatment at 1973 K applied to W previously consolidated by HIP at 1550 K did not produce further densification because of the presence of open porosity in the material. However, addition of 0.5 wt% Y2O3 yielded a material with very low porosity after the second HIP stage at 1973 K. In this case, complex (W-Y) oxides were found filling the residual pores. Addition of 2 or 4 wt % Ti to

W resulted in a fully dense material irrespective of the Y2O3 presence in the materials HIP treated at 1550K. The present results demonstrate that sound W-Ti/Y2O3 materials for full mechanical testing can be fabricated by HIP [Ref. W2]

V.3.4. W-EUROFER joining technologies

Commercial pure tungsten and oxide dispersed tungsten alloy containing 2% Ti and 0.47% Y_2O_3, have been joined to EUROFER 97 by means two alternative welding techniques: high temperature brazing using a high power diode laser (HTB-HPDL) and solid state diffusion bonding by high isostatic pressure (DB-HIP). In the first case, two different high temperature brazes were tested: a Nichrome (80Ni-20Cr) alloy with a melting point of 1400 °C and a Nitinol (55Ni-45Ti) alloy with a melting point of 1310 ºC. An additional brazing test using a pure Ti 1 mm thick foil (99.9 %) as filler materials was also made. For diffusion bonding, different metallic interlayers were used in the form of thin foils for the solid state bonding tests carried out using HIP: pure Cu (99.5 %) with 400 µm thickness and pure Ti (99.95 %) with 1500 µm thickness.

The main problem associated to brazing of dissimilar joints between W and Eurofer was the high residual stress at the bonding because of the great differences of thermal expansion coefficients of parent materials and brazed alloys. These stresses promoted subsequent cracking after brazing. In the case of brazing using NiCr alloy, it was very difficult to control the cracking of W sheet associated to the excessive thermal stress generated during cooling. The brittleness of tungsten favoured the nucleation of cracks in it, following with their growth across the brazing interface penetrating in the Ni-Cr filler. NiCr braze presented poor wettability to pure W and to Eurofer when low laser power densities were used but, by increasing laser power, it was possible to reach the required wetting of both parent materials of the dissimilar joint. Wetting of W-Ti-Y_2O_3 by NiCr braze was much more effective, presumably because of the active effect of titanium.

It was possible to produce brazed joints between pure W to Eurofer with NiTi wire and focusing the laser underneath the filler, with good superficial aspect and extended between both parent materials, showing a high degree of wettability with both parent sheets. Although cracking by CTEs mismatch was also present in brazed joints using NiTi wire, the intermediate CTE of this material in relation with Eurofer and W, decreased the thermal stress at the bond, reducing the risk of cracking.

Diffusion bonding by HIP between pure W and Eurofer has not been possible for the bonding conditions applied, in spite of the use of two different interlayer materials, copper and titanium. Nevertheless, it has been possible to form a continuous joint using Ti foils as interlayer when the W-Ti-Y_2O_3 alloy was used as parent materials. The bond interface between Eurofer and the interlayer was very complex, being mainly constituted by continuous layers of NiTi intermetallic compounds, although titanium carbonitrides and other secondary phases were also detected. This structure, in conjunction with the presence of porosity, might degrade the strength of this joint.

Joining conditions and joint characteristics have been described in an internal report

V.3.5. Modelling of Fe: He-defect interactions

Although there was no funding for the materials modelling effort under EFDA during 2007, we have continued our studies of the migration of He in Fe. Our work in 2006 showed that impurities play a very important role in the migration of He in Fe and the formation of He-vacancy complexes. Our hypothesis was that carbon was the impurity responsible for this effect. In collaboration with C. Chun Fu, from the CEA-Saclay, in France, we have extended the original model to explicitly include Carbon and its interaction with He and He-vacancy complexes. Dr. Fu calculated using density functional theory the binding energies of Carbon to different complexes, as well as the migration energy of Carbon. This information has been included into the rate theory model and has been used to reproduce the experimentally measured He desorption from irradiated Fe. These calculations show that indeed when Carbon is included in the model it is possible to reproduce these experiments, that are performed under very different conditions of temperature, implantation dose and sample depth. In this model no fitting of any of the energies of the different reactions is necessary, and only a single free parameter exists which is the carbon content, not known exactly for these experiments. Moreover, this model also explains the large discrepancies in the literature on the value for the vacancy migration energy in Fe obtained experimentally. A paper has been submitted to J. of Nuclear Materials [1] and two other papers will be submitted shortly to Physical Review. This work was presented at the ICFRM2007 meeting in Nice by C. Ortiz [2], and part was included in the invited talk of B. D. Wirth in the same meeting [3].

In order to validate this model, a new collaboration has started with the groups of Dr. Esteban at UPV/EHU and Dr. Ibarra at CIEMAT. These groups will perform experiments designed to test different parts of the model developed.

References:

[1] C.J. Ortiz, M.-J. Caturla, C.C. Fu and F. Willaime, Impurity effects on He diffusion in a-Fe, submitted to J. of Nuclear Materials.

[2] C.J. Ortiz, M.-J. Caturla, C.C. Fu and F. Willaime, Impurity effects on He diffusion in a-Fe, Oral communication, ICFRM 2007, Nice 10 – 14 December, 2007.

[3] B. Wirth, M.-J. Caturla, C.C. Fu, A. Kimura, R.J. Kurtz, K. Morishita, G. Odette, D. Xu and T. Yamamoto, Assessment of He Migration and Trapping Interactions with Microstructural Features in Ferritic Alloy, Invited presentation, ICFRM 2007, Nice 10 – 14 December, 2007.

V.4. Tritium Breeding and Materials: Breeding blanket

V.4.1. Extend computing tools for T cycle

V.4.2. Experimental determination of reference Sieverts' constant and diffusivity values for tritium in Pb-Li

The Absorption-Desorption technique has been used to analyse the H transport parameters in eutectic lead lithium alloy [ref. PbLi 1]. The first experimental campaign is based on subsequent gas loading and deloading phases in the experimental range: temperature from 532 K to 922 K, loading pressure of 10^5 Pa and measuring times of 12 hours in the loading phase and release phase. Preliminary values of Sieverts' constant and diffusivity have been obtained by modelling the individual test with a specific non-saturation diffusion model [ref. PbLi 2]. Further work has been performed by studying gas absorption in the loading phase at low gas pressure using big cylinders (15 mm diameter, 60 mm height) instead of the PbLi thin shavings used the previous campaign in order to minimise the influence of oxide in the H absorption [ref. PbLi3]. A serious damage in the facility is being repaired to continue with the experimental campaign during year 2008 [ref. PbLi4].

V.4.3. Microfission chamber development

See Section 6.4.1.10

V.4.4. EVEDA / IFMIF activation

In the framework of the EVEDA phase, neutron source, neutron flux and the corresponding dose rates on beam-off phase have been calculated in the vicinity of the accelerator components. And a comprehensive methodology to deal with the problem has been proposed. These activities have been performed by the Universidad de Educación a Distancia (UNED)

The d-d neutron source obtained using density profiles for the implanted deuterium computed with the proposed tools is found very different than that obtained using the traditional deuterium saturation density in copper at room temperature. And above all, the effect of considering d-Cu interactions at energies below 6 MeV are found critical in assessing the neutron source relevance for dose rates evaluations.

The d-d neutron source is negligible in terms of dose rate production when compared to the workers dose rate limit. Dose rate from deuteron activation has found also to be irrelevant. On the contrary, the d-Cu neutron source has a very significant effect. It is responsible of the dose rates at the end of the RFQ and in the DTL. Maximum decay gamma dose rate is observed at the end of the RFQ, where the deuteron energies are in the range between 4 and 5 MeV. At the external surface of the RFQ-end section, some days of cooling can be necessary for dose rate levels to fulfil dose rate limit for workers. At one meter distance, the limit could be fulfilled with a cooling time of about an hour.

As deuteron losses definition is the crucial input in the calculation of neutron activation and subsequent dose rates, different sets of deuteron losses computed along the last tree years have been lately compared and the effect upon residual dose rates and implications for hands-on maintenance activities discussed. The effect of the differences in the sets of deuteron losses have been shown to be very important on dose rates values. Using the most recent deuteron losses information we obtain dose rates values more than one order of magnitude lower than that obtained using former data.

As d-Cu reactions in the 4-5 MeV range have found the most relevant in regards to neutron source, and subsequent neuron activation a dose rates evaluations, an additional quality assessment of the cross sections data used for this range in EAF-2007 is undergoing. Moreover, cross checking of calculations for the neutron source resulting from d-Cu interactions is being performed using different approaches.

VI. OTHER ACTIVITIES CONTRIBUTIONG TO THE EURATOM FUSION PROGRAMME

VI.1. Training and Education

VI.1.1. Development of Eurasmus Mundus programme on Fusion (which initial teaching activities initiated on October 2006)

The Association EURATOM-CIEMAT has continued its involvement (making used of the TJ-II facility) in educational activities, dissemination of information about fusion to the general public and education of young researchers during 2007.

Eight PhD students have been directly involved (via their PhD work) in the TJ-II research programme and four Erasmus Mundus students (with EU grant) have been benefited from the TJ-II facilities (via the development of Erasmus Mundus programme on Fusion, http://www.em-master-fusion.org/).

VI.2. Public Information

VI.2.1. The Zivis Project

As it has been shown in Section 3.4 (Theory and Modelling) the LNF in collaboration with BIFI performed the experience of deploying a citizen supercomputer, based on BOINC middleware. The Zivis citizen supercomputer presented in Section 3.4 was not only a cheap computer infrastructure, but it is powerful tool for divulgating the main results and objectives of fusion research. The Town Hall of Zaragoza provided a strong support and even the Major made some public appearances and declarations, giving a political relevance to the project.

About 5000 persons participated in Zivis experience lending some cycles of their personal computers. Beyond these people, the project had a large diffusion among the society. More than 50 entries were detected in journals, radio and TV programmes and a huge number of visits to the web page of the project was registered. Accompanying the project, several performances and scientific conferences were given. In this way, the

citizens that participated giving their CPU time were also aware of the scientific results that were obtained using their computers.

VI.3. Socioeconomics

VI.3.1. Socioeconomic studies: EFDA-TIMES Model: Resource potential update

The objective of the task are the review, validation, improvement and documentation of the fossil resource potentials (different forms of oil, gas and coal) for the different regions of the EFDA-TIMES based on recent literature and databases. The review of the renewable resources was done in collaboration with ARC (GIS analysis). CIEMAT proposed a new structure for the modelling of renewable resources as well as the data to be used as potentials, based on both the literature (done by CIEMAT) and the GIS analysis (done by ARC in collaboration with CIEMAT). An update of the review done by CIEMAT is under-going and will be available in May 2008. Finally, CIEMAT collaborated with the other teams of EFDA responsible for the review of power plants and downstream transformation given the closed relations between the latter and the resource analysis. (1) (2) (3).

(1). EFDA Technology Work Programme 2006. EFDA-TIMES Model: Resources potentials update. Efda Reference: TW6-TRE-ETM-RES-Del 1, TW6-TRE-ETM-RES-Del 2, TW6-TRE-ETM-RES-Del 3. Final Report: Synthesis. M. Labriet, Y. Lechón, H. Cabal, M. Biberacher, S. Gluhak, D. Zocher, N. Dorfinger. CIEMAT Ref.: CIEMAT/ASE/F0030/SERF/1.

(2). EFDA Technology Work Programme 2006. EFDA-TIMES Model: Resources potentials update. Efda Reference: TW6-TRE-ETM-RES-Del 1, TW6-TRE-ETM-RES-Del 2, TW6-TRE-ETM-RES-Del 3. Final Report-Appendix A, Literatura review. M. Labriet, Y. Lechón, H. Cabal. CIEMAT Ref.: CIEMAT/ASE/F0030/SERF/2.

(3). EFDA Technology Work Programme 2006. EFDA-TIMES Model: Resources potentials update. Efda Reference: TW6-TRE-ETM-RES-Del 1, TW6-TRE-ETM-RES-Del 2, TW6-TRE-ETM-RES-Del 3. Final Report: Appendix B (GIS Approach). M. Labriet, Y. Lechón, H. Cabal, M. Biberacher, S. Gluhak, D. Zocher, N. Dorfinger. CIEMAT Ref.: CIEMAT/ASE/F0030/SERF/3

VI.3.2. Socioeconomics studies: Social perception of Fusion Research

Investigating lay understanding and reasoning about fusion technology by means of a group-based methodology suitable to take lay participants through a learning process about fusion

According with the Technical Specifications, two research stages were developed by Ciemat and Cardiff University during 2007: the design a group-based methodology suitable to take lay participants through a learning process about fusion, and the implementation of this method to investigate reasoning process about fusion by lay publics, and how such reasoning changes as they learn more about the technology.

The first objective of the research (i.e. the design of the group-based method) was addressed in the 1st Intermediate Report delivered to EFDA by the end of June 2007. That report included a review of relevant literatures for the design and implementation of the novel methodology - from both the conceptual (lay understanding of new technologies; the concept of a technology signature; nuclear branding) and the methodological perspective (group-based methods and problem structuring methods); the procedure followed to identify and select the informative materials to be used as stimulus in the group-based method (including interviews to check the suitability of the selected materials); and the practical design of the methodology to be applied in the next stage of the project.

The second objective (i.e. implementation of the method) was addressed in the 2nd Intermediate Report delivered to EFDA by the end of December 2007. That report addressed the details of a pilot study (comprising a single pair of groups) carried out prior to the data collection, in order to check the suitability of all parts of the method, and to fine-tune it as necessary. It explained the procedure followed to recruit the suitably-selected lay citizens for the six discussion groups (each meeting on two occasions). Next, it focussed on the details of the data gathering process. Finally, it introduced our approach to the data analysis and some very preliminary insights of the implementation of the group-based method, as well as its evaluation.

The final Report of this Task is foreseen for June 2008.

The main findings of this on-going work have been submitted and accepted in two international congresses to be held in Spain next September 2008: the First ISA (International Sociological Association) Forum of Sociology [ref. TW6-TRE-FESS-B1_1], and the ESREL (European Safety and Reliability Association –ESRA- and Society for Risk Analysis Europe -SRA-E) Annual Conference [ref. TW6-TRE-FESS-B1_2] [ref. TW6-TRE-FESS-B1_3].

VI.4. Activities related to the Broader approach

VI.4.1. IFMIF/EVEDA Project

VI.4.1.1. Accelerator Facilities: RF system

The RF Power System activity concerns the Engineering Design of the RF source required for IFMIF (RFQ, Buncher Cavities and DTL cells) and the construction of the RF sources for experimental validation on the prototype accelerator.

For the prototype accelerator, the reference RF Power System includes:

- 2 complete 1 MW RF Power Chains to feed the RFQ
- 1 complete 1 MW RF Power Chain to feed the first DTL tank
- 2 complete 60 kW RF Power Chains to feed the 2 buncher cavities of the MS

During 2007 an alternative solution to the Alvarez type Drift Tube Linac (DTL) has been proposed, this solution is based on the use of superconducting Half-Wave Resonators (HWR). For this reason, during this year two different RF systems have been studied and evaluated: one for the reference solution that uses 1 MW chains (above described) and another for the superconducting (SC) solution.

The RF system for the superconducting solution requires a higher number of RF chains but with a lower power:

Power amplifiers	**60 kW**	**105 kW**	**200 kW**
SC resonators	-	18	24
RFQ cavity	-	-	8
Buncher cavity	2	-	-
Total for 1 linac	2	18	32
Total for 2 linacs	**4**	**36**	**64**

Hereunder, the work during 2007 for each of the RF System main components is described, considering both options (reference and SC solution):

- **Amplifier Integration, Transmission Lines and Singular Elements**

During 2007, it has been decided the use of coaxial transmission lines instead of waveguide after analyzing the advantages and disadvantages of both options. Moreover, it has also been decided the use of a circulator and the corresponding dummy load for each RF chain. Basic characteristics of transmission lines and singular elements have been identified [Ref RF System 1]. Concept design of transmission lines and singular elements has been done. Contact with possible vendors has been established and a cost estimate of a 1 MW circulator has been received from industry.

For the superconducting option, different solutions for the RF system have been evaluated in order to feed the Half Wave resonators with the required RF power. One of the studied possibilities has been to power a series of 4-8 superconducting resonators by one high power amplifier (1 MW) and using fast ferrite high power phase shifters for the individual control of the resonators. However, finally the solution based on smaller RF amplifiers feeding individually the superconducting resonators seems to be more appropriate [Ref RF System 2]. For this solution, a preliminary design of the RF amplifiers implementation has been carried out based on removable boards containing all the two chains main components except the HVPS and the transmission lines. These removable modules would allow a fast maintenance and a may provide a higher reliability and availability.

Also, for the SC option, a preliminary design of the two foreseen coaxial lines (EIA 6"1/8 and EIA 9"3/16) has been carried out and a cost estimate has been received from industry.

- **Electrical DC High Voltage Power Supplies**

Main requirements of needed power supplies have been identified and an estimation of the installed and consumed power has been calculated. A set of preliminary alternative schematics of HVDC power supplies for the diacrode's anode has been conceived.

A preliminary technical specification of the diacrode's anode HV source has been written including the electrical and protection requirements.

In the case of the HWR superconducting option, a preliminary design has been conceived including the estimation of the installed and consumed power of the HVPS for the RF amplifiers. Were defined:

- The number, main parameters and dimensions of the potential HV sources
- The scheme of the switchyard for the connection to the HV network (6.6 kV)

- A layout proposal of the HV sources in the accelerator prototype building
- Also, two estimations for a 200 kW RF chain HVPS have been received from industry

- **Low Level RF Regulation & Local Control System**

A preliminary design of the LLRF system has been carried out. Collaboration between CIEMAT and CELLS (the Institution which develops and operates the ALBA Synchrotron) has been established to develop the IFMIF-EVEDA LLRF system.

VI.4.1.2. Accelerator Facilities: Beam Dump & HEBT

The accelerator prototype of the EVEDA phase requires a beam dump to stop the beam at the end of the accelerator and a beamline to transport the beam from the exit od the linac to the beam dump. The objective of this working package is the design and construction of these components. CIEMAT is the institute responsible of this delivery.

A first design of the High Energy Beam Transport (HEBT) line has been performed, using as input data the 9 MeV beam characteristics at the exit of the normal-conducting DTL cavity. Several configurations of the EVEDA-HEBT line have been studied, using different codes (Parmila, WinAgile and finally TraceWin). The line is composed of three quadrupole triplets, two for controlling the beam along the line and the last one to expand the beam with the aim of obtaining a deposited power density lower than 300 W/cm2 in the beam stop. In order to reduce the backscattering neutron radiation into the accelerator elements, a bending magnet has been inserted in the line. The total length of the line is about 12 meters, leaving enough free space for the diagnostic plate and for possible IFMIF diagnostics.

With regard to the beam dump, the main activities performed or initiated during 2007 have been the following:

- Study of activation by neutrons and deuterons for different materials for beam facing material selection
- First preliminary calculations of the cooling system
- Thermomechanical analysis with ANSYS for a conical beam stop
- Dose calculations (still on-going) to elucidate the best option of beam dump implantation into the building (dedicated room or sarcophagus).

VI.4.1.3. Accelerator Facilities: Diagnostics

As a starting point for this activity, a mini-workshop with beam instrumentation experts from different accelerators was gathered in June at CIEMAT. The goal of the meeting was to have some feedback of the techniques used at similar accelerators which could be interesting for IFMIF-EVEDA. After this workshop, an internal report was issued [IN-IF-ACBI-001]. The document includes an evaluation of the technical requirements of the devices for the measurement of each parameter, the advantages and drawbacks of these techniques. In addition, a preliminary estimation of the location and position of the beam diagnostics in the IFMIF-EVEDA beamline is given. Finally, the techniques used in similar accelerators for the different beam parameters are summarized. Once the final list of beam diagnostics was established, the work has been focused on the conceptual design of the beam position, fluorescence profile and transverse halo monitors. In addition, beam dynamics simulations have been performed in order to study the feasibility and accuracy of the measurement of the mean energy, energy spread and transverse and longitudinal emittance.

VI.4.1.4. Accelerator Facilities: DTL & MS

During 2007 no activities have been performed concerning the drift tube linac and matching section, as an alternative proposal to the reference design, based on superconducting half wave resonators, was being evaluated. Therefore, this activity was set on hold, until a decission on its implementation is taken by the Broader Approach Steering Committee. Preliminary discussions with CEA took place to decide the sharing between France and Spain in case that the superconducting option is finally chosen for the IFMIF-EVEDA accelerator.

VI.4.1.5. Accelerator Facilities: Safety

The Safety and Radioprotection tasks concerning IFMIF-EVEDA accelerator have been performed by the Universidad Nacional de Educación a Distancia (UNED). These activities started on September 2007. During this period, the main task was to provide expertise on safety and mainly on radioprotection issues with regard to the basic design of the EVEDA building. With this aim, a preliminary set of assumptions of the deuteron beam losses and corresponding neutron source terms was established [AccSafety1] and then an identification of the nuclear safety and radioprotection issues was done.

The main source terms identified correspond to points where high beam losses are expected: the Faraday cup located after the ion source, the matching section and the beam dump.

Biological shielding preliminary calculations have been performed for the design of the prototype accelerator building. The results have been crosschecked between CEA and UNED. A good agreement was obtained. Assuming a 0.56 % hydrogen content (in weight) the thickness of accelerator vault's walls has been set to 1.50 m, in order to be compliant with the Japanese external dose rate limitation of 12.5 μSv/h outside the accelerator vault.

The validation of a comprehensive computational methodology able to deal with the different radioprotection and safety identified issues is ongoing.

VI.4.1.6. Test and Target activities: Modelling Li behaviour in the target

The nuclear reactions in the target will produce a neutron flux which will be used for irradiation of specimens of candidate materials in the fusion field. To achieve the desired neutron flux, the IFMIF target fluid dynamics plays an important role since the lithium free surface should be stable to avoid an altered neutron field. During EVEDA phase, calculations and experiments are needed and it is essential to have codes capable to correctly simulate the IFMIF operation conditions. The activities related with the modelling of IFMIF lithium jet during 2007 were focused in the validation of CFX 10.0 code, specially, the turbulence models validation.

The validation process for IFMIF fluid dynamic calculations was performed by comparing experimental data obtained in a IFMIF scaled water facility with calculation results, for different water velocities (3.5, 8 and 20 m/s at the nozzle exit) and with different turbulence models used (*k-ε, k-ω*, *SST, SST* for transitional turbulence and *SMC,* [ref IN-IF-TFTM-001].

The main conclusion is that, in order to correctly simulate the velocity profile in the IFMIF nozzle, the use of the *SST* for transitional turbulence model is recommended in cases with relaminarization effects. On the contrary, for fully turbulent problems, like IFMIF case, it is recommended the use of *SMC*, *k-ω* or *SST* models, obtaining acceptable results with *k-ε* model.

Some 3D calculations were performed in the case of IFMIF target in order to obtain information about:

- The shape of the free surface under problematic situations like a small solid lithium drop (1 mm) in the nozzle exit edge.

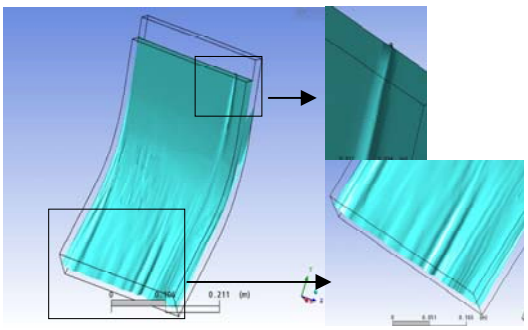

- The temperature distribution in flowing lithium under different beam power deposition profiles (14 kW/cm^3, 28 kW/cm^3 and 1000 kW/cm^3 as maximum value of Bragg curve).

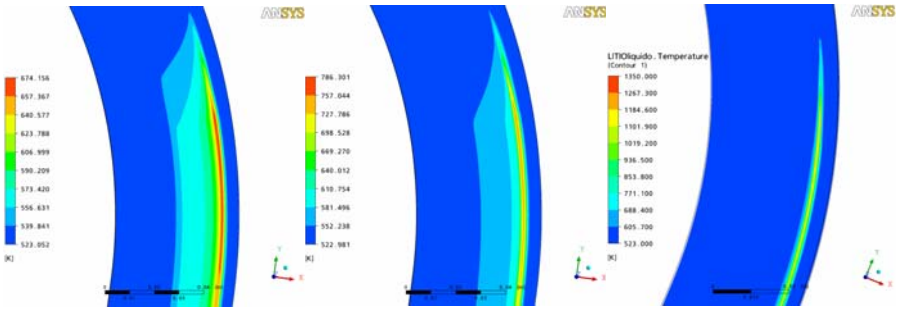

14 kW/cm^3 28 kW/cm^3 1000 kW/cm^3

VI.4.1.7. Test and Target activities: Target diagnostics

Diagnostics for the lithium target will be crucial for the operation of IFMIF. Several parameters as the lithium temperature, target thickness or wave pattern must be monitored during operation. As a result of an international collaboration expected dose rates were calculated at several locations where IFMIF diagnostics will be located. A summary of expected problems due to radiation damage has been done. The diagnostics considered cover topics as laser systems, IR cameras, windows assemblies, mirrors or surface diagnostics.

The main conclusions are that many components of the proposed diagnostics will be exposed to a radiation field generating important effects and could eventually lead to malfunctioning. The optical components of any diagnostic system may be weak points. The contact electrical probe is also a point of concern due its proximity to the target. Radiation effect on these critical components shall be revised in detail in order to assure the high performance required for the target system. [ref TAR] (*"Radiation Effects in IFMIF Li Target Diagnostic Systems" J.Molla, R.Vila, T. Shikama, H.Horiike, S.Simakov, M.Ciotti and A.Ibarra]* (paper accepted but unpublished)

VI.4.1.8. Test and Target activities: RH Engineering

Draft proposals have been produced to improve the design of the Test Cell in IFMIF for an enhanced remote handling. The proposals can be classified in:

- Modifications in the geometry of the Test Cell (TC) in order to improve the access at the bottom of the TC and facilitate the recovery of Li spills and accidentally dropped elements: The removal of one or various steps at the bottom of the TC and the addition of horizontal panels at the middle of the TC to divide the upper and lower volumes of the TC has been proposed.
- Proposals to provide access at the Back Plate through modified Plugs and to lighten the Test Cell Covers: The change in the order of the Shielding Plugs of the TC has been assessed and the Test Cell Covers of the TC have been split in different geometries to improve the access and to achieve a weight less than 25 tons per unit.
- Proposals to improve the installation and removal of Vertical Test Assemblies (VTAs): Wedged VTAs to avoid jamming and VTAs having dissimilar steps in order to achieve a staggered introduction of the VTAs have been devised.

The reports corresponding to these proposals are in process of publication.

A review of the Remote Handling operations carried out in the Test Facilities of IFMIF has been carried out. The sequence of operations is compiled in a tree structure and has been produced by means of a Visual Basic code. The series of operations are important to assess the time required for maintenance, find and solve issues during the maintenance operations and gradually increase the detail in the definition of the operations to be carried out.

VI.4.1.9. Test and Target activities: Medium Flux modules engineering

The scope of CIEMAT concerning the Medium Flux Test Modules (MFTM) of IFMIF, during the EVEDA phase, is the design of some rigs for the Tritium Release Module (TRM). The present objective of the TRM is to achieve tritium release measurements for the ceramic breeding blankets validation. Since liquid breeder blankets are very promising and its validation there has not been foreseen up to now, the future work of CIEMAT in the rigs design will be also focused in such a type of blankets.

During 2007, the aim of CIEMAT about the MFTM engineering has been the analysis of the current status of the module and the establishment of the starting point for the rigs design.

A detailed design of the rigs that will be allocated in the Tritium Release Module are not developed up to now. In order to start with the rig development for a particular

experiment, a first evaluation of the rig behaviour under the medium flux conditions has been performed during 2007. Two different conceptual designs of a rig have been analyzed:

- Design based in the CDE report conceptual design in which the temperature control of the samples is performed by changing the thermal conductivity of a gas gap.
- Design based on the HFTM rig (performed by FZK) in which the temperature control is achieved by means of electrical heaters.

Both designs are cooled by helium surrounding the rig by a very narrow channel. Tritium released by the specimens in the case of a ceramic breeder material will be swept up by another helium stream flowing through the rig in both cases.

Thermal hydraulic calculations have been performed to analyze the temperature of the samples obtaining that both designs allow the desired temperature in the rig. Taking into account that electrical heaters are also needed in beam off periods, a design based on the HFTM rigs was proposed as starting point of TRM rigs design. In order to get confidence on the used codes (CFX 10.0) for the thermal hydraulic calculations, a validation exercise using different turbulence models (*k-ε, k-ω*, *SST, SST* for transitional turbulence, *SMC, …)* has been performed. The calculation results have been compared with experimental data obtaining a suitable turbulence model (SST for transitional turbulence) to be used in future calculations [ref IN-IF-TFTM-001].

No conceptual design of the module to perform the experiments focused on the Liquid Breeder Validation has been initiated. Liquid metal blankets are very promising since allow a high operating temperature, an adequate tritium breeding ratio without beryllium neutron multiplier, low pumping power required and, also, an easy maintenance. Nevertheless, several problematic issues should be study to validate this blanket concept, for instance, the tritium permeation throughout the blanket walls. Next steps of CIEMAT in the MFTM engineering will be focused in the design of a tritium permeation experiment to validate the Liquid Breeder concepts.

VI.4.1.10. Test and Target activities: Microfission chamber validation activities

Part of the CIEMAT tasks related to the EVEDA phase of IFMIF is the validation of a fission microchamber for the IFMIF Test Cell.

Microfission chambers may be a very useful tool for operation of IFMIF, giving information on-line on the irradiation conditions. Several experiments are required to

validate the microchamber in the harsh environment of the Test Cell. A prototype needs to be developed able to provide information on the neutron flux and capable to survive the hard irradiation conditions in the IFMIF Test Cell. This includes the procurement of a prototype, simulation and preliminary tests, irradiation tests and the final design. A review of previous works by ENEA-Frascati (Italy), CEA-Cadarache (France) and Nuclear Physics Institute (NPI)-Prague (Czech Republic) [FC_1, FC_2] has been performed, and where the design of sub-miniature fission chambers for IFMIF – HFTM was studied.

The main identified purposes of the fission chambers are to control neutron fluxes in the Test Cell, measure differences in their spatial distribution and control fluence rate variations in the neutron source. Due to the high neutron fluxes and energetic particles (80% of neutrons will have energies above 1 MeV) they must be very efficient for fast neutrons, operating in an energy range between 1 – 50 MeV. Therefore, sensitivity at that energy range becomes a crucial point and one of the main requirements of the fission chambers. This sensitivity mainly depends on the coating fissile material, therefore several candidates with appropriates fission cross sections have been explored. Additionally, new burn-up and inventory evolution calculations have been now performed with the ACAB numerical code [FC_3], which takes into account actualized libraries (EASY2005) with cross section values up to 55 MeV (previous works only considered values below 20 MeV). One of the main requirements is that burn-up of the coating material should be minimal at the end of the irradiation period, since it is necessary to ensure a well functioning during the 11 months of the IFMIF operation (total fluxes up to 10^{22} neutrons·cm^{-2}). Results show that best fissile candidates for the measurement of high energy neutrons in the HFTM are ^{238}U and ^{237}Np, due to their fission cross sections and because their burn-up after one year of irradiation is under 4%. For the IFMIF MFTM the burn-up after one year of irradiation has been found to be negligible (i.e. <1% in most of cases).

The next step has been to study the procurement of a microchamber prototype. There are several companies which supply fission chambers, but up to now, those with a small diameter are manufactured by PHOTONIS [www.photonis.com] under CEA licence. The exploration of a number of microfission chambers commercially available has showed that 1.5 mm diameter chambers, which were the foreseen ones in previous studies, are too fragile and unreliable to be used in IFMIF, being advisable the use of wider chambers (at least 3 mm diameter).

This constraint in size has lead to propose new locations to place this neutron diagnostic, since it is too wide to be located inside the HFTM. Therefore the final part of the work has been focused on propose new locations to place the fission chambers. The best solution remains to be an open work that must be clarify in the next months.

[FC_1] C. Blandin, B. Esposito, "Design of sub-miniature fission chambers for the IFMIF-High Flux Test Module", Final Report EU Contract "ENEA contribution to IFMIF optimisation and cost reduction" ERB 5005 CT 90 0059 (EFDA/99-506) (Nov 2000).

[FC_2] B. Esposito, "Final Report of IFMIF Task D9 Construction and testing of prototype miniature fission chambers for IFMIF". EFDA task TW0-TTMI-00D9 (Sept 2003).

[FC_3] J. Sanz, "ACAB Activation Code for Fusion Applications: User's Manual V5.0", Lawrence Livermore National Laboratory UCRL-MA-143238 (2000).

VI.4.1.11. Design Integration: RAM evaluation

A RAM joint team has been created to develop RAM study in IFMIF. The first step was to compile all IFMIF's RAM information and evaluate the current state of RAM studies in IFMIF. The main conclusion is that there isn't a complete RAM study for IFMIF including the changes on CDA (00).

Riskspectrum has been proposed as right software to develop RAM analysis. It's necessary a powerful tool and made for this kind of studies and Riskspectrum is a professional and interactive tool for reliability and safety analysis and today is used at approximately 40% of the worlds nuclear power plants and other important PRA activities.

The target facility has been modelled using Riskspectrum and applying the changes on CDA (00) to make a bench market with previous RAM developed by Markov Chains. To create a powerful model it's necessary to encode all the basic events and a encode proposal have been done. This must be the same for all the designers and applied in the IFMIF design.

An actualization and extension of IFMI CDA (00) data base is beginning to develop.

VI.4.2. JT-60 SA Cryostat

VI.4.2.1. Activities in the Broader Approach. The Cryostat for JT-60SA

Spain is a voluntary contributor for the Japanese JT-60SA Tokamak. This machine is part of the JA-EU Broader Approach Agreement. JT-60SA is an abbreviation of JT-60 Super Advance. Spain will contribute, in-kind, with the fabrication of the Cryostat component.

Along the year 2007, the engineering group of the Lab. Nal de Fusión-Ciemat has participated in several meetings in relation with this project. It was also organized a

meeting, held at Madrid the 26th and 27th of March of 2007, especially dedicated to the Cryostat component. Three persons from Japan (JAEA), one from EU and experts of two Spanish Companies along with Ciemat engineers were involved in the meeting. The main conclusion of this meeting was to divide the cryostat in two parts: the gravity support and the main body including the top lid. The gravity support is the first piece needed to start the assembly, in-situ, of the whole tokamak, therefore the first part to be urgently manufactured. The agreement was to finish the detail design and technical specifications of this part and to prepare the call for tenders at the end of 2007. Moreover two Ciemat engineers stayed at JAEA in July and August, for one month, to study in-situ the site where the tokamak will be installed and also to see the status of the conceptual design of the cryostat main body. After this visit and for different reasons the conceptual design of the gravity support has been redesigned and different structural analysis has been performed inside the Ciemat.

Due to a general design review of the JT-60SA project carried out by experts from EU and Japan to reduce the cost, an important delay on the engineering activities has been produced and thus the detail design of the gravity support and conceptual design of the main body is still pending at the end of 2007. In spite of that, some calculation and design activities were carried out until the end of the year.

Finally, two Spanish companies have been working in different studies in relation with this project, in order to obtain a better understanding of the future manufacturing problems.

VI.4.3. DEMO R&D

VI.4.3.1. SiC/SiC characterization

A first batch of samples has been prepared. Commercial SiC 2 mm thick sheets (reaction bonded and hot pressed) have been purchased from Goodfellow. A Nd-YAG laser has been adapted in order to cut the SiC sheets to the appropriate size for the corresponding experiments and sample holders.

Preliminary results of electrical conductivity and dielectric loss have been performed to obtain pre-irradiation values.

VI.4.3.2. Insulators ceramics

Ceramics containing Li were produced at Ciemat (two different types: Li2SiO3 and Li4SiO4). Both types were irradiated with 1.8 MeV electrons in order to characterize and also to study the material stability in the presence of a radiation field. The samples were

irradiated at 75 C and during irradiation radioluminescence measurements were performed at different doses. In the case of the LiSiO3 sample several RL bands around 420, 500, 600 and 750 nm respectively were observed. All these bands decreased with irradiation time exhibiting a rapid initial decrease (very likely a purely electronic process) and then the observed decrease was much slower probably related to displacement events.

The Li4SiO4 sample when irradiated exhibited radioluminescence intensity around 100 times smaller than the Li2SiO3. In this case the RL spectrum did not exhibited band structure. Both the lack of RL band structure and the very low RL intensity indicate that the cristalinity of the material is not as good as in the case of the Li2SiO3 material. Radioluminescence measurements demonstrate to be a rapid and good tool to evaluate the quality of Li ceramics.

VI.5. Technofusion

The development of thermonuclear fusion as an inexhaustible and environmentally sustainable energy source is one of the great technological world challenges. Research on this field is one of the prime focuses of the European Union research programs and, in the next few years, approximately 400 M€ will be invested in it per year. Recently, the agreement for the construction of ITER has been signed. ITER project will demonstrate the scientific feasibility of this technology at a cost of about 10000 M€ for a period of 20 years. Besides the European Union, the United States, the Russian Federation, the People's Republic of China, the Republic of South Korea, Japan and India are also parties of the ITER project.

The production of commercial electric power from thermonuclear fusion demands additional research projects that are now being planned. The main ones are:

- IFMIF, a facility to qualify the materials that will be used in a fusion reactor
- JT60-SA, a superconductor tokamak that will make possible to test alternative concepts for ITER operation and, although it is still under discussion
- CTE, a tokamak to study the response of big components to radiation

All this shows that within the next 20-30 years, a great development on thermonuclear fusion research and its associated technologies is going to take place. It is believed that the main effort will be displaced towards the development of the different technologies

involved in the systems which are part of a fusion reactor and it will require the design and construction of great multinational projects.

Spain has a unique opportunity to outstand on the participation in this new technological field since the European Agency in charge of the European contributions management and control to ITER project and other "Fast Track" projects will be sited in Barcelona.

In our country most of the thermonuclear fusion research has been developed at CIEMAT, in Madrid, where the Stellarator TJ-II, a big magnetic confinement fusion device was constructed. Spanish participation in fusion technologies development projects, known as European Program on Fusion Technology, has been mainly focus on the development and characterization of materials. This activity became a significant success which has turned CIEMAT the reference laboratory in Europe on insulating materials for Fusion. But it is clearly needed to make a special effort to increase the participation on other technological areas and reinforce the present ones.

VI.6. Keep in Touch activities on Inertial Confinement Fusion

VI.6.1. Radiation Hydrodynamics and Jet Impact Fast Ignition

Radiation hydrodynamics simulations in relation with radiative shocks experiments hold at high-energy laser installations relevant for astrophysical situations have shed into light the importance of radiative losses on the shocks topology and dynamics. These losses can bend the shock, decrease significantly the time needed to reach the stationary regime and sharpen the luminosity of the shock around a privileged direction. In the context of inertial fusion, numerical tests are performed of radiation transport in order to quantify the differences between the Sn model and the M1 model. Advantages and drawbacks of each method are remarked in order to know which is better suited to model a given physical situation. We show that in the simple case of a Marshak wave, the differences can reach almost 20% on the matter temperature, and we are developing a series of case tests to enhance this comparison [ASTRON_ASP07_1]. Calculations using ARWEN for Jet Impact Fast Ignition has also been performed [PV_JIFI_IAEA_2].

VI.6.2. Activation and Safety

The primary damage behaviour of the low activation steel Eurofer was studied under irradiation in the high flux test module of IFMIF [TRANS_1, TRANS_2] and in the first structural wall of the magnetic (ITER, DEMO) and inertial (HYLIFE-II, HAPL) fusion energy reactors [DEMO_IFSA_1]. The depletion of the main constituents of Eurofer, Fe and Cr, is not significant. However, the prediction of minor constituents of Eurofer, such as Ti, V and Mn, increase in all cases, except for HYLIFE-II. In general, the concentration of newly generated elements is insignificant. The highest generation of Re and Os occurs in HYLIFE-II due to a softer neutron environment. The evolution of the elemental composition during irradiation shows a linear dependence with the irradiation time. There are a few exceptions such as B, Co and Ni. The total H and He production are comparable to some initial constituents and this production is due to (n,xH) and (n,xHe) reactions in Fe. We have calculated the effect of activation cross section uncertainties in the assessment of transmutation using the Monte Carlo method implemented in ACAB [NUCDAT_1, NUCDAT_2, NUCDAT_3]. The transmutant uncertainty analysis shows that the maximum relative errors for H and He production are in HFTM/IFMIF, 6.5% and 5.2%, respectively. We have found significant uncertainties in the transmutation responses for B, C, Al, P, Cr, Ni, Nb and Ta. In the case of H- and He- gas production the maximum uncertainty is below 7%.

VI.6.3. Tritium Handling

Primary phase of tritium emission to the atmosphere in a fusion system follows with a secondary phase (tritium deposited in the surface soil and vegetables). The meteorological conditions of the environment are critical in the final consequences. We perform calculations with detail analysis of meteorological parameters every hour, different velocity of deposition under normal operation, and considering that in eventual cases there is always tritium in the means; the concentrations were measured at times of more rain intensity and speed smaller than the wind. We conclude that if the season of vegetable growth coincides with a high intensity of rain, the tritium concentrations internal doses are maximal. 3D neutronics calculations for complex geometry are performed for KOYO-FI and ITER and assessment of fluid dynamics in Blanket Modules for inertial and magnetic concepts [NEUT_IFSA_1].

VI.6.4. Materials Radiation Damage

Fe-Cr system is the basis for the low activation steels that are being developed in the EU fusion materials community. A series of Fe-Cr alloys in the range from 1-15 at% Cr were produced under well controlled conditions from high purity elements by arc-melting in an

Argon atmosphere at CIEMAT. These alloys are being irradiated with Fe ions at different temperatures in the form of thin foils suitable for transmission electron microscopy (TEM) characterization in CIEMAT. We look for a better understanding of the basic mechanisms of damage production and microstructure evolution under irradiation in Fe-Cr alloys. Simulations in FeCr are starting to be performed in addition to those already done for comparison of Fe with/without magnetic interatomic potentials [MAT_IAEA_1, MAT_2, MAT_3]. The production of high levels of He during operation of future fusion reactors could affect the mechanical properties of structural materials, particularly in austenitic steels. We study the particular case of Ni using kinetic Monte Carlo with input from molecular dynamics calculations and *ab initio* data available in the literature, some of them will be reviewed by new *ab initio* calculations. From these calculations, relevant mechanisms of He diffusion and He-V complex stabilities are revealed that provide insight on the initial stages of bubble and void nucleation in f.c.c. metals. A very large work has been performed in the identification of the irradiation primary parameters of ceramics such as silica in IFE and MFE [SILICA_1] and the identification of the basic defects and cascades formation in such materials [SILICA_2]. A very important work was developed in the identification of the role of H in the materials, its diffusion and the effects of stochiometry [SILICA_3] in silica when production of defects. A new parallel kinetic Monte Carlo has been developed and used now for extension to higher doses [KMC_PAR_1], and the study of partial dislocation in fcc metals using dislocation dynamics has also been studied.

VI.6.5. Atomic Physics

VI.6.5.1. Calculation of atomic properties including plasma effects.

The determination of the atomic magnitudes is a subject of special relevance in plasma physics since they are essential in the determination, for example, of level populations, radiative properties or thermodynamic magnitudes. However, these magnitudes are modified with respect to the isolated situation when an ion is surrounded by a plasma. The study of their variations is the object of many theoretical and experimental investigations. In this sense, we have developed analytical potential for the determination of atomic properties of non-hydrogenic ions immersed both in strongly and weakly coupled and plasmas, which has allowed us to analyze the plasma influence. In particular, we have studied the plasma effect on the photoionization cross section of non-hydrogenic ions in weakly coupled plasmas [ref CAP_1], since the photionization process is a subject of special relevance in plasma physics because it is extremely sensitive to the details of the atomic structure and the correlation effects and can be used for plasma

diagnosis. Furthermore, we have performed an analysis of the effects of strongly coupled plasmas on the atomic magnitudes by using a new parametric potential developed with this purpose [ref CAP_2] which is able to model many-electron atoms, which is the most remarkable issue of this work since there are very few studies about them.

VI.6.5.2. Colisional-radiative calculations of plasmas.

Plasmas under NLTE conditions are ubiquitous both in laboratory and astrophysics. To diagnose and understand such plasmas, the collisional-radiative calculations are the first step and therefore, the development of new codes to carry out these calculations or the improvement of the existing ones remains as an area of great interest of plasma physics. In that sense, we have elaborated a flexible collisonal code named ABAKO [ref CRC_1] based on analytical potentials which can be applied to low-to-high Z plasmas in a wide range of plasma conditions, covering CE, LTE and NLTE, and optically thin and thick situations. Moreover, ABAKO has the advantage with respect to other kinetics codes of low pc-time-consuming. The results obtained by using this code were successfully compared with other provided by outstanding international laboratories in the last two NLTE Codes Workshops. In particular, our results corresponding to the 4^{th} NLTE workshop, which was hold in Las Palmas de Gran Canaria in 2005 and organized by our research team where the most relevant international laboratories devoted to plasma physics participated, were published in [ref CRC_2]. With this code we have made an exhaustive study of the level populations of carbon plasmas (which is one of the most important element under investigation both in magnetic confinement and astrophysics) providing a useful map to determine the carbon plasma regimes in terms of the plasma temperature and electron density [ref CRC_3] and also a first study of its spectrally resolved and mean opacities [ref CRC_4] by using an additional module for ABAKO called RAPCAL which makes the calculation of the radiative properties. Furthermore, in this line of research we have also carried out a similar analysis for aluminium plasmas [ref CRC_5] and some preliminary studies about the influence of the plasma self-absorption have been done [ref CRC_6]. This kind of plasmas has been of particular interest during the last two decades and much experimental and theoretical effort has been employed to investigate their radiative properties. However, in spite of these studies there is still a lack of complete understanding of the radiative properties of aluminium plasmas and new studies and results are always welcomed.

VI.6.5.3. Analytical opacity formulas.

Finally, at the same time, we have continued with the development of analytical expressions that permit to evaluate the mean opacities of plasmas under a wide range of plasmas conditions in a fast and accurate way. This kind of expressions is very relevant in hydrodynamic codes since the use of spectrally resolved opacities for each mesh point would take a huge calculation time. We presented a first work [ref AOF 1] where analytical expressions were proposed to calculate Planck and Rosseland mean opacities in a wide range of plasma densities and temperatures. The expressions were fitted to mean opacities obtained using very accurate atomic data (under DLA approach and including configuration interaction) and with level populations calculated solving a level-by-level collisional-radiative steady state model, using ABAKO and RAPCAL codes. Furthermore, in this work an extensive validation of the results was carried out by comparing them with data available in the bibliography.

Annex I

PUBLICATIONS of the Association EURATOM-CIEMAT in 2007 (compiled in May 2008)

SUMMARY

Articles published in journals and books	73
Articles accepted for publication or submitted	28
Technical reports	14
Presentations in conferences and workshops	79
PhD thesis	3
Advanced Studies Diplomas	2

1. Journals, books

Electron cyclotron wave power loss in fusion plasmas: a model comparison
F. Albajar, M. Bornatici and F. Engelmann
Nucl. Fusion **47** (2007) 1101-1105

Residual magnetic field coils for the neutral beam test facility (NBTF)
J. Alonso, J. Botija, G. Barrera, A. Lopez-Fraguas, M. Liniers and A. Soleto
Fusion Engineering and Design **82** (2007) 920-925

Hydrogen recycling and puffing at a poloidal limiter of TJ-II
E. de la Cal, J. Guasp, F.L. Tabarés, D. Tafalla, A. Alonso, P. Carvalho[a], A. Salas, B. Zurro and TJ-II Team.
J. Nucl Mater **363-365** (2007) 764

Fractional generalization of Fick's Law: a microscopic approach
I. Calvo, R. Sánchez, B.A. Carreras, and B.Ph. Van Milligen
Phys. Rev. Lett. **99** (2007) 230603

Continuous Time Random Walks in periodic systems: fluid limit and fractional differential equations on the circle
I Calvo, B A Carreras, R Sánchez and B Ph van Milligen
J. Phys. A: Math. Theor. **40** (2007) 13511-13522

Dynamics of a 1-D model for the emergence of the plasma edge shear flow layer with momentum conserving Reynolds stress
I. Calvo and B. A. Carreras.
Physics of Plasmas **14** (2007) 102507

ECCD Experiments in Heliotron J: Recent Results Regarding the Dependence on Magnetic Configuration and Wave Polarization
A.Cappa, K.Nagasaki, G.Motojima, T.Mizuuchi, H. Okada, S.Kobayashi, K.Kondo, H.Arimoto,W.Watanabe, M.Nosaku, H.Yasuda, F.Sano and A.Fernández.
Plasma Fusion Research: Rapid Communications **2** (2007) 030

Ion kinetic transport in the presence of collisions and electric field in TJ-II ECRH plasmas
F. Castejón, L. A. Fernández, J. Guasp, V. Martín-Mayor, A. Tarancón, and J. L. Velasco.
Plasma Phys. Control. Fusion **49** (2007) 753–776

Weakly Relativistic and Nonrelativistic Estimates of EBW Heating in the TJ-II Stellarator
F. Castejón, A. Cappa, M. Terechshenko, S. S. Pavlov, and A. Fernández.
Fusion Science & Technology **52** (2007) 230-239

Erratum: "Relativistic plasma dielectric tensor evaluation based on the exact plasma dispersion functions concept" [Phys. Plasmas 13, 072105 (2006)]

F.Castejón, S.S. Pavlov
Physics of Plasmas **14** (2007) 019902

Zivis: Deployment of a citizen supercomputer for stellarator calculations
F.Castejón
Stellarator News **110** (2007)

Cambio climático y sus consecuencias
Ed. Generalitat Valenciana. Valencia, 2007
ISBN 978-84-482-4771-3
Capítulo 15: *La fusión como solución a los desafíos*
F.Castejón

Perturbation of tokamak magnetic surfaces by applied toroidally asymmetric magnetic fields
I.T. Chapman, T.C. Hender, ...E. de la Luna, ... and JET EFDA Contributors
Nucl. Fusion **47** (2007) L36-L40

11th EU-US Transport Task Force workshop on transport in fusion plasmas
J.W. Connor, C. Angioni, P.H. Diamond, G.W. Hammett, C. Hidalgo, A. Loarte and P. Mantica
Nucl. Fusion **47** No 4 (2007) 361-369

Studies on proton irradiation-induced modifications of KU1 and KS-4V quartz glasses ultraviolet transmission properties
B. Constantinescu, R. Bugoi, E.R. Hodgson**,** R. Vila, P. Ioa
J. Nucl. Mater **367-370 (** 2007) 1048-1051

Assessment of Global Stellarator Confinement: Status of the International Stellarator Confinement Scaling Data Base
A Dinklage, E Ascasibar, CD Beidler, J Geiger, JH Harris, A Kus, S Murakami, S Okamura, R Preuss, F. Sano, U Stroth, Y Suzuki, J Talmadge, V Tribaldos, KY Watanabe, H Yamada, M Yokoyama
Fusion Science and Technology **51** (2007) 1-7

Physical model assessment of the energy confinement time scaling in stellarators
A. Dinklage, H. Maaßberg, R. Preuss, Yu.A. Turkin, H. Yamada, E. Ascasibar et al.
Nucl. Fusion **47** (2007) 1265-1273

ITER Physics Basis: Chapter 7: Diagnostics
A.J.H. Donné, ..., J. Sanchez, ..., et al.
Nucl. Fusion **47** (2007) S337-S384

Structural pattern recognition methods based on string comparison for fusion databases
S. Dormido-Canto, G. Farias, R. Dormido, J. Vega, J. Sánchez, N. Duro, H. Vargas, G. Rattá, A. Pereira, A. Portas
Fusion Engineering and Design **83** (2008) 421-424

Transitions to improved core electron heat confinement triggered by low order rational magnetic surfaces in the stellarator TJ-II

T. Estrada, F. Medina, D. López-Bruna, E. Ascasíbar, R. Balbín, A. Cappa, F. Castejón, S. Eguilior, A. Fernández, J. Guasp, C. Hidalgo and S. Petrov.
Nucl. Fusion **47** (2007) 305-312

Gyrotron Radiation affected by a controlled modulated reflector: high power experiment
A.Fernández, N.Kharchev, A.Psechnichnikov, Y.Bondar, K.Sarksyan, A.Tolkachev and M.Petelin.
International Journal of Infrared and Millimeter Waves **28** (2007) 705-711

ECCD Experiments in the TJ-II Stellarator
A.Fernández, A.Cappa, F.Castejón, J.M.Fontdecaba, K.Nagasaki
Fusion Science and Technology, **53** (2008) 254-260

Alternative cleaning techniques for the removal of carbon deposits
J. A. Ferreira, F. L. Tabarés, D. Tafalla
J. Nucl Mater **363-365** (2007) 888

Cryo-Trapping Assisted Mass Spectometry for the analysis of complex gas mixtures
J.A. Ferreira, F. L Tabarés
J. Vac. Sci. Technol. A **25** (2007) 246

Removal of carbon deposits in narrow gaps by oxygen plasmas at low pressure
J. A. Ferreira, F. L. Tabarés,a and D. Tafalla
J. Vac. Sci. Technol. A **25** (2007) 746

Power transmission of the Neutral Beam Heating beams at TJ-II.
C. Fuentes, M. Liniers, J. Guasp, J. Botija, J. Doncel, X. Sarasola, G. Wolfers, J. Alonso, R. Carrasco, G. Marcon, M. Acedo, E. Sanchez, M. Weber, M. Medrano, A. Soleto, J. Tera, D. Ciric
Fusion Engineering and Design **82** (2007) 926-932

Experimental progress on zonal flow physics in toroidal plasmas
A. Fujisawa, T. Ido, ...C. Hidalgo et al.
Nucl. Fusion **47** (2007) S718-S726

PKA Energy Spectra and Primary Damage identification in Amorphous Silica under different neutron energy spectra
M. L. Gámez, M. Velarde, F. Mota, J. Manuel Perlado, M. León, A. Ibarra

J. Nucl. Mater **367-370** (2007) 282-285

Electron heat transport comparison in the Large Helical Device and TJ-II
J. García, J. Dies, F. Castejón, K. Yamazaki
Physics of Plasmas **14** (2007) 102511

Electrical and mechanical behaviour of improved platinum on ceramic bolometers
M. Gonzalez, E.R. Hodgson

Fusion Engineering and Design **82** (2007) 1277-1281

Surface Electrical Degradation of Helium Implanted SiO2
S.M. Gonzalez de Vicente, A. Moroño, and E.R. Hodgson.
Journal of Nuclear Materials **367-370** (2007) 1014-1017

Surface electrical degradation for low mass ion implanted SiO2: Dependence on ion mass, energy, and dose rate
S. M Gonzalez de Vicente, A. Moroño, E. R. Hodgson,
Fusion Engineering and Design **82** (2007) 2567–2571

Microstructural and Optical Features of a Eu-Monazite.
T. Hernández and P. Martín
Journal of the European Ceramic Society **27** (2007) 109-114

Mirrors for Diagnostic and Remote Handling Applications in ITER. Problems with Specifications for Commercial Mirrors.
T. Hernández, P. Martín, E.R. Hodgson
Fusion Engineering and Design **82** (2007) 1258-1262

Water Hydraulic Polymer Components Ander Irradiation. Mechanical Properties.
T. Hernández, E.R. Hodgson.
Fusion Engineering and Design **82** (2007) 2035-2039.

Radiation induced ion currents in vacuum due to residual He and H, and their expected effect on insulating surfaces
E. R. Hodgson, A. Moroño, S.M. Gonzalez de Vicente
Fusion Engineering and Design **82** (2007) 2567-2571

Radiation effects on the deuterium diffusion in SiO2
A. Ibarra, A. Muñoz-Martín, P. Martín, A. Climent-Font, E.R. Hodgson
J. Nucl. Mater **367-370** (2007) 1003-1008

Recent EU activities for IFMIF EVEDA in the framework of the Broader Approach
A. Ibarra, A. Moslang, R. Laesser, R. Ferdinand, R. Andreani, E. Surrey, B. Riccardi, V. Heinzel, H. Klein, U. Fishcer, R. Forrest, M. Gasparotto
Fus. Eng. & Design **82** (2007) 2422-2429

Analysis of magneto hydrodynamic instabilities in TJ-II plasmas
R. Jiménez-Gómez, E. Ascasíbar et al.
Fusion Science and Technology **51** (2007) 20-30

Active contol of type I edge-localized modes with n=1 perturbation fields in the JET tokamak.Y.
Y. Liang, H.R. Koslowski, P.R. Thomas, E. Nardon,.... E. de la Luna, ... and JET EFDA contributors.
Physical Review Letters **98** (2007) 265004

Active control of type-I edge localized modes on JET

Y Liang, H R Koslowski, P R Thomas, E Nardon, ..., E De La Luna, ... and JET-EFDA Contributors
Plasma Phys. Control. Fusion **49** (2007) B581-B589

Prospects for steady-state scenarios on JET.
X. Litaudon, J.P.S. Bizarro, C.D. Challis, F. Crisanti, ...E. de la Luna,.... And JET EFDA contributors.
Nuclear Fusion **47** (2007) 1285-1292

Development of steady-state scenarios compatible with ITER-like wall conditions
X Litaudon, G Arnoux, M Beurskens,... E De La Luna, ... and the JET-EFDA Contributors
Plasma Phys. Control. Fusion **49** (2007) B529-B550

Edge plasma pressure measurements using a mechanical force sensor on the tokamak ISTTOK
T. Lunt, C. Silva, H. Fernández, C. Hidalgo, M.A. Pedrosa, P. Duarte, H. Figueiredo and T. Pereira
Plasma Phys. Controll. Fusion **49** (2007) 1783

Power plant conceptual studies in Europe
D. Maisonnier, D. Campbell,... M. Medrano et al.
Nucl. Fusion **47** (2007) 1524-1532

Fusión nuclear, una opción energética para el futuro
A. Medialdea, J. Sánchez
Revista de la Sociedad Nuclear Española **271** (2007)

Characterization of ripple-trapped suprathermal electron losses by their bremstrahlung emission in the soft x ray range at the TJ-II Stellarator
F Medina, M A Ochando, A Baciero and J Guasp
Plasma Phys. Control. Fusion **49** (2007) 385–394

Plasma potential evolution study by HIBP diagnostic during NBI experiments in the TJ-II stellarator
A.V. Melnikov, A. Alonso, E. Ascasíbar, R. Balbín, A.A. Chmyga, Yu.N. Dnestrovskij, l.G. Eliseev, T. Estrada, et al.
Fusion Science and Technology **51** (2007) 31-37

Assesment of transport in NCSX
D. R. Mikkelsen, H. Maasberg, M. C. Zarnstorff, C. D. Beidler, W. A. Houlberg, W. Kernbichler, H. Mynick, D. A. Spong, P. Strand, and V. Tribaldos
Fusion Science and Technology **51** (2007) 166-180

Pulse propagation in a simple probabilistic transport model
B.Ph. van Milligen, B.A. Carreras, V.E. Lynch and R. Sánchez
Nucl. Fusion **47** (2007) 189

The role of fused silica stochiometry on the intrinsic defects concentration
J.Molla, F.Mota, M.Leon, A.Ibarra, M.J.Caturla, J.M.Perlado
Journal of Nuclear Materials **367-370** (2007) 1122-1127

Radioluminescence behaviour for electron irradiated KS-4V
A. Moroño and E.R. Hodgson,
Journal of Nuclear Materials, **367-370** (2007)1107-1111

Radiation effects on the optical and electrical properties of CVD diamond
A. Moroño, S.M. Gonzalez de Vicente, E.R. Hodgson,
Fusion Engineering and Design **82** (2007) 2563-2566

Identification and characterization of defects produced in irradiated fused silica through molecular dynamics
F.Mota, M.-J.Caturla, J.M.Perlado, A.Ibarra, M.Leon, J.Molla, A.Kubota
Journal of Nuclear Materials, **367-370** (2007) 344-349

Control of non-inductive current in Heliotron J
G. Motojima, K. Nagasaki, ... A. Cappa and F. Sano
Nucl. Fusion **47** (2007) 1045-1052

A standard data access layer for fusion devices R&D programs
A. Neto, H. Fernandes, D. Alves, D.F. Valcárcel, B.B. Carvalho, J. Ferreira, J. Vega, E. Sánchez, A. Peña, M. Hron and C.A.F. Varandas
Fusion Engineering and Design **82** (2007) 1315-1320

On the damping of edge radial electric fields and flows in the TJ-II stellarator
M. A. Pedrosa, C. Hidalgo, B. A. Carreras, C. Silva, and L. García
Stellarator News, June 2007

Sheared flows and turbulence in fusion plasmas
M A Pedrosa, B A Carreras, C Hidalgo, C Silva, M Hron, L García, J A Alonso, I Calvo, J L de Pablos and J Stöckel
Plasma Phys. Control. Fusion **49** (2007) B303-B311

The role of a fast ion component on the heating of the plasma bulk
D Rapisarda, B Zurro, V Tribaldos, A Baciero and TJ-II team
Plasma Phys. Control. Fusion **49** (2007) 309–324

Remote control of data acquisition devices by means of message oriented middleware
E. Sánchez, A. Portas, A. Pereira, J. Vega and I. Kirpitchev
Fusion Engineering and Design **82** (2007) 1365-1371

Overview of TJ-II experiments
J. Sánchez et al
Nucl. Fusion **47** (2007) S677-S685

On the mechanism of carbon film deposition by PACVD in the presence of nitrogen. A Cryo-Trapping Assisted Mass Spectrometric Study
F. L Tabarés, JA Ferreira, and D. Tafalla.
Chem. Vap. Depos **13(6-7)** (2007) 335-344

Studies of film formation and erosion by hydrocarbon injection at the plasma edge of TJ-II.

D. Tafalla, F.L. Tabarés, I. García-Cortés, E.de la Cal, J.A. Ferreira and A. Hidalgo.
J. Nucl Mater **363-365** (2007) 252

Ion Chemistry in Cold Plasmas of H_2 with CH_4 and N_2
I. Tanarro, V. J. Herrero, A. M. Islyaikin, I. Méndez, F. L. Tabarés, and D. Tafalla
J. Phys. Chem. A **111** (2007) 9003 – 9012

Preliminary assessment of the safety of IFMIF
N. P. Taylor, B. Brañas, E. Eriksson, A. Natalizio, T. Pinna, L. Rodríguez-Rodrigo, S. Ciattaglia, R. Lasser.
Jour. Nucl. Mater **367-370** (2007) 1537

Experimental electron heat diffusion in ECH plasmas of the TJ-II stellarator
V.I. Vargas, D. López-Bruna, J. Herranz, F. Castejón and the TJ-II Team
Nucl. Fusion **47** (2007) 1367-1375

Real-time lossless data compression techniques for long-pulse operation
J. Vega, M. Ruiz, E. Sánchez, A. Pereira, A. Portas and E. Barrera
Fusion Engineering and Design **82** (2007) 1301-1307

Materiales para los futuros reactores de fusión
R. Vila, P. Fernandez, A. Moroño
Revista de la Sociedad Nuclear Española **271** (2007)

Thermally induced EMF in unirradiated MI cables
R. Vila, E. R. Hodgson.
Journal of Nuclear Materials **367-370** (2007)1044-1047

TIEMF in unirradiated Cu cored MI cables.
Rafael Vila, Eric Richard Hodgson.
Fusion Engineering and Design **82** (2007) 1271–1276

Core electron-root confinement (CERC) in helical plasmas
M. Yokoyama, H. Maaßberg, C.D. Beidler, V. Tribaldos, K. Ida, T. Estrada, F. Castejon et al.
Nucl. Fusion **47** (2007) 1213-1219

Bopp operators and phase-space spin dynamics: application to rotational quantum Brownian motion
D Zueco and I Calvo
J. Phys. A: Math. Theor. **40** (2007) 4635-4648

Edge turbulence measurements in toroidal fusion devices
S J Zweben, J A Boedo, O Grulke, C Hidalgo, B LaBombard, R J Maqueda, P Scarin and J L Terry
Plasma Phys. Control. Fusion **49** (2007) S1-S23

2. Accepted or submitted for publication

Conceptual design of the blanket mechanical attachment for the Helium-Cooled Lithium-Lead reactor.
G. Barrera, B. Brañas, J. Lucas, J.Donce1, M. Medrano, A. García, L. Giancarli, A. Ibarra, A. Li Puma, D Maisonnier, P. Sardain.
Fusion Engineering and Design **83** (2008) 6-20

CFD validation to the IFMIF Li-jet fluiddynamics
N. Casal, S. Gordeev, A. Garcia, F. Martin-Fuentes, A. Ibarra
Submitted to Fusion Engineering and Design.

Computation of EBW heating in the TJ-II Stellarator
F. Castejón, A. Cappa, M. Tereshchenko, and A. Fernández
Submitted to Nuclear Fusion.

The exact plasma dispersion functions in the complex region
F. Castejón and S. S. Pavlov
Nucl. Fusion **48** (2008) 065008

Estimation of pump-out and positive radial electric field created by electron cyclotron resonance heating in magnetic confinement devices
F. Castejón, S. Eguilior, I. Calvo, D. López-Bruna, and J. M. García-Regaña
Physics of Plasmas **15** (2008) 012504

PAPI based federation as a test-bed for a common security infrastructure in EFDA sites
R. Castro, J. Vega, A. Portas, D.R. López, S. Balme, J.M. Theis, P. Lebourg, H. Fernandes, A. Neto, A. Duarte, F. Oliveira, F. Reis, K. Purahoo, K. Thomsen, W. Schiller and J. Kadlecsik
Fusion Engineering and Design **83** (2008) 486-490

Physical and chemical studies of the removal of hydrogenated carbon films by nitrogen glow discharges
J.A. Ferreira, F.L. Tabarés
Submited to J. Phys: Conf. Series

Parameter dependence of the perpendicular velocity shear layer formation in TJ-II plasmas
L. Guimarais, T. Estrada, E. Ascasíbar, M.E. Manso, L. Cupido, T. Happel, E. Blanco, R. Jiménez-Gómez, M.A. Pedrosa, C. Hidalgo, I. Pastor and A. López-Fraguas
Submitted to Plasma and Fusion Research.

Microstructural and Electrical Features of Lithium doped Ce-Monazite
T. Hernández, R. Vila, J.R. Jurado, E. Chinarro, J. Molla, P. Martín
Accepted in Solid State Ionics

Effect of the Phosphorous/Cerium Ratio in the Properties of Sintered Ce-Monazite.
T. Hernández and P.Martín

Accepted in Journal of Alloys and Compounds

Insulator degradation due to radiation induced ion and dark currents in vacuum , E.R. Hodgson, A. Moroño, and S.M. Gonzalez.
J. Nucl. Mater. (in press)

Electrical surface degradation of electron irradiated sapphire and silica A.Moroño, E.R. Hodgson and S.M. González de Vicente.

J. Nucl. Mater. (in press).

Surface electrical degradation due to ion bombardment of ITER insulators,E.R. Hodgson, A. Moroño, and S.M. Gonzalez
J. Nucl. Mater. (in press).

Vacuum ultraviolet excitation of the 4.4 eV emission band in neutron irradiated KU1 and KS4Vquartz glasses
M. León, P. Martín, R.Vila, J. Molla, R.Roman and A.Ibarra
*Nuclear Instruments and Methods in Physics Research Section B: Beam Interactions with Materials and Atoms, **In Press, Corrected Proof**, Available online 23 March 2008.*

Thermal Stability of Neutron Irradiation Effects on KU1 Fused Silica
M. Leon, P.Martín, A. Ibarra, D. Bravo, F.J. Lopez, A. Rascon and F. Mota.
J. Nucl Materials **374** (2008) 386-389

Gamma irradiation induced defects in different types of fused silica

M. León, P. Martin, A. Ibarra, E.R. Hodgson
Submitted to J. Nucl. Mater.

Radiation induced absorption and luminescence of selected alternative radiation resistant glasses
P. Martín, A. Moroño and E.R. Hodgson,
J. Nucl. Mater (in press)

Radiation Effects in IFMIF Li Target Diagnostic Systems
J.Molla, R.Vila, T. Shikama, H.Horiike, S.Simakov, M.Ciotti, A.Ibarra
Submitted to J. Nucl. Mater.

Molecular dynamics study of Structure transformation and H effects in silica under displacement cascades
F.Mota, M.-J. Caturla, J.M. Perlado, J. Mollá, A. Ibarra
Submitted to J. Nucl. Mater.

On-line reprogramming of data acquisition systems during shots
A. Pastoriza, P Manrubia, F. Sastre, M. Ruiz, E. Barrera, J. Vega, R. Castro, A. Portas, A. Pereira, P. Castro, G. Rattá.
Submitted to Fusion Engineering and Design.

First applications of structural pattern recognition methods to the investigation of specific physical phenomena at JET
G.A. Rattá, J. Vega, A. Pereira, A. Portas, E. de la Luna, S. Dormido-Canto, G. Farias, R. Dormido, J. Sánchez, N. Duro, H. Vargas, M. Santos, G. Pajares and A. Murari
Fusion Engineering and Design **83** (2008) 467-470

Solar sintering of alumina ceramics: Microstructural development
R. Román, I. Cañadas, J. Rodríguez, T. Hernández, M. González,
Solar Energy, In Press, Uncorrected Proof, Available online 1 May 2008

Data reduction in the ITMS system through a data acquisition model with self-adaptive sample frequency
M. Ruiz, JM. López, G. de Arcas, E. Barrera, R. Melendez and J. Vega.
Fusion Engineering and Design **83** (2008) 358-362

An event-oriented database for continuous data flows in the TJ-II environment
E. Sánchez, A. de la Peña, A. Portas, A. Pereira, J. Vega, A. Neto and H. Fernandes
Fusion Engineering and Design **83** (2008) 413-416

Cleaning efficiency of carbon films by oxygen plasmas in the presence of metallic getters
F L Tabarés, J A Ferreira, D Tafalla, I Tanarro, V Herrero, I Méndez, C Gómez-Aleixandre and J M Albella
Submited to J. Phys: Conf. Series

Intelligent methods for data retrieval in fusion databases
J. Vega and EFDA contributors
Fusion Engineering and Design **83** (2008) 358-362

Data mining technique for fast retrieval of similar waveforms in Fusion massive databases
J. Vega, A. Pereira, A. Portas, S. Dormido-Canto, G. Farias, R. Dormido, J. Sánchez, N. Duro, M. Santos, E. Sánchez and G. Pajares
Fusion Engineering and Design **83** (2008) 132-139

Ion heating in transitions to CERC in the stellarator TJ-II
J.L. Velasco, F. Castejón, L.A. Fernández, V. Martin-Mayor, A. Tarancón and T. Estrada
Nucl. Fusion **48** (2008) 065008

3. Technical reports

BSM Attachment Arrangement & EPP Hydraulic Analysis
José Botija, Ángela García, Esther Rincón, y Xabier Sarasola
EFDA task: TW5-TPDS-DIASUP

ITER diagnostic procurement package PP01: Plasma Position Reflectometry. First Intermediate Report.
T. Estrada and G. Pérez
EFDA task: TW6-TPDS DIADES. April 2007

ITER diagnostic procurement package PP01: Plasma Position Reflectometry. Second Intermediate Report
T. Estrada and G. Pérez
EFDA task: TW6-TPDS DIADES. July 2007

Irradiation Effects in Ceramics for Heating and Current Drive, and Diagnostic Systems: Report on in-situ testing of resistive type bolometers using alumina, aluminium nitride, and silicon nitride substrates: temperature and ionization effects
M. Gonzalez and E.R. Hodgson
Final report TW5-TPDC-IRRCER, December 2007.

Sistema de control remoto de los espejos de las líneas de transmisión de microondas del TJ-II
A.López-Sánchez, A.Fernández, A.Cappa, J.de la Gama, J.Olivares, R.García, M.Chamorro
Informe técnico CIEMAT, **1108**, junio 2007.

ITER diagnostic procurement package PP11: Radial Neutron Camera and Equatorial Visible/IR Wide Angle Viewing System. First Intermediate Report
J.L. de Pablos, A. Manzanares, J.A. Alonso, E. de la Cal and C. Hidalgo
EFDA task: TW6-TPDS DIADES . May 2007

ITER diagnostic procurement package PP11: Radial Neutron Camera and Equatorial Visible/IR Wide Angle Viewing System
Second Intermediate Report.
J.L. de Pablos, A. Manzanares, J.A. Alonso, E. de la Cal and C. Hidalgo
EFDA task: TW6-TPDS DIADES. September 2007

ITER diagnostic procurement package PP12: Core-plasma LIDAR Thomson Scattering. First Intermediate Report.
I. Pastor, G. Veredas and J. Herranz
EFDA task: TW6-TPDS DIADES. May 2007

ITER diagnostic procurement package PP12: Core-plasma LIDAR Thomson Scattering. Second Intermediate Report
I. Pastor, G. Veredas and J. Herranz
EFDA task: TW6-TPDS DIADES. July 2007

Beam diagnostics for IFMIF-EVEDA
I. Podadera, B. Brañas
IN-IF-ACBI-001, CIEMAT (2007)

Feasibility study of CMR sensors for ITER
J.A. Romero
EFDA task: ITER TW5-TPDS-DIADEV deliverable 2c. March 2007

Hotcell Functions during ITER Dismantling and Phases of Hotcells and Radwaste Buildings Dismantling.
M. Vázquez, S. Vidaechea, O. Asuar, B. Brañas, P. Díaz-Arocas, E. Milla, P. Zuloaga
Informe CIEMAT IN-IT-EISS-004. Diciembre 2007.
Informe final de tarea EFDA TW5-TES-SL53.8b.

Study of thermally–induced electrical signals (TIEMF) in coated cables for in-vessel coils. Final report
R.Vila and E.R.Hodgson
UT06_TPD_TIEMF

Preliminary study on alternative RF power systems for superconducting Half-Wave resonators in IFMIF accelerator
M. Weber, P. Méndez, I. Kirpitchev, M. Falagan, A. Soleto, A. Ibarra
Informe técnico CIEMAT, , 2007.

4. Conferences and Workshops

15th IEEE NPSS Real Time Conference 2007. Fermilab, Batavia, IL (USA). April 29 – May 4, 2007
(http://computing.fnal.gov/cd/rt07/).

Two criteria for On-line Detection of Oscillations in Nuclear Fusion Experiments
N. Duro, J. Sánchez Moreno, S. Dormido-Canto, R. Dormido, G. Farias, H. Vargas, J. Vega.

8th International Reflectometer Workshop (IRW8), St.Petersburg, Russia. May 2-4 2007
http://plasma.ioffe.ru/irw8/

1. Study of Doppler reflectometry capability to determine the perpendicular velocity and the k-spectrum of the density fluctuacions using a 2D full-wave code"
E. Blanco, T. Estrada, and E. Holzhauer

2. Recent results of reflectometry measurements in TJ-II"
T. Happel, T. Estrada, L. Cupido1, E. Blanco, M. A. Pedrosa and R.Jiménez-Gómez

17th Topical Conference on Radio Frequency Power in Plasmas. Clearwater, Florida (USA). May 7-9 2007.
http://www.ornl.gov/sci/fed/rf2007/

Electron Bernstein Waves Heating Project in the TJ-II stellarator
A.Fernández, J.Caughman, A.Cappa, F.Castejón and M.Tereshchenko

European Consulting Committee for Neutral Beam Injection CCNB I/2007 Meeting, CEA, Cadarache. May 23-24 2006
http://efdasql.ipp.mpg.de/ccnb/ccnbindex.htm

A Target Calorimeter for the "in situ" characterization of Beams at TJ-II
M. Liniers, C. Fuentes, G. Wolfers, M. Weber, G. Marcon, R. Carrasco,J. Guasp, M. Acedo, E. Sánchez, X. Sarasola, J. Botija, J. Alonso,J. Tera

6th IAEA Technical Meeting on Control, Data Acquisition and Remote Participation for Fusion Research. Inuyama (Japan). June 4-8 2007.(http://tm2007.nifs.ac.jp/).

1. Support tools for the EFDA RP collaboration
Stéphane Balme, Piroska Giese, Jesús Vega.

2. PAPI based federation as a test-bed for a common security infrastructure in EFDA sites
R. Castro, J. Vega, A. Portas, D. R. López, S. Balme, J.M. Theis, P. Lebourg, H. Fernandes, A. Neto, A. Duarte, F. Oliveira, F. Reis, K. Purahoo, K Thomsen, W. Schiller, J. Kadlecsik.

3. Comparison of structural pattern recognition methods for fusion databases
S. Dormido-Canto, G. Farias, R. Dormido, J. Sánchez, N. Duro, H. Vargas, J. Vega, G. Rattá, A. Pereira, A. Portas.

4. On-line reprogramming of data acquisition systems during shots
A. Pastoriza, P Manrubia, F. Sastre, M. Ruiz, E. Barrera, J. Vega, R. Castro, A. Portas, A. Pereira, P. Castro, G. Rattá.

5. Structural pattern recognition for image processing in fusion plasmas
D. Raju, J. Vega, P. Castro, G. Rattá, A. Murari, G. Vagliasindi and JET EFDA Contributors.

6. First applications of structural pattern recognition methods to the investigation of specific physical phenomena at JET
G. A. Rattá, J. Vega, A. Pereira, A. Portas, E. De la Luna, S. Dormido-Canto, G. Farias, R. Dormido, J. Sánchez, N. Duro, H. Vargas, M. Santos, G. Pajares, A. Murari and JET EFDA Contributors.

7. PAPI EE. Adapting PAPI to Shibboleth
C. Rodríguez, D. López, A. Daryanani, D. García, R. Castro, J. Vega .

8. Data reduction in the ITMS system through a data acquisition model with self-adaptive sample frequency
M. Ruiz, G. Arcas, J.M. López, E. Barrera, R. Meléndez, J. Vega.

9. An event-oriented database for continuous data flows in the TJ-II environment
E. Sánchez, A. de la Peña, A. Portas, A. Pereira, J. Vega, A. Neto, H. Fernandes.

10. Intelligent methods for data retrieval in fusion databases
J. Vega and JET EFDA Contributors.

34th EPS Conference on Plasma Physics. Warsaw, Poland. July 2-6 2007
http://www.eps2007.ifpilm.waw.pl/

1. Fast camera installation and operation in JET
J.A. Alonso et al.
P2.124

2. Local emission profiles from impurity ions and visible bremsstrahlung in the TJ-II stellarator
A. Baciero et al.
P5.089

3. Study of the statistical properties of fluctuations in the plasma boundary region of the TJ-II stellarator
J. Brotankova et al.
P1.086

4. Spatially resolved H-alpha study of hydrogen recycling at a limiter in ECRH plasmas of TJ-II
E. de la Cal et al.
P2.029

5. One-dimensional transition model with momentum conservation
I. Calvo et al.
P4.057

6. Gaussian beam optimization for O--X mode conversion
A. Cappa et al.
P5.054

7. Localized temperature and velocity measurements of C VI ions using active CXRS spectroscopy in the TJ-II stellarator
J.M. Carmona et al
P2.146

8. Dynamics of plasma electric field of positive radial electric field created by ECRH-pump out
F. Castejón et al.
P4.089

9. First results of Fast Ion Losses in the TJ-II stellarator
D. Jiménez-Rey et al.
P5.114

10. Active Control of Type-I Edge Localized Modes on JET
Y. Liang, ..., E. De La Luna, ...et al.
I5.004 (Invited talk)

11. Recycling and density control in TJ-II plasmas based on 1-D transport calculations. D. Lopez-Bruna et al.
P1.098

12. Measurements of inboard-outboard asymmetry of pedestal temperature collapse during Type I ELMs in JET
E. de la Luna et al.
P5.085

13. Sheared flows and turbulence in fusion plasmas
M.A. Pedrosa et al.
I2.020 (Invited talk)

14. Electron diffusivity profiles in ECH plasmas of the TJ-II Heliac
V.I. Vargas et al.
P1.120

15. A comparative study of impurity and proton poloidal rotation in the TJ-II stellarator B. Zurro et al.
P5.110

17th International Vacuum Congress (IVC-17). Stockholm, Sweden. July 2-6 2007.
http://www.congrex.com/IVC17icss13/

1. Physical and chemical studies of the removal of hydrogenated carbon films by nitrogen glow discharge.
J.A. Ferreira and F.L. Tabarés.

2. Cleaning efficiency of carbon films by oxygen plasmas in the presence of metallic getters.
F.L. Tabarés, J.A. Ferreira and D.Tafalla, I. Tanarro and V.Herrero, C. Gómez-Aleixandre and J.M.Albella.

14 th International Conference on Radiation Effects in Insulators (REI - 2007) 28 August - 01 September 2007 Caen (France)
Vacuum ultraviolet excitation of the 4.4 eV emission band in neutron irradiated KU1 and KS-4V quartz glasses
M. León, P.Martín R. Vila, J. Molla, R. Roman and A. Ibarra

Joint 32nd International Conference on Infrared and Millimetre Waves and 15th International Conference on Terahertz Electronics. Cardiff (UK). September 2-7 2007.
http://www.astro.cf.ac.uk/irmmw-thz2007/

EC waves polarization control in the TJ-II Stellarator
A.Fernández, D.Wagner, A.Cappa, G.Müller and A.Tolkachev

ASEVA Workshop 2007: WS-21 Hydrogen as a Future Energy Carrier. Ávila, Spain. September. 3-5 2007.
http://www.icmm.csic.es/aseva/ws21.html

Hydrogen Retention in the first wall of TJ-II under plasma operation.
F.L. Tabarés, J.A. Ferreira and D. Tafalla

5th International Conference on Inertial Fusion Sciences and Applications. Kobe (Japan), September 9-14 2007.
http://www.ile.osaka-u.ac.jp/ifsa07/

1. Molecular dynamics study of defects in amorphous silica; generation and migration
F. Mota, J. Molla, J.M. Caturla, A. Ibarra, J.M. Perlado

2. Primary Damage Identification in Amorphoys Silica and Carbon, and Microscopic Calculation of Defect Formation under Neutron Irradiation in Inertial Fusion
M. Perlado, M.J. Caturla, A. Ibarra, F. Mota, M.L. Gámez, M. Velarde, M. León, M. J. Mollá, E. Bringa

31 Reunión Bienal de Física. Granada, Spain. September 10-14 2007
http://physica.ugr.es/bienalgranada/

1. Interrelación entre flujos medios, campos eléctricos y turbulencia en plasmas del dispositivo stellarator TJ-II
J.A. Alonso, C. Hidalgo, M.A. Pedrosa, J.L. de Pablos et al

2. Ion kinetic transport in presence of collisions and electric field in TJ-II ECRH plasmas
F. Castejón et al.

3. Propiedades de la absorción y dispersión de microondas en el dispositivo de confinamiento de plasmas MLPUC
J.M. García-Regaña, F. Castejón, E. Anabitarte

4. Nuevo diagnóstico bidimensional de alta velocidad en JET
J. L. de Pablos et al.

5. Turbulencia y flujos en plasmas de fusión
M.A. Pedrosa, B.A. Carreras, C. Silva, C. Hidalgo, J.A. Alonso,,L. García, I. Calvo et al.

6. Estudio de fragmentación e ionización de hidrocarburos en el borde del plasma del stellarator TJ-II
F. L. Tabarés, J. A. Ferreira, D. Tafalla, I. García-Cortés, E. de la Cal

International Workshop on Burning Plasma Diagnostics. Varenna, Italy. September 24-28 2007
http://www.ispp.it/Courses_and_Workshops.html#2007

Critical Assessment of Pressure Gauges for ITER
Francisco L. Tabarés, David Tafalla and Isabel Garcia-Cortés

33ª Reunión Anual de la Sociedad Nuclear Española, Segovia, España. 26-28 September 2007

***1.** CFD calculations on the IFMIF Li-jet fluiddynamics (Oral)*
N. Casal, F. Martin-Fuentes, A. Garcia, A. Ibarra

2. Sistemas de manipulación remota para las instalaciones del Test de IFMIF (Oral)
A. Garcia, A. Ibarra, V. Queral, G. Micciche

3. Selección de materiales para el beam dump de la fase EVEDA de IFMIF (Oral)
J.M. Gomez, B. Brañas, A. Ibarra, J. Sanz, O. Cabellos

4. Cámaras de fisión miniaturizadas para medidas neutrónicas en IFMIF (Oral)
J.M. Gomez-Ros, M. Lis, A. Garica, A. Ibarra, O. Cabellos

5. El proyecto TecnoFusión: un centro singular para el desarrollo de la tecnología de Fusión : (Oral INVITADA)
A. Ibarra, J.M. Perlado

6. La Instalación Singular de Fusión: Un Centro Nacional para las Tecnologías de la Fusión: (Oral)
A. Ibarra, M.J. Perlado, B. Brañas, J. Sanchez, A. Garcia, F. Tabarés, M. Victoria

7. La participación Española en el Acuerdo para el Enfoque Amplio a la Fusión: (Oral INVITADA)

J. Sanchez, A. Ibarra, J. Alonso, E.R. Hodgson

8. Propuesta de plan de RAM para IFMIF (Oral)
C. Tapia, J. Dies, M. Papera, R. Lopez, G. Riba, A. Ibarra

9. Los nuevos paradigmas de interacción con los entornos experimentales de dispositivos de fusión
J. Vega, R. Castro, A. Portas, A. Pereira, P. Castro, G. Rattá, J. Sánchez, A. Pastoriza, P. Manrubia, F. Sastre, M. Ruiz, E. Barrera

10. El sistema de RF para IFMIF (Oral)
M. Weber, P. Mendez, I. Kirpitchev, M.A. Falagan, A. Ibarra

8th International Symposium on Fusion Nuclear Technology. Heidelberg (Germany). September 30-October 5 2007
http://iwrwww1.fzk.de/isfnt/

CFD calculations on the IFMIF Li-jet fluiddynamics
N. Casal, F. Martín-Fuertes, A. García, A. Ibarra, R. Barbero

Joint Conference of 17th International Toki Conference (ITC) on Physics of Flows and Turbulence in Plasmas and 16th International Stellarator/Heliotron Workshop (ISHW) 2007, Toki, Japan. October 15-19 2007
http://itc.nifs.ac.jp/

1. On the link between flows, turbulence and electric fields in the edge of the TJ-II stellarator
J.A. Alonso, C. Hidalgo, M.A. Pedrosa, J.L. de Pablos and the TJ-II team

2. Effect of rotational transform and magnetic shear on confinement
E. Ascasíbar, D. López-Bruna, F. Castejón, V. Tribaldos et al.

3. A systematic study of impurity ion poloidal rotation and temperature profiles using CXRS in the TJ-II stellarator
J.M. Carmona, K.J. McCarthy, R. Balbín, and TJ-II team

4. Searching for a flux-expansion divertor in TJ-II
F. Castejón, L. A. Fernández, A. López-Fraguas, V. Martin-Mayor, A. Tarancón and J. L. Velasco

5. Status of the International Stellarator/Heliotron Profile Database: The ISHPDB Collaboration
A. Dinklage, E. Ascasibar, C.D. Beidler, R. Brakel, R. Burhenn, F. Castejon, T. Estrada, H. Funaba, Y. Feng, J. Geiger, J.H. Harris, C. Hidalgo, K. Ida, M. Kobayashi, R. König, G. Kühner, A. Kus, D. Lopez Bruna et al.

6. Transitions to improved core electron heat confinement in TJ-II plasmas
T. Estrada, F. Medina, D. López-Bruna, E. Ascasíbar, R. Balbín, F. Castejón, C. Hidalgo and S. Petrova

7. Parametric dependence of the perpendicular velocity shear layer formation in TJ-II plasmas
L. Guimarais, T. Estrada, E. Ascasíbar, T. Happel, R. Jiménez-Gómez, M.A. Pedrosa, C. Hidalgo, I. Pastor and A. López-Fraguas

8. MHD activity measured with magnetic probes in TJ-II
R . Jiménez-Gómez, E. Ascasíbar, S. Yamamoto, G. Motojima, K. Nagaoka, J. A. Jímenez, T. Estrada, T. Happel, A. V. Melnikov, M. A, Pedrosa, C. Hidalgo, A. Alonso, A. Fernández, M. Liniers.

9. Modification of transport due to low order rationals of therotational transform in ECH plasmas of the TJ-II Heliac
D. López-Bruna, T. Estrada, F. Medina, J. Herranz, V. I. Vargas, A. Baciero, E. Ascasíbar, J. A. Romero, F. Castejón

10. Comparison of Impurity Transport in Different Magnetic Configurations
Kieran J. McCarthy, R. Burhenn, K. Ida, H. Maassberg, Y. Nakamura, N. Tamura

11. Quantifying profile stiffness
B.Ph. van Milligen, B.A. Carreras, R. Sánchez, V. Tribaldos, V.I. Vargas

12. ECCD Experiments in Heliotron J, TJ-II, CHS and LHD
K. Nagasaki, G. Motojima, A. Fernandez, A. Cappa, Y. Yoshimurac T. Notake, Heliotron J Team, TJ-II Team, CHS Team and LHD Team

13. Experimental studies and modelling of edge shear flow development in the TJ-II stellarator
M.A. Pedrosa, B.A. Carreras, C. Silva, C. Hidalgo, J.A. Alonso, L. García, I. Calvo, J.L. de Pablos, R.O. Orozco, D. Carralero and the TJ-II team

14. On the zonal flows identification in the plasma edge of the TJ-II stellarator
M.A. Pedrosa, C. Silva(*), C. Hidalgo, R.O. Orozco, D. Carralero and the TJ-II team

15. Impact of lithium-coated walls on plasma performance in the TJ-II stellarator
F.L. Tabarés, D. Tafalla, J.A. Ferreira, I. García-Cortés and the TJ-II Team.

13th International Conference on Fusion Reactor Materials (ICFRM13), . Nice, France, December 10-14 2007
http://www-fusion-magnetique.cea.fr/icfrm13/

1. Insulator degradation due to radiation induced ion and dark currents in vacuum
E.R. Hodgson, A. Moroño, and S.M. Gonzalez.

2. Surface electrical degradation due to ion bombardment of ITER insulators
E.R. Hodgson, A. Moroño, and S.M. Gonzalez.

3. Gamma irradiation induced defects in different types of fused silica
M. León, P. Martín, A. Ibarra, and E. R. Hodgson

4. Radiation induced absorption and luminescence of selected alternative radiation resistant glasses
P. Martín, A. Moroño and E.R. Hodgson

5. Radiation Effects in IFMIF Li Target Diagnostic Systems
J.Molla, R.Vila, T. Shikama, H.Horiike, S.Simakov, M.Ciotti, A.Ibarra

6. Electrical surface degradation of electron irradiated sapphire and silica
A.Moroño, E.R. Hodgson and S.M. González de Vicente

7. Molecular dynamics study of structure transformation and H effects in silica under displacement cascades
F. Mota, M.J. Caturla, J.M. Perlado, J. Mollá, A. Ibarra

8. Neutron induced activation in the EVEDA Accelerator materials: Implications for the accelerator maintenance
J. Sanz, M. Garcia, P. Sauvan, D. Lopez, C. Moreno, A. Ibarra, L. Sedano

9. TIEMF effect in ceramic coated cables
R. Vila and E.R. Hodgson

17th IEA Annex II Workshop on Radiation Effects in Ceramic Insulators. Nice, December 2007
Latest data on TIEMF
R.Vila

5. Ph. D. Thesis

“Estudio de la dinámica de iones por métodos espectroscópicos en TJ-II”
David Rapisarda
February 2007

"Transmisión del haz de neutros de calentamiento en TJ-II"
Cándida Fuentes
May 2007

“Caracterización de los plasmas de TJ-II y sus poblaciones supratérmicas con diagnósticos de rayos x”
Francisco Medina
May 2007

6. Advanced Studies Diplomas

"Integración del Diagnóstico de reflectometría para el control de posición del plasma de ITER".
Germán David Pérez Pichel
Octubre 2007

"Estructura federativa entre laboratorios de fusión basada en tecnología PAPI"
Rodrigo Castro Rojo
Junio 2007